Technische Universität München
TUM School of Natural Sciences

Multifunctional Flavins for Oxidation Catalysis

Alexandra Parvin Walter

Vollständiger Abdruck der von der TUM School of Natural Sciences der Technischen Universität München zur Erlangung einer Doktorin der Naturwissenschaften (Dr. rer. nat.) genehmigten Dissertation.

Vorsitz: Prof. Dr. Michael Groll

Prüfer der Dissertation:

1. TUM Junior Fellow Dr. Golo T. B. Storch
2. apl. Prof. Dr. Wolfgang Eisenreich
3. Prof. Dr. Oliver Trapp

Die Dissertation wurde am 03.11.2023 bei der Technischen Universität München eingereicht und durch die TUM School of Natural Sciences am 11.12.2023 angenommen.

This thesis was prepared at the Lehrstuhl für Organische Chemie I at the Technische Universität München under the supervision of Dr. Golo Storch between November 2019 and December 2023.

Publication List:

- A. Walter, G. Storch, *Angew. Chem. Int. Ed.* **2020**, *59*, 22505−22509. “Synthetic C6-Functionalized Aminoflavin Catalysts Enable Aerobic Bromination of Oxidation-Prone Substrates”
- A. Rehpenn[‡], A. Walter[‡], G. Storch, *Synthesis* **2021**, *53*, 2583−2593. “Molecular Editing of Flavins for Catalysis”
- R. Foja, A. Walter, C. Jandl, E. Thyrhaug, J. Hauer, G. Storch, *J. Am. Chem. Soc.* **2022**, *144*, 11, 4721−4726. “Reduced Molecular Flavins as Single-Electron Reductants after Photoexcitation”
- A. Rehpenn, A. Walter, G. Storch, *Chem. Sci.* **2022**, *13*, 14151−14156. „Molecular Flavin Catalysts for C-H Functionalisation and Derivatisation of Dehydroamino Acids”
- A. Walter, W. Eisenreich, G. Storch, *Angew. Chem. Int. Ed.* **2023**, *62,* e202310634. „Photochemical Desaturation and Epoxidation with Oxygen by Sequential Flavin Catalysis”

Conference Contributions:

- 22nd Lecture Conference ORCHEM **2022**, Münster, Deutschland. “Design and Reactivity of Molecular Flavin Catalysts” (Poster presentation)
- Hochschule Trifft Industrie **2022**, Biberach, Deutschland. „Synthetic Flavin Catalysts for Oxidation Catalysis” (Conference Talk)
- 5th International Symposium on Synthesis and Catalysis **2023**, Évora, Portugal. “Sequential Reactivity of Molecular Flavin Catalysts” (Poster presentation)

In this thesis, the relative configuration of racemates is represented by straight lines (bold or hashed). The absolute configuration of enantiomerically pure or enriched compounds is represented by wedge-shaped lines (bold or hashed)

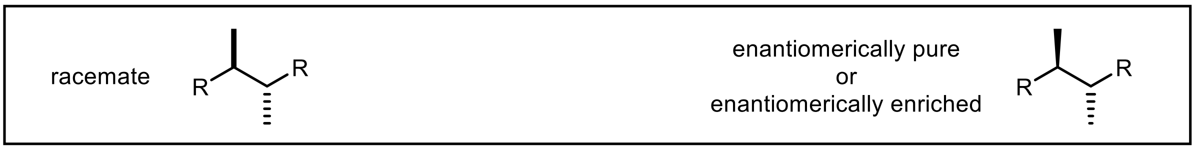

Acknowledgements

Allen voran möchte ich mich herzlich bei meinem Doktorvater *Dr. Golo Storch* für die Aufnahme in seinen Arbeitskreis und die exzellente Betreuung während meiner Promotion bedanken. Danke für dein Vertrauen in den letzten Jahren, deine motivierenden Worte und den fachlichen Rat, wenn die Flavine mal wieder nicht das getan haben, was sie tun sollten und die Freiheiten, die ich im Rahmen meiner Forschungsarbeiten erhalten habe. Ebenso möchte ich mich für dein offenes Ohr für alle Probleme und dein Verständnis in schwierigen Zeiten bedanken.

Bei *apl. Prof. Dr. Eisenreich*, *Prof. Dr. Oliver Trapp* und *Prof. Dr. Michael Groll* möchte ich mich herzlich für die Übernahme des Koreferats und des Prüfungsvorsitzes bedanken.

Ein besonderer Dank gilt *Kerstin Voigt* für die kompetente und schnelle Hilfe bei allen bürokratischen Fragen, sowie die netten Gespräche.

Bei *Dr. Stefan Breitenlechner* möchte ich mich für die Hilfe im Labor- und Praktikumsalltag bedanken. Deine stets freundliche und aufgeschlossene Art bereichert den Lehrstuhl! Ebenso möchte ich *Olaf Ackermann* für die gewissenhaften Messungen der HPLC-Proben sowie die Versorgung im Labor bedanken.

Prof. Dr. Wolfgang Eisenreich danke ich zusätzlich für die Unterstützung bei der Planung und Durchführung von NMR-Studien.

Für das Korrekturlesen dieser Arbeit und die konstruktiven Anmerkungen möchte ich mich bei *Tim Langschwager, Andreas Rehpenn, Richard Foja, Sascha Niedersteiner* und *Darren Wragg* bedanken.

Bei allen aktuellen und ehemaligen Mitgliedern des AK Storch: *Andreas Rehpenn*, *Golo Storch*, *Johannes Lamhauge*, *Lennart Brücher*, *Maxi Gretz*, *Maxi Schick*, *Max Schmid*, *Noah Richter*, *Quirin Fichtner*, *Richard Foja*, *Tim Langschwager*, *Ümit Beser* und *Zhengyang Dong* möchte ich mich für die schöne Zeit im Arbeitskreis bedanken. Gemeinsame Mittags-, Kaffee- und Teepausen sowie die AK-Ausflüge mit euch haben die Zeit im Arbeitskreis unvergesslich gemacht!

Für die großartige Zeit im Labor danke ich vor allem meinen aktuellen und ehemaligen Laborkollegen aus Box 1: *Andi* für die coole Zeit, auch als AK Storch nur aus uns beiden bestand und die angenehme Gesellschaft während der Mittagspausen, „Tim des Monats“ *Tim* für seine Marcel Reich-Ranicki und King Julien Imitationen, die mich immer zum Lachen gebracht haben, *Richard* für seine äußerst aufschlussreichen Einblicke in zeitgenössische

Kultur und Sprache und *Lilla Koser*, für die schöne Zeit während der Masterarbeit und der Promotion. Danke für die Gespräche, den Blödsinn, die aufmunternden Worte, die Hilfe bei Problemen aller Art und die Akzeptanz meiner Musikauswahl. Ihr seid echt coole Socken und ohne euch wären die letzten vier Jahre ziemlich langweilig gewesen!

Ebenso danke ich meinen ehemaligen Praktikumsbetreuern *Dominik Lenhart* und *Michi Grübel* für das Wissen, das sie mit mir geteilt und all die praktischen Tricks, die sie mir beigebracht haben. Dem gesamten Lehrstuhl für Organische Chemie 1 möchte ich für die herzliche Aufnahme und für die freundliche und schöne Atmosphäre im Labor danken.

Bei meinen Forschungspraktikanten *Christian Seitz, Andrei Bubeneck*, *Tim Langschwager, Christoph Buchelt*, *Franzi Elsen*, *Ümit Beser*, *Hannah Kallweit*, *Maxi Schick*, *Matthias Holzer*, *Lennart Brücher* und *Guo Zichen* sowie meinen Bachelorandinnen *Naz Karadeniz* und *Alesia Kokoneshi* bedanke ich mich herzlich für ihren Einsatz und ihre Hilfe im Labor.

Bei *Michael Kreitmeir*, *Johanna Wallner*, *Paul Pabst*, *Yasmin Selic*, *Simon Bodesheim* und *Sebastian Stigler* möchte ich mich für die schöne Zeit während des Studiums bedanken. Die WG-Zeit, gemeinsame Konzert- und Festivalbesuche sowie zahlreiche Koch-, Spiele- und Filmabende haben die letzten zehn Jahre in München unvergesslich gemacht.

Außerhalb des Laboralltags möchte ich mich bei meiner Mutter *Maria*, Schwester *Tina* und meinem Vater *Gholam* für ihre Unterstützung auf meinem bisherigen Weg bedanken. Ein besonderer Dank gilt auch meiner besten Freundin *Lisa* für die letzten 25 Jahre unzerbrechliche Freundschaft (Auf die nächsten 25!).

Last but not least möchte ich mich bei meinem Partner *Sascha* für sein grenzenloses Verständnis und seine Unterstützung bedanken. Danke, dass du immer die richtigen Worte findest, um mich zu motivieren und aufzubauen.

Abstract

In nature, flavoenzymes mediate various chemical transformations including *inter alia* reductions, oxidations, and oxygenations. This versatile reactivity can be explained by the flavin’s ability to switch between distinct catalytically active states under thermal or photochemical conditions. However, the limited stability and missing non-covalent substrate-binding and stabilisation of reactive intermediates in the active site restrict the application of molecular flavins in synthetic chemistry due to catalyst decomposition and decreased reactivity. This work focuses on overcoming these limitations and aims for achieving catalytic oxidations with molecular flavins in the organic laboratory. Here, the first biomimetic halogenation strategy using a molecular flavin catalyst and inorganic LiBr as halide source in organic media without the need of additional catalysts or mediators is presented. The designed molecular flavin catalysts contain two stacked *C*6-amino functionalised isoalloxazines. This structure increases the flavin’s stability and influences their reactivity, which allows for selective bromination of oxidation-prone phenolic substrates while decomposition of both the flavin and the substrate is significantly reduced compared to parent riboflavin tetraacetate (RFTA). Additionally, a flavin catalysed sequential *Saegusa-Ito* oxidation epoxidation sequence for the direct conversion of silyl enol ethers to *α*,*β*-epoxyketones is disclosed. The reaction relies on the sequential combination of two orthogonal reactivities of the flavin, namely the photooxidation of silyl enol ethers, followed by the reductive activation of O_2. Again, the instability of RFTA under the reaction conditions prompted us to switch to an improved molecular flavin catalyst. Sequential transformation of silyl enol ethers by flavin catalysis is not limited to the *Saegusa-Ito* oxidation epoxidation sequence, which is highlighted by further transformations including *inter alia* a *Saegusa-Ito* oxidation trifluoromethylation sequence. These results demonstrate how adjusting the flavins reactivity and stability by chemical modifications enable synthetically useful transformations. The presented studies serve as a starting point for further site-selective and sequential transformations.

Kurzzusammenfassung

In der Natur katalysieren Flavoenzyme unterschiedliche chemische Reaktionen, beispielsweise Reduktionen, Oxidationen und Oxygenierungen. Diese vielseitige Reaktivität lässt sich durch die Fähigkeit der Flavine erklären, unter thermischen oder photochemischen Bedingungen, zwischen verschiedenen, katalytisch aktiven Zuständen zu wechseln. Die begrenzte Stabilität und die Abwesenheit nicht-kovalenter Substratbindung sowie Stabilisierung reaktiver Intermediate im aktiven Zentrum schränken den Einsatz molekularer Flavine in der organischen Synthese jedoch ein, da diese Katalysatorzersetzung sowie eine verringerte Reaktivität zur Folge haben. Das Ziel dieser Arbeit ist es, diese Limitierungen zu überwunden und molekulare Flavine als Oxidationskatalysatoren in der organischen Synthese einzusetzen. Es wird die erste flavinkatalysierte, biomimetische Halogenierungsstrategie vorgestellt, die anorganisches LiBr als Halogenidquelle in organischem Lösungsmittel verwendet und keine zusätzlichen Katalysatoren oder Mediatoren benötigt. Die konzipierten, molekularen Flavine beinhalten zwei gestapelte, *C*6-aminofunktionalisierte Isoalloxazineinheiten, wodurch die Stabilität der Flavine erhöht und ihre Reaktivität gesteuert wird. Mithilfe dieser Flavine wird die Bromierung von oxidationsempfindlichen, phenolischen Substraten ermöglicht, während im Vergleich zu Riboflavin-Tetraacetat (RFTA) die Zersetzung des Flavins sowie der Substrate erheblich unterdrückt wird. Darüber hinaus stellt diese Arbeit eine *Saegusa-Ito* Oxidations-Epoxidierungssequenz zur direkten Umsetzung von Silylenolethern zu α,β-Epoxyketonen vor. Die Transformation beruht auf der sequenziellen Verknüpfung zweier orthogonaler Reaktivitäten des Flavins, der Photooxidation von Silylenolethern gefolgt von der reduktiven Aktivierung von O_2. Die Instabilität von RFTA unter den Reaktionsbedingungen führte auch hier zur Entwicklung und Anwendung eines molekularen Flavins mit verbesserter Stabilität. Diese flavinkatalysierte, sequenzielle Umwandlung von Silylenolethern ist nicht auf eine Oxidations-Epoxidierungssequenz beschränkt, was durch weitere Reaktionsfolgen, u.a. einer *Saegusa-Ito* Oxidations-Trifluormethylierungssequenz verdeutlicht wird. Die Ergebnisse dieser Arbeit zeigen, dass die erhöhte Stabilität sowie angepasste Reaktivität, die durch die chemische Modifikation der Flavine erreicht wurden, synthetisch wertvolle Umsetzungen ermöglichen. Die im Zuge dieser Arbeit durchgeführten Studien dienen als Ausgangspunkt für weitere selektive und sequenzielle Reaktionen.

Table of Contents

1. Introduction 1

2. Activation of Molecular Oxygen in Flavoenzymes 3

   2.1. Flavin-Dependent Monooxygenases 3

      2.1.1. Flavin-Dependent Halogenases 6

   2.2. Flavin-Dependent Oxidases 7

   2.3. Flavin-Dependent Dehydrogenases 8

3. Activation of Oxygen by Molecular Flavins 9

   3.1. Use of Flavins as mild H_2O_2 Source 9

   3.2. Stabilisation of Flavin-Hydroperoxides *via* Synthetic Modification 12

      3.2.1. *N*5-Alkylation 12

      3.2.2. *N*1-Functionalisation 16

      3.2.3. *N*10-and *N*3-Functionalisation 19

4. Photochemistry of Flavins 22

   4.1. Flavin-Mediated Photocatalytic Oxygenations 22

   4.2. Flavins as Photooxidants 24

5. Aim and Motivation 28

6. Synthetic C6-Functionalized Aminoflavin Catalysts Enable Aerobic Bromination of Oxidation-Prone Substrates 30

7. Photochemical Desaturation and Epoxidation with Oxygen by Sequential Flavin Catalysis 36

8. Summary 43

9. Licenses 48

10. List of Abbreviations 49

11. References 51

1. Introduction

Flavoenzymes are one of the most versatile enzyme classes which rely on non-metal cofactors flavin adenine dinucleotide (FAD) and flavin mononucleotide (FMN). Biosynthetically, both cofactors are derived from riboflavin, commonly known as vitamin B2 (Figure 1A).[1] Riboflavin was first described in 1879 as a bright orange compound isolated from cow's milk and therefore named *lactochrome*.[2] Different terms such as *ovoflavin*[3] and *hepatoflavin*[4] were used as well, relating to the source the compound was isolated from. Within the first half of the 20th century, its role as a constituent of the vitamin B complex was discovered[5] and the structure of riboflavin was determined and proven by chemical synthesis in the groups of Paul Karrer[6] and Richard Kuhn[7], both of which obtained the Nobel Prize for their research on vitamins. With increasing interest, the name riboflavin, derived from its ribityl side chain and its yellow colour (Latin: *flavus* - yellow), replaced the various terms previously used. Shortly after the identification of riboflavin, FMN was identified as the first cofactor in flavoenzymes[5] and its structure was confirmed in 1936 by chemical synthesis starting from synthetic riboflavin.[8] FAD was first mentioned in 1938 as the coenzyme in D-amino acid oxidase from liver, kidney and yeast.[9] Its previously postulated structure was confirmed in 1954 *via* synthesis from FMN.[10] These discoveries represent milestones in flavin research and since then a multitude of flavoenzymes, which mediate a variety of biochemical transformations have been discovered.[11]

Despite the versatile reactivity of flavoenzymes, both cofactors FMN and FAD share the same catalytically active moiety, the heterocyclic isoalloxazine core (Figure 1A). It can be excited by visible light and undergoes one- and two-electron transfer processes, which allows the flavin cofactor to switch between three distinct redox states: the oxidized (quinoid), the one-electron reduced (semiquinoid) and the two-electron reduced (hydroquinoid) state (Figure 1B).[12] Due to the presence of both acidic and basic centres at *N*1 and *N*5 (Figure 1B), all redox forms exist in pH-dependent acid-base equilibria.[13] These active states in combination with the enzymatic scaffold are responsible for the versatile reactivity of flavoenzymes in biochemical transformations.[14]

The largest class of flavoenzymes are the oxidoreductases,[11b] including flavin-dependent oxidases, monooxygenases/hydroxylases and dehydrogenases/reductases.[15] They catalyse an electron transfer from a suitable donor molecule to oxygen as an acceptor.[16] The bright yellow colour of flavins and their green fluorescence[17] is attributed to their absorption maximum in the range of blue light (λ = 450 nm[5]) and inspired chemists to use them in photocatalytic applications. One of the first examples mentioned in literature is the photocatalytic oxidation of indole acetic acid under aerobic conditions using synthetic riboflavin reported by *Galston* in 1949.[18]

Both ground state and photoexcited state of flavin cofactors catalyse chemical transformations *via* two separate half-reactions, namely an oxidative and a reductive half-reaction (Figure 1C). The oxidative half reaction involves the reduction of the cofactor by electron transfer from a substrate while the reductive half reaction describes the reduction of a substrate by the hydroquinoid flavin.[19] The majority of flavin cofactors are bound to the enzymatic scaffold *via* non-covalent interactions, most of which occur between the *N*10-ribityl carbohydrate chain of the cofactor and the peptide scaffold.[17] The enzyme controls the cofactors oxidation state, tunes its reactivity and aligns substrates, reactants or reactive intermediates.[1, 12] However, covalent linkage of the cofactor to an amino acid of the enzyme is observed in some flavoenzymes as well, which influences the redox potential of the flavin.[20] Covalent linkage is known to occur between either the *C*8α methyl group of FAD or FMN and a tyrosine, histidine, aspartic acid, or cysteine moiety of the peptide or the *C*6 carbon of the FMN isoalloxazine core and cysteine (Figure 1A, marked green).[21]

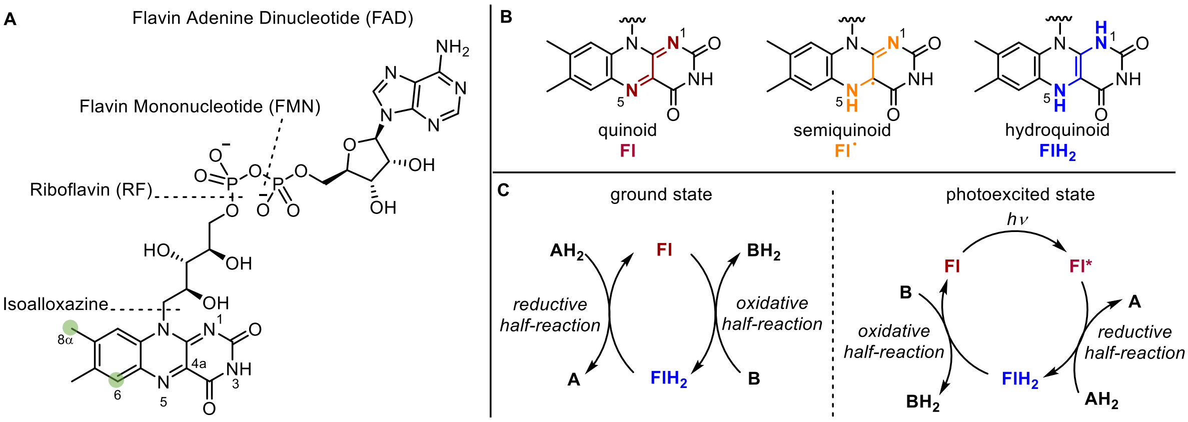
A
Flavin Adenine Dinucleotide (FAD)
Flavin Mononucleotide (FMN)
Riboflavin (RF)
Isoalloxazine
8α
6
5
4a
1
3
NH₂
OH
HO
B
quinoid
Fl
semiquinoid
Fl˙
hydroquinoid
FlH₂
C
ground state
photoexcited state
hν
AH₂
A
BH₂
B
Fl
FlH₂
Fl*
reductive half-reaction
oxidative half-reaction

Figure 1: A) Structure of flavin adenine dinucleotide; B) The three redox states of flavin cofactors; C) General mechanism for the reduction and oxidation of flavin cofactors.

2. Activation of Molecular Oxygen in Flavoenzymes

After reduction, hydroquinoid flavins are able to activate molecular oxygen *via* single-electron transfer (SET) and radical combination, yielding flavin-*C*4a-hydroperoxide intermediates (Figure 2).[12]

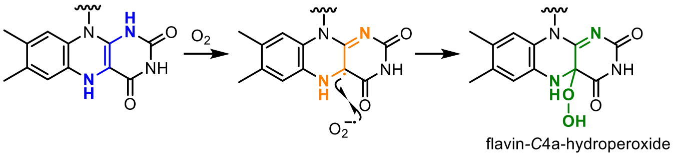

Figure 2: Reaction of hydroquinoid flavin with O_2 to flavin-*C*4a-hydroperoxide.

Flavoenzymes, which mediate oxygenation reactions *via* the formation of flavin-*C*4a-hydroperoxides are categorised as flavin-dependent monooxygenases while flavoenzymes that use O_2 as electron acceptor to regenerate the quinoid cofactor are categorised as flavin-dependent oxidases.[12, 16] Additionally, *bluB*, a flavin-dependent enzyme similar to oxidoreductase, is involved in the biosynthesis of the lower ligand 5,6-dimethylbenzimidazole (DMB) of vitamin B12. *BluB* demonstrates a unique O_2-activation-fragmentation sequence, where DMB is generated from a contraction of the isoalloxazine core of FMN along with D-erythrose-4-phosphate, originating from the ribityl chain. The exact fragmentation mechanism has not been elucidated so far. However, the proposed mechanisms involve initial formation of a FMN-*C*4a-hydroperoxide from reduced FMN and O_2.[22] Further flavoenzymes that activate molecular oxygen without the formation of *C*4a-hydroperoxide intermediates are flavin-dependent dehydrogenases, which react slowly or not at all with O_2.[12, 16] In the following, the use and activation of molecular oxygen by flavoenzymes will be discussed in more detail, highlighting crucial interactions between the cofactor and the enzymatic scaffold.

2.1. Flavin-Dependent Monooxygenases

Flavin-dependent monooxygenases react readily with molecular oxygen and can be further classified into three categories: i) one-component monooxygenases that use FAD as cofactor and have an additional binding site for NAD(P)H; ii) two-component monooxygenases where the reduction of the cofactor is carried out by a NAD(P)H-dependent reductase and the reduced cofactor is transported to the monooxygenase protein by diffusion; iii) internal monooxygenases where the cofactor is reduced by a suitable substrate which is subsequently oxygenated.[12]

Flavin-dependent monooxygenases rely on coenzyme NAD(P)H as hydride donor to generate the hydroquinoid cofactor **2** (Figure 3A). The reduced cofactor reacts with O_2 in a single-electron transfer (SET) step to generate the semiquinoid cofactor **3** and a superoxide radical ($O_2^{\bullet -}$), which form the flavin-*C*4a-hydroperoxide **4** by radical combination.[14] Its terminal oxygen atom can be transferred to a substrate molecule, *via* a neutral, electrophilic or deprotonated, nucleophilic *C*4a-peroxide species (Figure 3B),[12] forming the oxygenated product and flavin-*C*4a-hydroxy intermediate **5**. Regeneration of the quinoid cofactor **1** is achieved by elimination of one molecule of water. In the absence of a suitable substrate, elimination of H_2O_2 occurs.[12, 14] Oxygenation reactions catalysed by flavin-dependent monooxygenases include *inter alia* electrophilic halogenation of tryptophan[23] and *Baeyer-Villiger* oxidation[24] (Figure 3C).

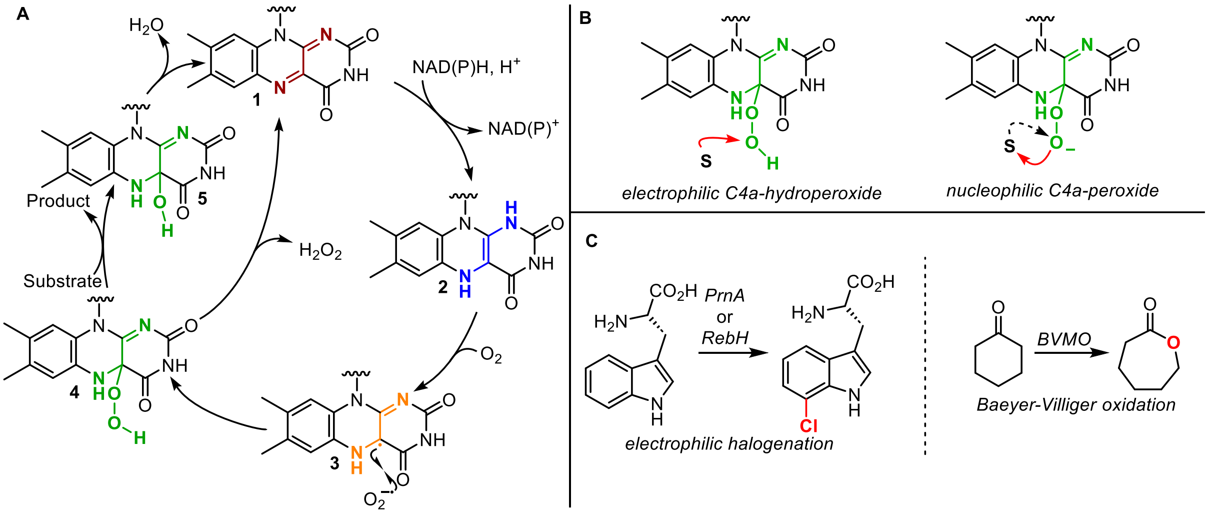
A
H_2O
1
NAD(P)H, H^+
NAD(P)$^+$
5
Product
Substrate
H_2O_2
2
O_2
4
3
O_2^-
B
electrophilic C4a-hydroperoxide
nucleophilic C4a-peroxide
S
C
PrnA
or
RebH
electrophilic halogenation
BVMO
Baeyer-Villiger oxidation

Figure 3: A) General catalytic cycle for flavin-dependent monooxygenases; B) Electrophilic and nucleophilic flavin-*C*4a-hydroperoxides; C) Chemical transformations catalysed by flavin-dependent monooxygenases; NAD(P)H: Nicotinamide adenine dinucleotide (phosphate).

The half-lives of flavin-*C*4a-hydroperoxides of different monooxygenase enzymes in absence of a suitable substrate differ a lot, which is attributed to stabilising interactions between the hydroperoxide and the enzymatic scaffold.[25] In two-component flavin-dependent monooxygenase *p*-hydroxyphenylacetate 3-hydroxylase (*HPAH*), a conserved serine moiety (Ser171) within the active site was found to stabilise the reactive intermediate by hydrogen bonding interactions between the O^γ of the Ser171 and the flavin *N*5-H, impeding the deprotonation at this position and therefore slowing down the elimination of H_2O_2.[25] In the same study, a conserved histidine moiety His396 was found to be involved in the formation of the enzymes *C*4a-hydroperoxide intermediate, possibly by protonation of the peroxide.

In addition to flavin-*C*4a-hydroperoxides, recent studies by the group of *Teufel* propose that some flavin-dependent monooxygenases, such as *RutA*, which catalyses the oxidative cleavage of uracil to 3-ureidoacrylate (Figure 4A) operate *via* a flavin-*N*5-hydroperoxide intermediate **8**. The latter is formed *via* SET from reduced, deprotonated flavin cofactor **6** to O_2 and radical combination (Figure 4B). O_2-pressurized X-ray crystallography of *RutA* revealed an uncharged O_2-binding site close to the *N*5 with non-polar amino acids Leu65, Val136, Ala206, Met67 and polar amino acids Thr105 and Asn134 being present. Apolar amino acids interact with hydrophobic O_2 while polar amino acids stabilize short-lived hydrophilic $O2^{\bullet-}$ respectively. Replacing the polar amino acid residues with apolar residues by mutation leads to drastically reduced activity, demonstrating the need for a controlled environment for the O_2 activation. The amino acid residues help to position O_2 close to the *N*5-atom, almost perpendicular to the longitudinal axis of the isoalloxazine core, while the distance to the *C*4a-atom is larger and the angle is less favourable for the formation of a covalent adduct. Comparing the binding sites for O_2 in *RutA* and *HPAH*, an enzyme whose formation of flavin-*C*4a-hydroperoxides has been studied in detail, revealed that *RutA* features a narrower binding pocket aligned with *N*5, presumably restricting the freedom of motion of O_2. Computational calculations also suggest that within the active site, substrate binding and O_2 activation sites are spatially separated by FMN and located at the *si*- and *re*-side of the cofactor, respectively. While the formation of a *C*4a-hydroperoxide intermediate would displace the cofactor, which impedes substrate binding and orients the peroxide away from the binding site, the flavin-*N*5-peroxide is bound similarly to the quinoid cofactor at the active site and can undergo facile *N*5-inversion, locating the peroxide moiety close to the substrate. The proposed mechanism (Figure 4C, left) involves nucleophilic attack of the deprotonated *N*5-peroxide **9** on the uracil **10**, generating a covalent intermediate **11** followed by C-N bond cleavage as the rate-determining step. After O-O bond cleavage, ureidoacrylate **14** and a *N*5-oxygenated flavin cofactor **13** are released from the enzyme, the latter of which is reduced to the quinoid cofactor in the cell. In addition to the proposed mechanism, a hydroxide ion OH^-, cleaved from flavin-*N*5-peroxide could potentially mediate the reaction (Figure 4C, right). However, the better nucleophilic properties of flavin-*N*5-peroxide due to the α-effect compared to HO^- indicate that a covalent mechanism is more plausible.[26]

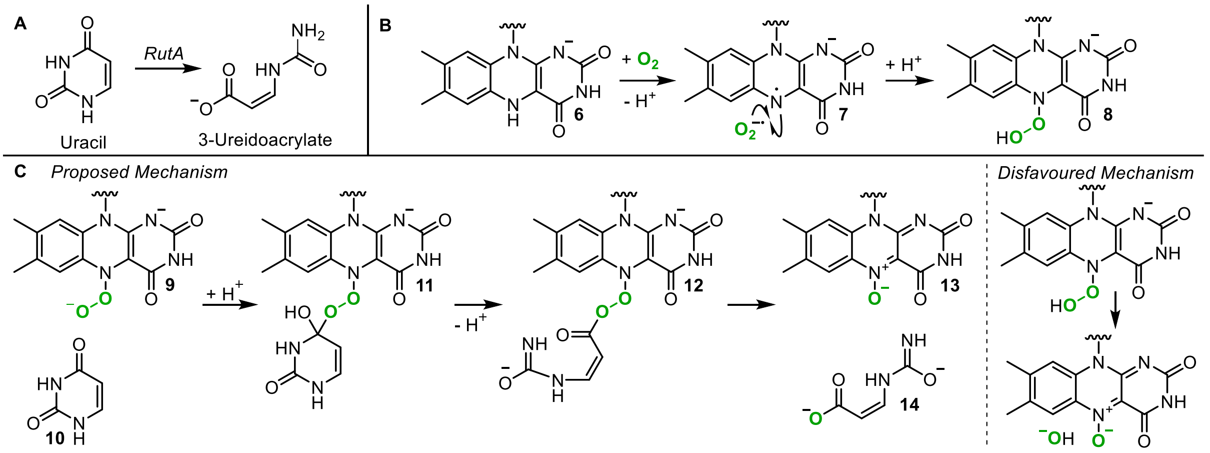

Figure 4: A) Oxidative cleavage of uracil to 3-ureidoacrylate catalysed by *RutA*; B) Proposed mechanism for the formation of flavin-*N*5-hydroperoxides; C) Proposed mechanism for the flavin-*N*5-peroxide catalysed cleavage of uracil.

Depending on the microenvironment of the enzyme's active site, formation of either *C*4a-hydroperoxides or *N*5-peroxides can be preferred. Comparing amino acid residues involved in the formation of the O_2 binding pocket of several group C flavin-dependent monooxygenases revealed a conserved *RutA*-like O_2 reactivity motif in many monooxygenases, suggesting that that the *N*5-peroxide as oxygen-transfer species might be more prevalent.[26] To this date, only a few enzymes that potentially utilize *N*5-peroxide intermediates as reactive intermediates have been reported. Therefore, only little is known about the reactivity of flavin-*N*5-peroxides, which are assumed to be primarily involved in carbon-heteroatom bond cleavage.[27]

2.1.1. Flavin-Dependent Halogenases

Flavin-dependent halogenases, belong to the class of monooxygenase enzymes. The first isolation and purification of a flavin-dependent halogenase was described in 2000 by the group of *van Pée*.[28] The enzyme *PrnA* catalyses chlorination of tryptophane to 7-chlorotryptophane. Since then, several halogenases that rely on FAD as cofactor and catalyse regioselective chlorination of tryptophane or pyrrole moieties to form important intermediates in the biosynthesis of natural products were identified.[29] Mechanistic investigations of tryptophan-7-halogenases *PrnA* and *RebH* revealed that an active site lysine (Lys79) is essential for the reaction.[30] The formation of flavin-*C*4a-hydroperoxide **17** with NADH as reductant under aerobic conditions occurs as discussed above (Figure 5A). In the presence of chloride ions, hypochloric acid is formed. The loss of activity in *PrnA* is observed when both residues, Lys79 and Glu346 are mutated to a different amino acid. The proposed mechanism for *PrnA* suggests a hydrogen bonding interaction between hypochloric acid and the free amine group of Lys79, as well as with the carboxylate of glutamic acid Glu346 (Figure 5B), which increases the electrophilicity of the chlorine atom and therefore facilitates the nucleophilic attack of tryptophane. Additionally, it is proposed that hydrogen bonding to Glu346 is vital for the precise positioning of the reactive intermediate as the reactivity is inhibited when it is exchanged for aspartic acid, which also features a carboxylate. [30a] For *RebH*, the proposed mechanism includes the activation of chlorine by the formation of an *N*-chloramine from Lys79 and hypochloric acid (Figure 5C).[30b]

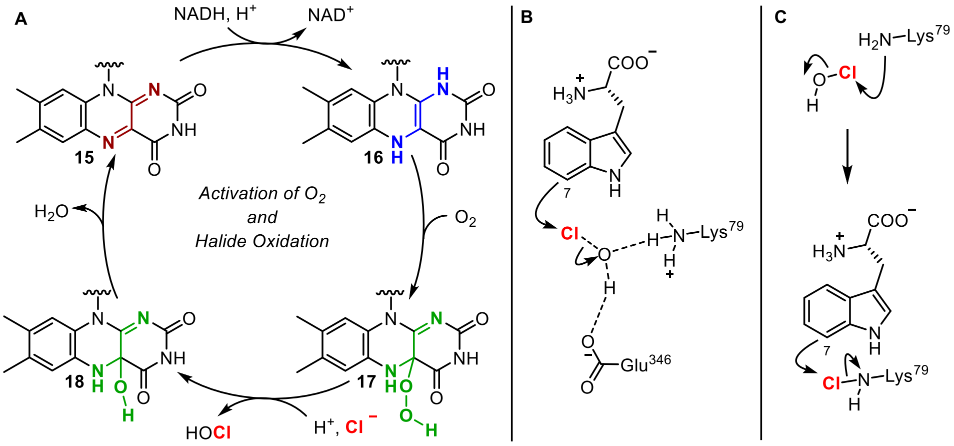

Figure 5: A) Proposed catalytic cycle for the O_2 activation and halide oxidation in flavin-dependent halogenases; B) Proposed activation of hypochloric acid *via* B) hydrogen bonding to Lys79 and Glu346 in *PrnA* and C) *via* formation of a chloramine species with Lys79 in *RebH*.

2.2. Flavin-Dependent Oxidases

In flavin-dependent oxidases the quinoid cofactor oxidizes a suitable substrate, leading to a reduced flavin and the oxidized product. O_2 is used as electron acceptor to regenerate the oxidized flavin cofactor. Hydrogen peroxide is formed *via* a one-electron transfer from the hydroquinoid cofactor **20** to O_2 and either subsequent combination of both radicals to the flavin-*C*4a-hydroperoxide **22** (Figure 6A, path A) or *via* a second electron transfer from the semiquinoid flavin **21** to the superoxide radical (Figure 6A, path B).[12, 31] Recent studies of pyranose-2-oxidase (*P2O*, Figure 6B, top) revealed that amino acid residues His548, Asn593 and Thr169 within the active site influence the formation and stabilisation of flavin-*C*4a-hydroperoxides. A protonated His548, located near the isoalloxazine, is suggested to facilitate the formation of flavin-*C*4a-hydroperoxides *via* a proton coupled electron transfer (PCET), where a proton from His548 is transferred to O_2 concomitant with the first single-electron transfer from deprotonated, hydroquinoid flavin (Figure 6B, bottom). His548 and Asn593 assist in the orientation of the resulting $HOO^{\bullet}$ radical for the formation of the *C*4a-hydroperoxide, which is stabilized by hydrogen bonding interactions to His548, Asn593 and Thr169.[32]

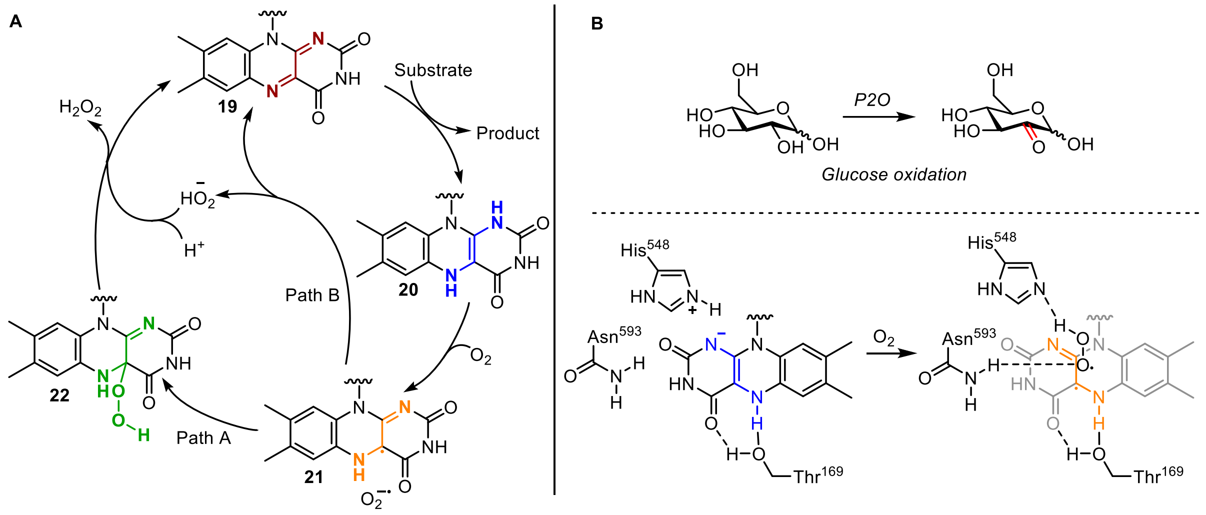

Figure 6: A) Proposed catalytic cycle for the O_2 activation in flavin-dependent oxidases; B) Top: Oxidation of Glucose mediated by flavin-dependent oxidase *P2O*; bottom: Hydrogen bonding interactions involved in the formation and stabilisation of flavin-*C*4a-hydroperoxide.

P2O is the first flavin-dependent oxidase known to form *C*4a-hydroperoxide intermediates. It has been suggested that a cavity at the enzymes active site, which is also observed in monooxygenases, might accommodate, and shield the hydroperoxide moiety in contrast to other flavin-dependent oxidases, where limited space or the lack of a controlled environment could inhibit the formation of flavin-*C*4a-hydroperoxides.[32-33]

2.3. Flavin-Dependent Dehydrogenases

Flavin-dependent dehydrogenases do not rely on molecular oxygen to regenerate the quinoid flavin. They exhibit no or only slow reactivity with O_2, generating H_2O_2 and $O_2^{\bullet-}$.[12] Cytokinin dehydrogenase (*CKX*) catalyses the oxidative cleavage of isopentenyladenine **23** to adenine **25** and 3-methyl-2-butenal **26** (Figure 7). Electron transfer from the hydroquinoid flavin to O_2 was found to be too slow for the latter to be the natural electron acceptor. However, several quinoids and 2,6-dichlorophenol indophenol (DCPIP) show high reactivity, suggesting that the innate electron acceptor is a similar compound.[34]

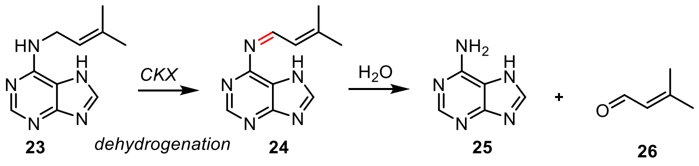

Figure 7: Dehydrogenation of isopentenyladenine mediated by flavin-dependent dehydrogenase *CKX*.

3. Activation of Oxygen by Molecular Flavins

The isolated flavin cofactor shows reduced activity[35] and stability[36] in chemical transformations compared to the whole flavoenzyme, presumably due to the lack of stabilising interactions between the cofactor and the enzymatic scaffold.[19] In the case of oxygenase activity, the lifetime of flavin-*C*4a-hydroperoxides generated by an isolated cofactor compared enzyme bound flavin is strongly decreased, resulting in rapid elimination of H_2O_2.[5, 37] Thus, two possibilities for the application of synthetic flavins in organic synthesis emerge: i) utilisation of unmodified flavins as mild H_2O_2 sources or ii) modification of the isoalloxazine core to increase reactivity and stability of the intermediate *C*4a-hydroperoxide.

3.1. Use of Flavins as mild H_2O_2 Source

Non-enzyme bound flavins rapidly release H_2O_2, which can be utilised in further chemical transformations. One example is the *Fleming-Tamao* oxidation of alkoxysilanes to the respective alcohols. A NADH analogue, *N*-Benzyl-1,4-dihydronicotinamide (BzlNAH), is used as a thermal reductant for riboflavin tetraacetate (RFTA, Figure 8A) in the dark under aerobic conditions.[38] The generated H_2O_2 is used to oxidize silanes (Figure 8B) in presence of a fluoride source, which is proposed to stabilise reactive intermediates and transition states.[38-39]

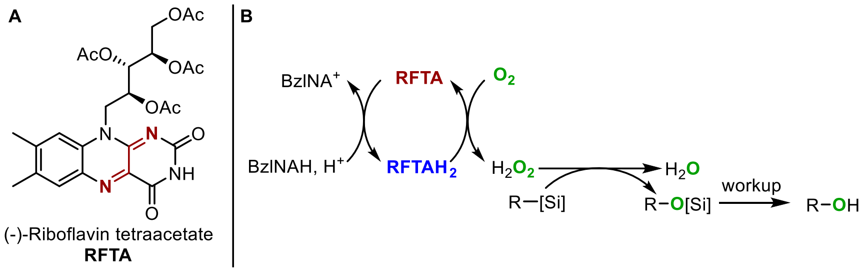

Figure 8: A) Chemical structure of RFTA; B) Proposed reaction cycle for the flavin catalysed *Fleming-Tamao* oxidation.

A detailed study concerning the aerobic reduction of olefins catalysed by cationic and neutral flavins was published in 2011. While cationic flavins show higher activity, neutral flavin **27** (Figure 9A) is more stable and quantitative yields are achieved by increasing the reaction time. Upon reduction with hydrazine (NH_2NH_2) under aerobic conditions, flavin **27** is proposed to release H_2O_2, bound in a 1:1 flavin-H_2O_2 complex **30**, along with one molecule of diimide (Figure 9B). H_2O_2 oxidizes a second molecule of NH_2NH_2 to diimide *via* *N*-oxygenation and dehydration. Reduction of the olefin along with N_2 formation proceeds from a 1:1 flavin-diimide complex **31**. Two molecules of diimide are produced in one catalytic cycle by combination of an anaerobic and an aerobic oxidation step. Acceleration of the reaction is observed with increasing amount of NH_2NH_2, suggesting that the rate determining step is the oxidation of NH_2NH_2 by the flavin catalyst. With this system, reduction of nine olefins is possible in high yields without the formation of side products such as sulfoxides in sulfur containing olefins (Figure 9C).[40]

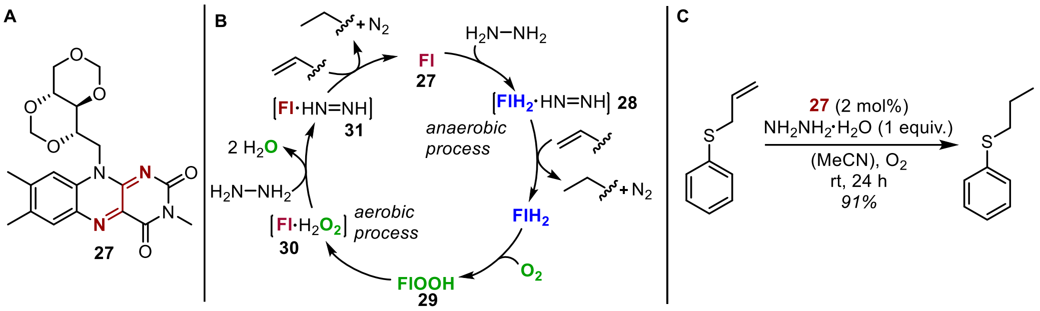
A
27
B
+ N2
H2N−NH2
Fl
27
[FlH2·HN=NH] 28
[Fl·HN=NH]
31
anaerobic
process
2 H2O
H2N−NH2
+ N2
aerobic
process
[Fl·H2O2]
30
FlH2
O2
FlOOH
29
C
S
27 (2 mol%)
NH2NH2·H2O (1 equiv.)
(MeCN), O2
rt, 24 h
91%
S

Figure 9: A) Chemical structure of flavin catalyst **27**; B) Proposed catalytic cycle for the flavin-catalysed reduction of olefins; C) Chemoselective hydrogenation of sulfur-containing olefins.

In 2016 the group of *König* reported the biomimetic chlorination of electron rich, aromatic compounds using photoexcited riboflavin tetraacetate and acetic acid as a H_2O_2 shuttle. *para*-Methoxybenzyl alcohol is used as a reductant for photoexcited RFTA, generating H_2O_2 under aerobic conditions upon irradiation with blue light (Figure 10, left). Acetic acid is essential for the chlorination as it forms peracetic acid, which acts as a mediator by generating an electrophilic chlorination species upon reaction with Cl^-. This mimics an enzymatic environment of halogenases, where the peptide scaffold is proposed to bring reactant and substrate in proximity to each other as well as stabilise reactive intermediates. HCl is necessary as a chloride source, as its strong acidity shifts the equilibrium between H_2O_2 and peracetic acid towards the peracid. With this system, chlorination of electron rich arenes and acetophenones is feasible in good yields (Figure 10, right).[41]

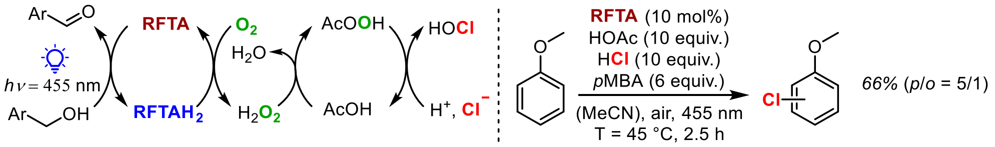
Ar O
hν = 455 nm
Ar OH
RFTA
RFTAH2
O2
H2O
H2O2
AcOOH
AcOH
HOCl
H+, Cl−
O
RFTA (10 mol%)
HOAc (10 equiv.)
HCl (10 equiv.)
pMBA (6 equiv.)
(MeCN), air, 455 nm
T = 45 °C, 2.5 h
O
Cl
66% (p/o = 5/1)

Figure 10: Proposed reaction cycle for the peracetic acid mediated formation of HOCl mediated by flavin-photocatalysis (left) and example for the application of flavin-catalysed biomimetic chlorination (right).

In 2018 *Seel et al*. reported the photobiocatalytic halogenation of aromatic compounds using photoexcited FMN for H_2O_2 generation along with vanadium-dependent haloperoxidases (VHPOs) and a halide salt. As VHPOs are sensitive towards H_2O_2, a constant but low concentration is crucial for the reaction, which is achieved by a low FMN loading and can be further controlled by adjusting the intensity of the light source. To circumvent the necessity of an additional reductant for the flavin cofactor, buffer solutions, necessary in enzymatic reactions for adjusting and maintaining pH-values, were tested for their ability to reduce FMN. Those containing tertiary amines, such as MES-buffer were found to be suitable electron donors, leading to H_2O_2 production upon irradiation with blue light (Figure 11, left). With *Am*VHPO from cyanobacterium *Acaryochloris marina* as the halogenating enzyme and KBr as halide source, bromination of aromatic compounds is observed in moderate to good yields and changing the enzyme to *Ci*VHPO from *Curvularia inaequalis* as well as the halide salt to KCl facilitates aromatic chlorinations (Figure 11, right).[42]

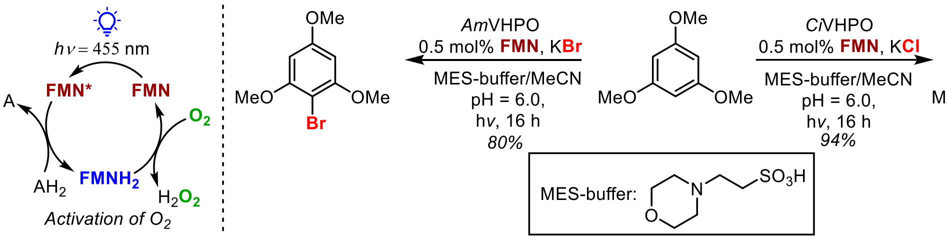

Figure 11: Photocatalytic generation of H_2O_2 (left) and Application of FMN in the photobiocatalytic bromination (right).

In a recent example by the group of *Iida*, RFTA was employed in an aerobic cross-dehydrogenative coupling of toluenes and *ortho*-phenylenediamines to form benzimidazoles.[43] Electron rich toluenes are transformed into the respective aldehydes by benzylic oxidation in presence of O_2. Mechanistic proposals[44] include a first SET from toluene to the excited RFTA***** followed by deprotonation, generating semiquinoid RFTAH$^\bullet$ and a benzylic radical, which is further oxidized to the respective arylaldehyde in presence of O_2. Semiquinoid RFTAH$^\bullet$ is proposed to undergo disproportionation to $RFTAH_2$ and RFTA. Condensation of arylaldehyde with the phenylenediamine yields benzimidazoline, which is oxidized by RFTA to benzimidazole (Figure 12). Alternative pathways for the last step involve oxidation by O_2 or H_2O_2.[43] The reaction is limited by the excited state redox potential of RFTA (E^0(**RFTA/RFTA$^{\bullet-}$**) = −0.81 V *vs* SCE)[45], which is only strong enough to oxidize activated benzylic substrates, such as electron rich methoxytoluenes.[44a]

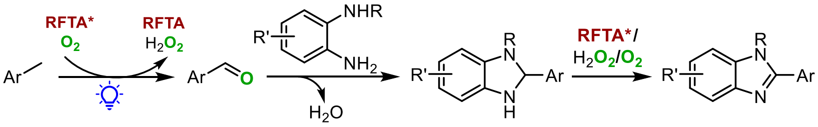

Figure 12: Proposed reaction scheme for the **RFTA**-catalysed aerobic cross dehydrogenative coupling of toluenes and *o*-phenylenediamines.

The same group reported the use of RFTA in a flavin-iodine dual catalytic system for the dehydrogenative coupling of chalcones **32** and amidines **33** to tetrasubstituted imidazoles **35** (Figure 13). RFTA as well as H_2O_2 can regenerate I_2 by oxidation of iodide. Iodine mediates the coupling reaction by activating **32** *via* halogen-bonding. α-Iodination of the product from *Michael* addition of **33** to **32** leads to intramolecular cyclization to a 4,5-dihydroimidazole intermediate **34**, which is dehydrogenated to imidazole **35** by RFTA as well as H_2O_2, I_2 or O_2.[46]

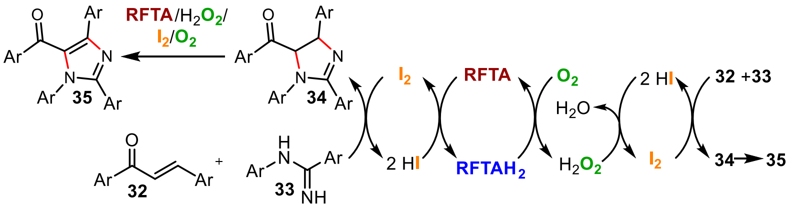

Figure 13: Proposed mechanism for the dehydrogenative coupling mediated by an RFTA-iodine dual catalytic system.

3.2. Stabilisation of Flavin-Hydroperoxides *via* Synthetic Modification

The stability of enzyme-bound flavin-*C*4a-hydroperoxides in absence of a substrate depends on the enzyme as well as the applied conditions. In bacterial luciferase isolated from *Vibrio campbellii*, decomposition of the *C*4a-hydroperoxide occurs at a rate of 0.002 s^{-1} (T = 4 °C, pH = 8.0). The formation and collapse of enzymatic *C*4a-hydroperoxides can be monitored by UV-VIS spectroscopy,[47] while non-enzymatic, flavin-*C*4a-hydroperoxides could not be detected, presumably due to their fast decomposition.[37, 48] Different approaches including modifications at the *N*1, *N*3, *N*5 and *N*10 position for increasing stability of flavin-hydroperoxides have been reported in the past in order to increase their applicability in organic synthesis.[48a, 49]

3.2.1. *N*5-Alkylation

One of the first approaches to stabilise flavin-*C*4a-hydroperoxides was to introduce substituents at the *N*5-position. In 1977, *Bruice* compared the reactivity of reduced *N*5-alkylated flavins towards O_2 in protic solvents.[48b] Spectroscopic data revealed that *N*5-alkylated flavins, in presence of a large excess of O_2, give flavin-*C*4a-hydroperoxide as major product in methanol[48b] and they were found to be stable in aprotic solvents, such as dioxane.[50] Flavin-*C*4a-hydroperoxides derived from flavinium salts can be accessed by addition of H_2O_2 or by reduction of the flavin in presence of O_2.[50] *Murahashi* and coworkers used a flavinium salt and H_2O_2 in the oxidation of thioethers and secondary amines where flavin-*C*4a-hydroperoxides show a 10^4 times higher catalytic activity compared to H_2O_2 alone.[51]

Sulfide Oxidation

The first flavin mediated aerobic oxidation of sulfides and amines was reported by *Imada* and *Murahashi*, catalysed by cationic flavinium salt **36** with hydrazine hydrate as reductant. The overall mechanism (Figure 14A) involves the reduction of cationic flavin **36** *via* nucleophilic addition of hydrazine to **36**. After *β*-elimination, reduced flavin **38** and diimide are released. Diimide itself is a strong reductant and transforms another equivalent of **36** to **38**, which then reacts with O_2 *via* SET and radical combination to flavin-*C*4a-hydroperoxide **39**. *Hammett* analysis of differently substituted sulfides suggests that oxygenation occurs *via* nucleophilic attack of the substrate onto **39**, generating the oxygenated product and flavin-*C*4a-hydroxide **40**. Elimination of H_2O closes the catalytic cycle.[52] Acidic alcohols such as trifluoroethanol as solvent were essential as they feature a high solubility of O_2 and prevent quenching of **39** by NH_2NH_2 since hydrogen bonding interactions between the solvent and hydrazine[53] decrease its nucleophilicity.[52] The elimination of H_2O from **40** is determined to be the rate-limiting step and only occurs in presence of an acid, which is released during the catalytic cycle, and protonates **40**.[48a] Quantitative oxidation of sulfides and amines is achieved without overoxidation. Secondary and tertiary amines require higher temperatures and higher catalyst loadings, presumably due to the increased basicity of the substrates, leading to neutralisation of the acid necessary for the regeneration of **36** from **40** (Figure 14B).[52]

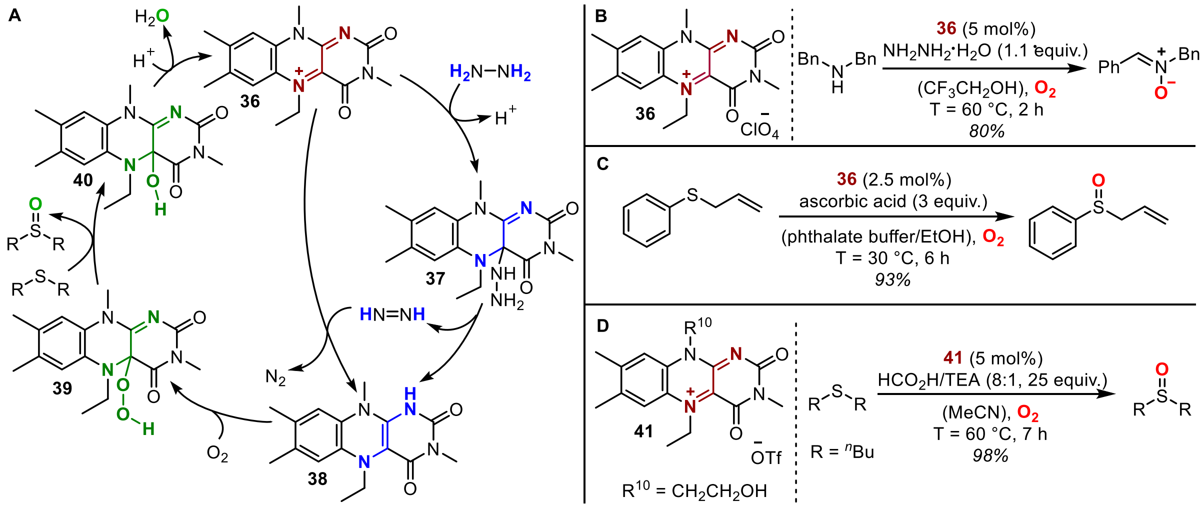
A
H2O
H+
36
H2N–NH2
H+
40
37
R–S(=O)–R
R–S–R
HN=NH
N2
39
O2
38
B
36
ClO4
Bn–NH–Bn
36 (5 mol%)
NH2NH2·H2O (1.1 equiv.)
(CF3CH2OH), O2
T = 60 °C, 2 h
80%
Ph, N+, Bn, O−
C
36 (2.5 mol%)
ascorbic acid (3 equiv.)
(phthalate buffer/EtOH), O2
T = 30 °C, 6 h
93%
D
R10
41
OTf
R10 = CH2CH2OH
R–S–R
R = nBu
41 (5 mol%)
HCO2H/TEA (8:1, 25 equiv.)
(MeCN), O2
T = 60 °C, 7 h
98%

Figure 14: A) Proposed catalytic cycle for the aerobic sulfoxidation mediated by **36**; B) Flavin catalysed aerobic oxidation of dibenzylamine with $N_2H_4•H_2O$ as sacrificial reductant; C) Flavin catalysed aerobic oxidation of sulfides with ascorbic acid as sacrificial reductant; D) Flavin catalysed aerobic oxidation of sulfides with HCO_2H/TEA as sacrificial reductant.

Following these results for the aerobic oxidation of sulfides and amines with hydrazine as a reductant, *Imada* reported the aerobic sulfoxidation in aqueous media using ascorbic acid as sacrificial reductant (Figure 14C). The mechanism proceeds as discussed above. The reaction is strongly pH-dependent which is explained by pH-dependent protonation states of ascorbic acid and a pH-dependent dehydration of **40** to **36**.[54] Besides ascorbic acid and hydrazine, a mixture of formic acid/triethylamine (TEA) as reductant for cationic flavin catalyst **41** was reported for the oxidation of sulfides (Figure 14D).[55]

Hydrogenation of Olefins

The group of *Imada* reported the use of flavinium salt **36** along with hydrazine for the generation of diimide, which is then used in the reduction of olefins. Here, **36** as well as its respective *C*4a-hydroperoxide **44** are used for the oxidation of hydrazine to diimide, which is then used for the reduction of olefins. The oxidation of hydrazine proceeds as described previously, yielding a 1:1 flavin-diimide complex **42** (Figure 15A). Hydrogenation of the olefin occurs faster than the liberation of N_2H_2, preventing its disproportionation to N_2 and hydrazine. **43** then reacts with O_2 to **44**, which oxidizes another equivalent of NH_2NH_2 to diimide. In aprotic solvents, the *α*-effect of NH_2NH_2 is responsible for its strong nucleophilicity, leading to rapid oxygenation by **44**. High yields are obtained and functional groups as amines and sulfides are tolerated in acetonitrile (Figure 15B). The selectivity of **36** can be switched by exchanging the solvent for acidic alcohols.[40, 56] Under otherwise identical conditions, a thioether containing olefin is converted to the respective hydrogenated sulfoxide as in trifluoroethanol, deactivation of NH_2NH_2 *via* hydrogen bonding interactions occurs, rendering it less nucleophilic.[53] Thus, oxygenation of the more nucleophilic sulfide by **44** is preferred. The rate of hydrogenation of olefins by cationic flavinium salts was found to be strongly dependent on the O_2 concentration[40], as the reaction rate increases with increasing O_2 content, while it shows only weak dependency on the NH_2NH_2 concentration. This suggests that the reaction between O_2 and hydroquinoid **43** to **44** is the rate determining step. In contrast to flavin **27**, which is used in a similar reaction, the reaction is proposed to proceed *via* a *C*4a-hydroperoxide and not *via* H_2O_2 released by the catalyst. Additionally, the rate determining step for the hydrogenation of olefins catalysed by **36** is the regeneration of the catalyst by elimination of H_2O from **46** to **36**, whereas for **27** the rate determining step is the oxidation of hydrazine to diimide.[40, 56]

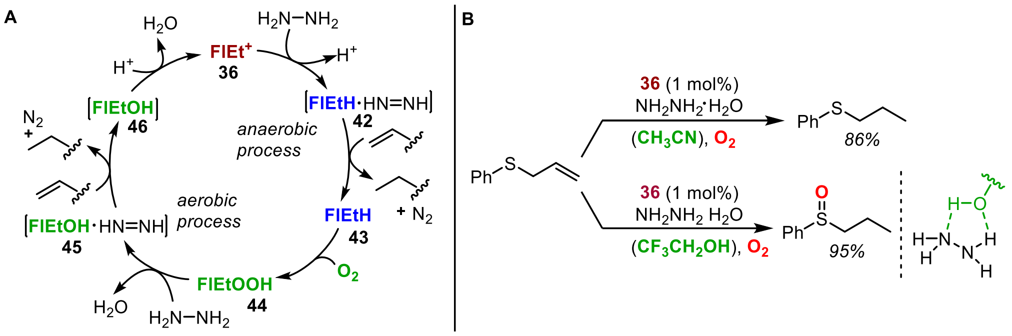
A
H_2O
H_2N-NH_2
FlEt+
36
H^+
H^+
[FlEtOH]
46
[FlEtH·HN=NH]
42
N_2 +
anaerobic process
aerobic process
FlEtH
43
+ N_2
[FlEtOH·HN=NH]
45
FlEtOOH
44
O_2
H_2O
H_2N-NH_2
B
Ph S
36 (1 mol%)
$NH_2NH_2·H_2O$
(CH_3CN), O_2
Ph S
86%
36 (1 mol%)
NH_2NH_2 H_2O
(CF_3CH_2OH), O_2
O
Ph S
95%
H–O
H–N
H N H
H

Figure 15: A) Proposed catalytic cycle for the reduction of olefins mediated by **36**; B) Chemoselectivity of flavin-catalysed reduction of olefins is influenced by the solvent.

Baeyer-Villiger Oxidation

An aerobic, chemoselective *Baeyer-Villiger* oxidation of cyclobutanones using riboflavin derived flavinium salt **47** (Figure 16A, left) was reported by *Imada*. The overall mechanism involves the reduction of **47** by zinc dust in the presence of molecular oxygen. Anionic, deprotonated flavin-*C*4a-peroxide is proposed as an intermediate, which facilitates a nucleophilic attack on the carbonyl moiety of the cyclobutanone **48**. Rearrangement of the *Criegee* intermediate (Figure 16B, right) then yields the respective lactone product **49**. A solvent mixture of MeCN and EtOAc with H_2O as proton source was necessary to obtain high yields (Figure 16B, left). No epoxidation and only traces of heteroatom oxidation is observed in presence of olefins or sulfides in contrast to the use of a combination of flavin **47** and H_2O_2 or *m*CPBA.[57]

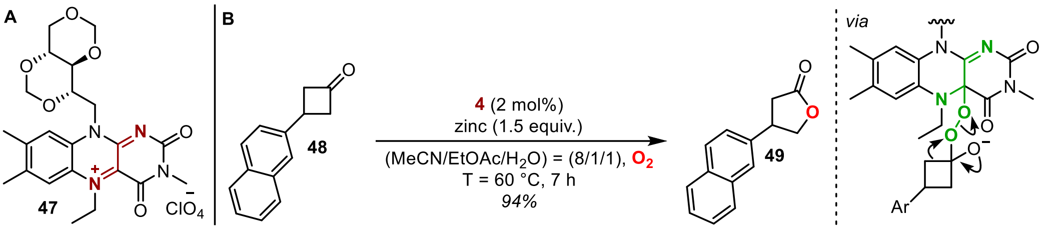
A
47
ClO_4^-
B
48
4 (2 mol%)
zinc (1.5 equiv.)
(MeCN/EtOAc/H_2O) = (8/1/1), O_2
T = 60 °C, 7 h
94%
49
via
Ar

Figure 16: A) Chemical structure of flavinium salt **47**; B) Example for the application of **47** in the aerobic *Baeyer-Villiger* oxidation of cyclobutanones (left) and proposed *Criegee* intermediate (right).

Flavin/Iodine Dual Catalytic System

*N*5-Alkylated flavinium salt **50** (Figure 17A) is used in coupled flavin-iodine catalytic systems for sulfenylation of imidazo[1,2-*a*]pyridines with thiols (Figure 17B, left). Flavin **50**, I_2 and O_2 are essential for the catalytic system. The overall mechanism involves the flavin mediated oxidation of iodide to I_2, yielding reduced **FlEtH**, which forms **FlEtOOH** in presence of O_2 (Figure 17B, right). **FlEtOOH** can again oxidise two equivalents of iodide to I_2 and after elimination of H_2O, **FlEt**$^+$ is regenerated. The reaction works with both thiols and the respective disulfides as reactants, however GC monitoring of the reaction progress revealed that sulfenylation takes place only after significant amounts of disulfide are formed, presumably *via* oxidation with **FlEt**$^+$. In the I_2 mediated catalysis a sulfenyl iodide is formed which mediates the sulfenylation reaction by nucleophilic attack of imidazo[1,2-*a*]pyridines onto the former. This reaction leads to product formation concomitant to the release of iodide.[58]

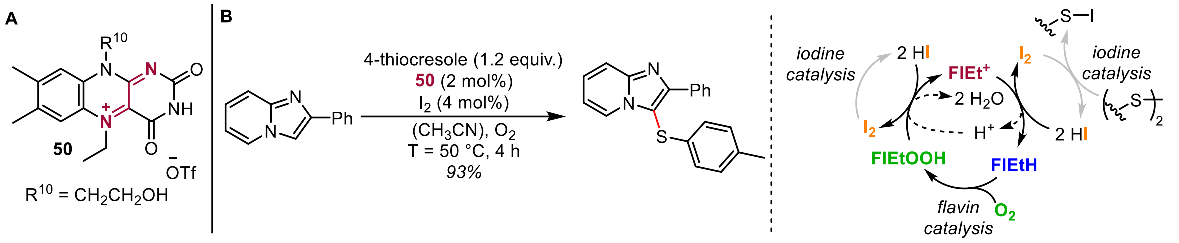

Figure 17: A) Chemical structure of flavinium salt **50**; B) Example for its application in a flavin-iodine mediated oxidative C−S bond formation (left) and proposed reaction cycle for the flavin-iodine dual catalytic system (right).

3.2.2. *N*1-Functionalisation

*N*5-alkylated flavinium salts that lack substitution at the *N*10-position but feature additional substitution at the *N*1-position are classified as alloxazinium salts. They differ from the *N*5-alkylated isoalloxazinium salts in their chemical behaviour, as they are less electrophilic, which can be determined by their flavinium salt-pseudobase equilibrium.[48a] In contrast to *N*5-alkylated alloxazinium and isoalloxazinium salts, *N*1,*N*10-ethylene bridged flavinium salts form adducts with nucleophiles *via* addition to the *C*10a carbon atom, instead of the *C*4a position or the *N*5-atom.[59]

Alloxazinium salts

The group of *Cibulka* reported a method for the hydroxylation of boronic acids using alloxazinium salt **51** (Figure 18A) under aerobic conditions. With this procedure, stoichiometric amounts of strong oxidants such as *m*CPBA can be replaced by catalytic amounts of **51**, O_2 and a sacrificial reductant. Flavin **51** is reduced by NH_2NH_2 in presence of O_2, resulting in the respective *C*4a-hydroperoxide. Various aryl- as well as alkylboronic acids are converted to the respective alcohols and functional groups prone to oxidation, such as pyridines **52** are tolerated (Figure 18B, left). For substrates that are not compatible with hydrazine (*e.g.*, arylaldehydes and styrenes) a protocol using ascorbic acid as reductant was developed. Reduction of the alloxazinium salt as well as hydroperoxide formation is suggested to occur in analogy to the isoalloxazinium salts. Adduct formation between the boronic acid and the hydroperoxide followed by transformation to the respective borate (Figure 18B, right) then leads to the release of the hydroxylated product **53**.[60]

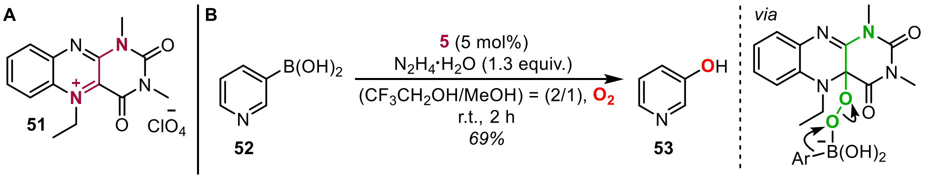
A
51
ClO_4^-
B
$B(OH)_2$
52
5 (5 mol%)
$N_2H_4 \cdot H_2O$ (1.3 equiv.)
($CF_3CH_2OH/MeOH$) = (2/1), O_2
r.t., 2 h
69%
OH
53
via
Ar
$B(OH)_2$

Figure 18: A) Chemical structure of alloxazinium salt **51**; B) Example for the application of **51** in the aerobic hydroxylation of arylboronic acids (left) and proposed borate intermediate (right).

The first aerobic *Dakin* oxidation of arylaldehydes with flavins was reported by the group of *Foss* in 2012. *N*5-alkylated alloxazine-hydroperoxide **54** (Figure 19A) is synthesized by reductive amination at *N*5 of the respective alloxazine and exposure to oxygen. For the catalytic reaction, *Hantzsch* ester is used as a reductant in presence of O_2 for regeneration of the hydroperoxide. $NaHCO_3$ is used as a mild base for the deprotonation of the flavin hydroperoxide in combination with 5% water in acetonitrile as solvent to ensure solubility of the base and hydrolysis of the aryl formate ester (Figure 19B). Electron withdrawing substituents on the flavin hydroperoxides increased the efficiency in *Dakin* oxidation, however, regeneration of the hydroperoxide by reaction of the hydroquinoid alloxazine with O_2 is slower. Therefore, unsubstituted flavin **54** turned out to be the most effective.[61]

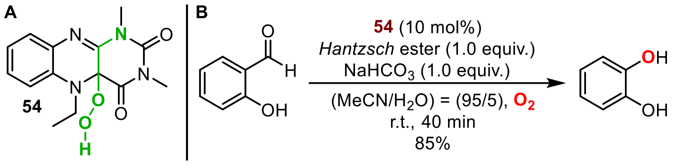

Figure 19: A) Chemical structure of alloxazine-*C*4a-hydroperoxide **54**; B) Example for the flavin-catalysed *Dakin*-oxidation.

Several examples of flavin-iodine coupled systems using alloxazinium salts have been reported by the group of *Iida*. The overall reaction mechanisms for the respective transformations are comparable to the one described for isoalloxazinium salts (see section 3.2.1). Using this method, aerobic, oxidative formation of C−C, C−N and C−S bonds gives access to various heterocyclic compounds.[62] The same group reported an electrochemical method for the aerobic oxidation of sulfides catalysed by an alloxazinium salt. Chemical reductants are replaced by low voltage, and under O_2, high chemoselectivities are observed.[63]

N1,N10-Ethylene Bridged Flavinium Salts

Flavinium salt **55** (Figure 20A) has been applied in the benzylic oxidation of unactivated benzylic substrates. Compared to neutral RFTA, the singlet excited state redox potential of **55** is significantly increased ($E^0(^1\mathbf{55}^*/\mathbf{55}^{\bullet-})$ = +2.67 V *vs*. SCE, $E^0(^1\mathbf{RFTA}^*/\mathbf{RFTA}^{\bullet-})$ = +1.67 V *vs* SCE), allowing for oxidation of substrates, that are otherwise inaccessible for the oxidation with flavins, such as *para*-trifluoromethyl toluene **56** and *para*-nitrobenzylic alcohol **58** (Figure 20B, left). In presence of O_2, oxidation of benzylic substrates yields the respective benzaldehydes by flavin mediated oxidation. Depending on the nature of the substrate, a photocatalytic as well as a thermal, organocatalytic pathway leads to the formation of the respective benzylic acid **57**.[44b] For *para*-nitrobenzylic aldehyde, transformation to the carboxylic acid is observed exclusively *via* the organocatalytic pathway, presumably by nucleophilic attack of flavin-*C*10a-hydroperoxide onto the aldehyde, as proposed by *Carbery* (Figure 20B, right).[44b, 64] For *para*-trifluoromethylbenzylic aldehyde, photocatalytic oxidation to the acid by excited flavin **55** in presence of O_2 was found to take place as well. Depending on the additives, chemoselective oxidation of *para*-nitrobenzylic alcohol **58** to either the aldehyde **59** or the carboxylic acid **60** can be achieved (Figure 20C). Strong acids, such as trifluoroacetic acid, prevent the formation of flavin-*C*10a-hydroperoxide, while weaker acids, such as formic acid, allow their formation to some extent, facilitating the organocatalytic oxidation pathway. The addition of molecular sieves to the reaction mixture also prevents the formation of flavin-hydroperoxides by decomposing H_2O_2 to H_2O.[44b]

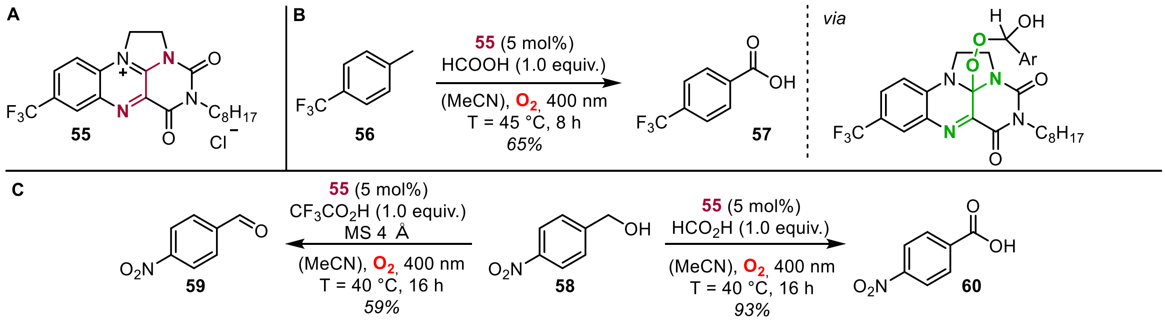

Figure 20: A) Chemical structure of *N*1,*N*10-bridged flavinium salt **55**; B) Flavin-catalysed benzylic oxidation of *p*-trifluorotoluene to the respective benzylic acid (left) and proposed intermediate in the organocatalytic pathway (right); C) Influence of the additives on the chemoselectivity.

In analogy to neutral flavins as well as *N*5-alkylated isoalloxazinium salts and alloxazinium salts, a *N*1,*N*10-bridged flavinium salt has been applied in a flavin-iodine dual catalytic system. The oxidative transformation of aryl tosylhydrazones to 1,2,3-thiadiazoles with sulfur is realised in presence of catalytic amounts of flavin and NH_4I as iodine source. [65]

3.2.3. *N*10-and *N*3-Functionalisation

Besides cationic flavinium salts bearing alkyl substituents to activate either *C*4a or *C*10a positions, neutral flavins with modifications at the *N*10-backbone or *N*3-side chain have been found to stabilise hydroperoxide intermediates as well.

Polymer supported flavin **61** with a peptide sequence tethered to the *N*3-position as a mimic for the enzymatic scaffold has been found to stabilise hydroperoxide intermediates and facilitates chemoselective, aerobic sulfide oxidation and *Baeyer-Villiger* reaction. Lumiflavin-3-acetic acid was tethered to L-proline, which induces a γ-turn into the peptide and brings it close to the active site (Figure 21A). Tyrosine as the second amino acid is proposed to undergo hydrogen bonding interactions with the *C*4-carbonyl group of the flavin while the carboxylic acid moiety of aspartic acid as third amino acid is proposed to interact with the *C*4a-hydroperoxide moiety. The length of the alkyl spacer with which the flavin was immobilised on the polymer was found to influence the activity as well. Longer alkyl chains increased the activity, presumably by increasing the flavins conformational flexibility and facilitating substrate accessibility.[66]

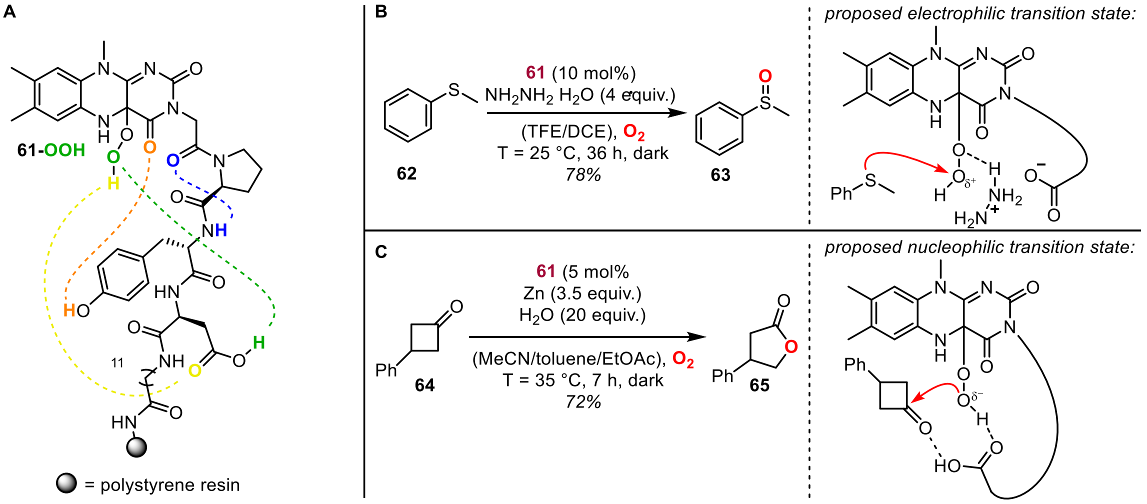
A
61-OOH
● = polystyrene resin
B
61 (10 mol%)
NH2NH2 H2O (4 equiv.)
(TFE/DCE), O2
T = 25 °C, 36 h, dark
78%
62
63
proposed electrophilic transition state:
C
61 (5 mol%
Zn (3.5 equiv.)
H2O (20 equiv.)
(MeCN/toluene/EtOAc), O2
T = 35 °C, 7 h, dark
72%
64
65
proposed nucleophilic transition state:

Figure 21: A) Chemical structure of flavin-*C*4a-hydroperoxide obtained from flavin **61** with proposed intramolecular hydrogen bonding interactions; B) Oxidation of thioanisole *via* electrophilic **61**-OOH; C) *Baeyer-Villiger* oxidation of cyclobutanone *via* nucleophilic **61**-OOH.

Aerobic oxidation of thioanisole **62** (Figure 21B, left) using flavin **61** is achieved in almost quantitative yield without overoxidation to the sulfone. A *Hammett*-study suggests that the oxidation takes place *via* an electrophilic flavin-*C*4a-hydroperoxide, with the oxygen transfer to the substrate being the rate determining step. Hydrazine is suggested to form an ion pair with the carboxylic acid residue in the peptide, which renders the flavin-*C*4a-hydroperoxide intermediate more electrophilic (Figure 21B, right). The *Baeyer-Villiger* oxidation of 3-phenylcyclobutanone **64** (Figure 21C, left) on the other hand is proposed to involve a nucleophilic flavin-*C*4a-hydroperoxide. Both coordination and activation of the hydroperoxide and the carbonyl moiety of the ketone by the aspartic acid residue are proposed to account for the nucleophilicity of flavin-*C*4a-hydroperoxide (Figure 21C, right). Since zinc is used as reductant instead of hydrazine, participation of a cationic Zn species cannot be ruled out. In both reactions, 3-methyllumiflavin and a polymer supported lumiflavin derivative, both lacking the peptide sequence tethered to *N*3, show no significant activity, highlighting the importance of the peptide sequence for catalytic activity. Participation of singlet oxygen was ruled out as well by performing the reactions in the dark.[66]

In 2018 *Chevalier et al.* reported the aerobic *Baeyer-Villiger* oxidation in water mediated by FMN incorporated in a water-soluble polyethyleneimine polymer modified with guanidinium and octyl groups ($\mathrm{PEI_{guan\text{-}oct}}$) in order to mimic an enzymatic environment. Electrostatic interactions between the negatively charged phosphate moiety of FMN and the guanidinium moieties of the polymer localise the cofactor within a hydrophobic microenvironment and prevent it from being displaced by an excess of substrate (Figure 22A). Studies regarding its reactivity towards NADH as an electron donor show significantly increased activity of the FMN-polymer compared to unmodified FMN. Under aerobic conditions, the reduced cofactor is anticipated to generate a flavin-*C*4a-hydroperoxide intermediate and potential stabilisation *via* hydrogen-bonding interactions with the polymer could facilitate *Baeyer-Villiger* oxidation. Asymmetric cyclobutanone **66** is chosen as a substrate to compare reactivity and chemoselectivity of the catalytic system to other known oxygenation systems (Figure 22B). In contrast to the use of *m*CPBA, no epoxide byproducts and a high selectivity for lactone **67** over **68** are observed, comparable to the results obtained with H_2O_2 and acetic acid. Increasing yields with increasing pH indicate a mechanism *via* a nucleophilic peroxide species. A control experiment using H_2O_2 in the absence of FMN also leads to lactone formation, which is why product formation *via* hydrogen bound H_2O_2 cannot be excluded. However, since a lower yield of 29% was observed in the uncatalyzed reaction participation of both, H_2O_2 and flavin-hydroperoxide is suggested.[67]

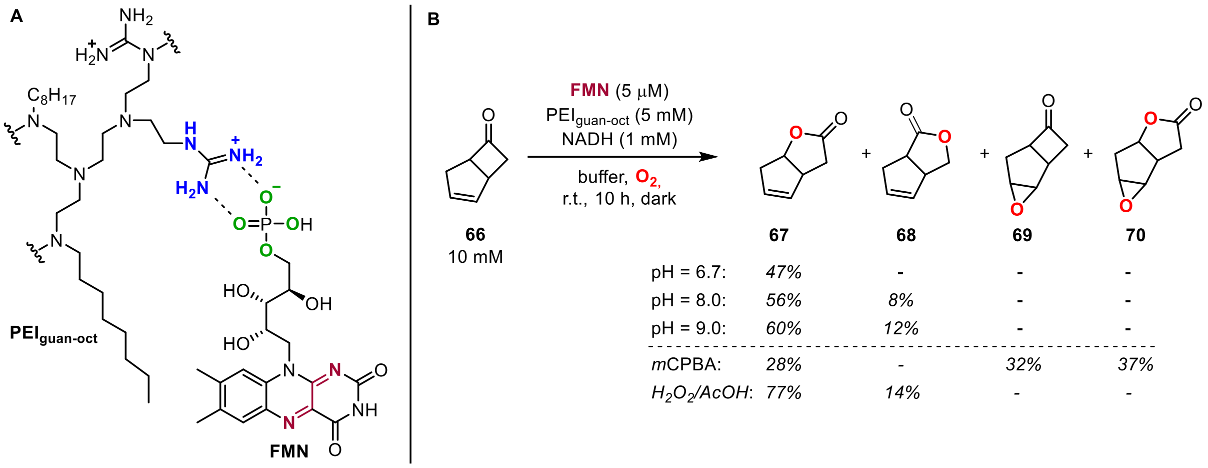
A
NH2
H2N+
C8H17
N
H
NH2+
H2N
O−
O=P−OH
O
HO
OH
HO
N
N
O
NH
O
PEIguan-oct
FMN
B
FMN (5 µM)
PEIguan-oct (5 mM)
NADH (1 mM)
buffer, O2,
r.t., 10 h, dark
66
10 mM
67
68
69
70

	67	68	69	70
pH = 6.7:	*47%*	-	-	-
pH = 8.0:	*56%*	*8%*	-	-
pH = 9.0:	*60%*	*12%*	-	-
*m*CPBA:	*28%*	-	*32%*	*37%*
H_2O_2/AcOH:	*77%*	*14%*	-	-

Figure 22: A) Proposed hydrogen bonding interactions between FMN and polyethyleneimine-polymer; B) *Baeyer-Villiger* reaction catalysed by artificial flavoenzyme compared to conventional methods and pH-influence on chemoselectivity.

4. Photochemistry of Flavins

Quinoid flavins absorb light in the visible spectrum with an absorption maximum in the blue range (λ = 450 nm).[5] Upon excitation, flavins reach their singlet excited state, and undergo fast intersystem crossing (ISC) to the longer lived triplet excited state ($\Phi_T = 0.375 \pm 0.05$ for riboflavin in aqueous solution at pH = 7.0[68], $\Phi_T = 0.54$ for *N*3-Me-RFTA in methanolic solutions[69]).[70] Photoexcitation of flavins leads to significantly increased redox potentials (E^0(**RFTA/RFTA**$^{\bullet-}$) = −0.81 V *vs* SCE, E^0(^{3}**RFTA*/RFTA**$^{\bullet-}$) = +1.37 V *vs* SCE, E^0(^{1}**RFTA*/RFTA**$^{\bullet-}$) = +1.67 V *vs* SCE)[45] and therefore facilitates reactions that are not feasible in the ground state. Due to its prolonged lifetime, the triplet excited state is the key catalytic species in many photochemical transformations. However, both singlet and triplet excited state can be involved in photochemical oxidations, occurring *via* SET from a suitable substrate to the flavin, generating a flavin radical anion (reductive quenching).[70] Due to the basicity of the latter, protonation can occur, which is known as a proton coupled electron transfer (PCET), when proton- and electron transfer are concerted. Regeneration of the flavin cofactor proceeds either *via* electron transfer to a sacrificial oxidant (Figure 23A) or to an intermediate (redox neutral process, Figure 23B). Additionally, the long lifetime of the flavins triplet excited state allows for photosensitization processes *via* energy transfer to a suitable substrate.[19]

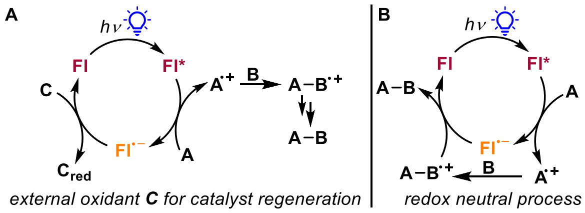

Figure 23: Reaction cycles for flavin based photocatalysis A) with the use of an oxidant **C** and B) for a redox neutral process.

4.1. Flavin-Mediated Photocatalytic Oxygenations

In the photocatalytic, aerobic oxidation of sulfides, two competing mechanisms are involved (Figure 24A). Sulfoxidation can occur *via* a singlet oxygen pathway (Figure 24A, i), where triplet excited ^{3}**RFTA*** facilitates triplet energy transfer to ground state $^3O_2$, resulting in $^1O_2$ and ground state **RFTA**. $^1O_2$ reacts with a sulfide to a zwitterionic persulfoxide intermediate **71**, which reacts with a second sulfide to two molecules of sulfoxide **72**. The competing electron transfer mechanism (Figure 24A, ii and iii) involves reaction of a sulfide radical cation **73**, generated by oxidation with ^{3}**RFTA***, with either superoxide anion $O_2^{\bullet-}$ or $^3O_2$

followed by electron transfer, leading to the persulfoxide intermediate **71**..[71] Significantly increased efficiency of the photooxidation in deuterated MeOH compared to non-deuterated MeOH indicates a singlet oxygen pathway, as the lifetime of $^1O_2$ is higher in deuterated solvents.[71-72] In protic solvents such as MeOH or EtOH, the $^1O_2$ pathway predominates while in MeCN/H_2O mixtures, electron transfer mechanism is enabled as well, allowing for the oxidation of sulfides, which are less susceptible to $^1O_2$ (Figure 24B).[71b] To further improve efficiency of flavins in the photocatalytic sulfoxidation *Zhao*, *Guo* and coworkers synthesized *C*7,*C*8-dibrominated flavin **74** with the aim to improve ISC by the heavy atom effect (Figure 24C). Indeed, flavin **74** showed enhanced photocatalytic activity compared to the respective non-brominated flavin **75**, presumably due to increased $^1O_2$ sensitization and $O_2^{\bullet-}$ generation.[73]

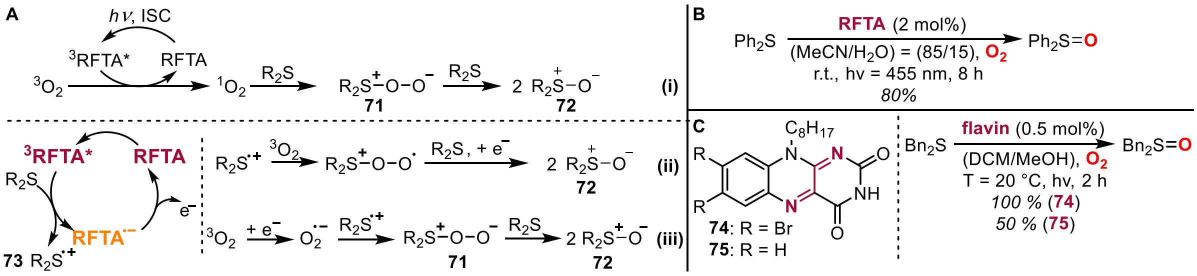
A
hν, ISC
³RFTA*
RFTA
³O₂
¹O₂
R₂S
R₂S⁺-O-O⁻
71
R₂S
2 R₂S⁺-O⁻
72
(i)
³RFTA*
RFTA
R₂S
e⁻
RFTA˙⁻
73 R₂S˙⁺
R₂S˙⁺
³O₂
R₂S⁺-O-O˙
R₂S, + e⁻
2 R₂S⁺-O⁻
72
(ii)
³O₂
+ e⁻
O₂˙⁻
R₂S˙⁺
R₂S⁺-O-O⁻
71
R₂S
2 R₂S⁺-O⁻
72
(iii)
B
Ph₂S
RFTA (2 mol%)
(MeCN/H₂O) = (85/15), O₂
r.t., hv = 455 nm, 8 h
80%
Ph₂S=O
C
C₈H₁₇
R
R
N
N
N
NH
O
O
74: R = Br
75: R = H
Bn₂S
flavin (0.5 mol%)
(DCM/MeOH), O₂
T = 20 °C, hv, 2 h
100 % (74)
50 % (75)
Bn₂S=O

Figure 24: A) Flavin catalysed photochemical aerobic sulfoxidation *via* $^1O_2$ sensitization (top) and electron transfer mechanism (bottom); B) Photocatalytic, aerobic oxygenation of diphenylsulfide mediated by RFTA; C) Increased efficiency of **74** compared to **75** due to improved ISC.

In a recent example, a RFTA-2Sc^{3+} complex was used for the oxyfunctionalisation of alkynes to α-keto ketals. O_2 is used as oxidant for RFTA$^{\bullet-}$, generating superoxide $O_2^{\bullet-}$. The increased redox potential of photoexcited **[RFTA-2Sc^{3+}]*** (E^0(**^{1}[RFTA-2Sc3$^+$]*/[RFTA$^{\bullet-}$-2Sc^{3+}]**) = +2.45 V *vs* SCE, E^0(**^{1}RFTA*/RFTA$^{\bullet-}$**) = +1.67 V *vs* SCE) facilitates single-electron oxidation of diaryl acetylenes **74** containing electron withdrawing groups (Figure 25) and after nucleophilic addition of an alcohol R^3OH, radical intermediate **75** is generated. **[RFTA$^{\bullet-}$-2Sc^{3+}]** then mediates a SET to O_2, generating $O_2^{\bullet-}$, which is captured by **75**, yielding the desired product **76** after nucleophilic addition of a second molecule R^3OH and elimination of H_2O. Labelling experiments with $^{18}O_2$ and $H_2{}^{18}O$ confirm the incorporation of one oxygen atom from O_2 into the carbonyl group and exclude H_2O as oxygen source. The addition of TEMPO to the reaction indicates the participation of radical species since product formation is inhibited. Additionally, participation of $^1O_2$ produced by sensitization could be excluded as the addition of the $^1O_2$ scavenger Co(acac)$_3$ as well as using deuterated MeOH does not influence the product yield. On the other hand, product formation is inhibited in presence of a 1,3-diphenylisobenzofuran, a superoxide inhibitor.[74]

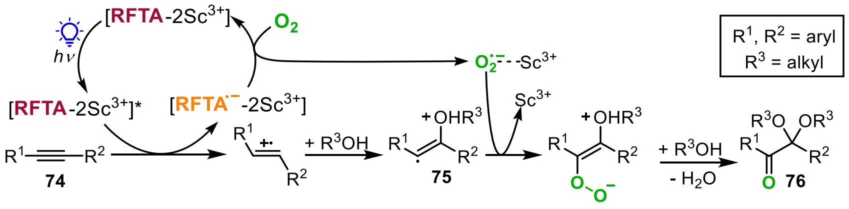

Figure 25: Proposed catalytic cycle for the [RFTA-$2Sc^{3+}$]-mediated oxyfunctionalisation of diaryl alkynes.

4.2. Flavins as Photooxidants

As mentioned previously, photoexcitation of flavins facilitates oxidation reactions that are not feasible in its ground state. However, riboflavin shows limited photostability, resulting in decomposition for example by intramolecular photoreduction or photodealkylation mainly *via* activation of the ribityl side-chain.[36] Through acetylation of the ribityl backbone as well as alkylation of the *N*3-position photostability compared to riboflavin can be increased.[75] In aerobic reactions, where O_2 is used to regenerate the oxidized flavin, removal of the H_2O_2 by-product during the reaction was essential to ensure sufficient stability of the catalyst. This can be achieved by adding molecular sieves[45] or iron complexes[44c] to the reaction mixture, which decompose H_2O_2.

RFTA is used as photocatalyst in various photochemical transformations in combination with an oxidant for catalyst regeneration. In the photooxidation of *in-situ* generated hemiaminals **78** to amides **79**[45] (Figure 26A) as well as *E*/*Z* isomerization of *E*-cinnamic acids **80** followed by cyclisation to yield coumarins **81**[76] (Figure 26B), O_2 is used as terminal oxidant for the reduced flavin, which is formed after a second SET/protonation step or hydrogen atom transfer (HAT). Degradation of the catalyst was circumvented by addition of molecular sieves[45] or sequential catalyst addition[76]. In the RFTA-mediated cyclisation of thiobenzanilides **82** to benzothiazoles **83**, $K_2S_2O_8$ is used for the reoxidation of RFTA$^{\bullet-}$ (Figure 26C).[77] *N*3-Methylated RFTA in combination with nitrobenzene for the regeneration of quinoid flavin is used as photocatalyst in an azodicarboxylate-free version of the *Mitsunobu* reaction (Figure 26D). The photoexcited flavin oxidises triphenyl phosphine to the triphenylphosphine radical cation, which reacts with the alcohol or the carboxylic acid to phosphoranyl radical intermediates. Further oxidation of the latter give the respective alkyloxy- or acyloxyphosphonium species **84** and **85** respectively.[78]

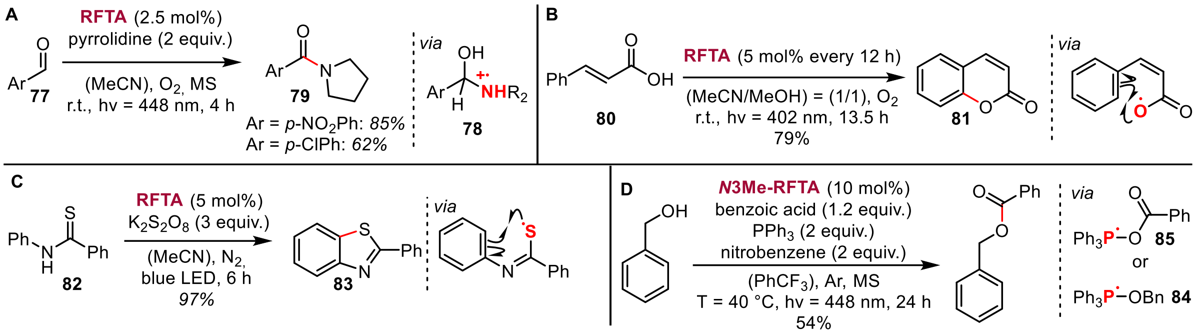
A
RFTA (2.5 mol%)
pyrrolidine (2 equiv.)
(MeCN), O2, MS
r.t., hv = 448 nm, 4 h
77
79
Ar = p-NO2Ph: 85%
Ar = p-ClPh: 62%
via
78
B
RFTA (5 mol% every 12 h)
(MeCN/MeOH) = (1/1), O2
r.t., hv = 402 nm, 13.5 h
79%
80
81
via
C
RFTA (5 mol%)
K2S2O8 (3 equiv.)
(MeCN), N2,
blue LED, 6 h
97%
82
83
via
D
N3Me-RFTA (10 mol%)
benzoic acid (1.2 equiv.)
PPh3 (2 equiv.)
nitrobenzene (2 equiv.)
(PhCF3), Ar, MS
T = 40 °C, hv = 448 nm, 24 h
54%
via
85
or
Ph3P-OBn 84

Figure 26: Application of RFTA as photocatalyst with the use of external oxidants in A) the photooxidation of *in-situ* generated hemiaminals, B) a coupled isomerization-oxidative cyclisation of *E*-cinnamic acids to coumarins, C) the oxidation of thiobenzanilides to benzothiazoles and D) the oxidation of phosphines for an azodicarboxylate free esterification.

Examples for the application of flavins in redox neutral processes involve *inter alia* the decarboxylative cyanation of aliphatic carboxylic acids **86** mediated by RFTA (Figure 27A). A PCET to the catalyst followed by decarboxylation yields heteroatom stabilised carbon-centred radicals which are coupled with tosylcyanide, yielding nitriles **87**.[79] Riboflavin tetrabutyrate has been used in a similar approach by the group of *MacMillan* for the oxidative functionalisation of *C*-terminal carboxylates **88** where the resulting stabilised radical **89** is coupled with a *Michael* acceptor for site selective peptide functionalisation (Figure 27B). Selectivity for *C*-terminal carboxylic acids over internal ones is achieved due to the higher oxidation potential of the latter.[80] Water soluble cofactor FMN was used in an oxidative dearomatisation of phenolic substrates **91** (Figure 27C). The proposed mechanism involves the formation of a phenolate in aqueous buffer, facilitating the SET to form a phenoxyl radical, which is trapped by O_2. SET from the semiquinone leads to a peroxy intermediate, which is transformed to the dearomatized product, possibly by oxidation of the buffer. Participation of singlet oxygen is not fully excluded as the addition of an $^1O_2$ quencher diminished the yields.[81]

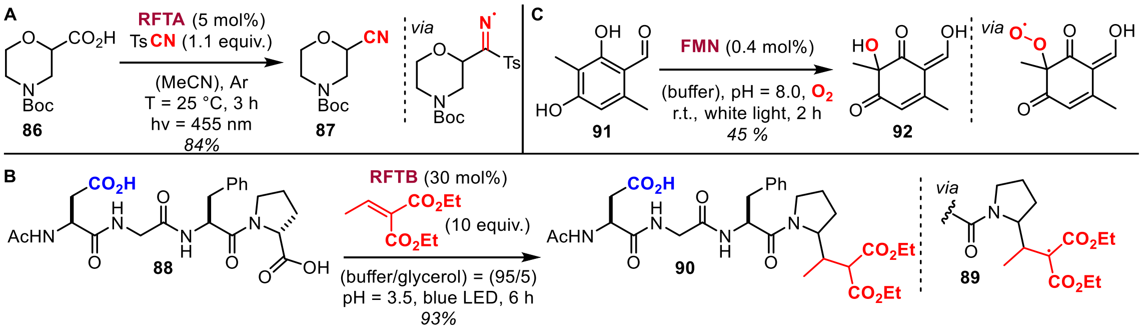
A
RFTA (5 mol%)
TsCN (1.1 equiv.)
(MeCN), Ar
T = 25 °C, 3 h
hv = 455 nm
84%
86
87
via
C
FMN (0.4 mol%)
(buffer), pH = 8.0, O2
r.t., white light, 2 h
45 %
91
92
via
B
RFTB (30 mol%)
(10 equiv.)
(buffer/glycerol) = (95/5)
pH = 3.5, blue LED, 6 h
93%
88
90
via
89

Figure 27: A) Decarboxylative cyanation of aliphatic carboxylic acids; B) Site-selective decarboxylative alkylation of peptides; C) Oxidative dearomatisation of phenols.

While the redox potential of riboflavin derivatives is strong enough to perform the above-mentioned transformations, oxidation of more challenging substrates with higher redox potentials are not feasible. Several approaches were made to overcome these limitations by optimizing the catalytic system or by modifying the catalyst itself *via* covalent modification of the isoalloxazine core or by non-covalent interactions. One example for the latter is the addition of *Lewis* acidic rare earth metal cations, such as Sc^{3+} which increases the excited state redox potential of RFTA by forming a RFTA-$2Sc^{3+}$ complex and allows for the oxidation of unactivated benzylic substrates[82] and electron poor diaryl alkynes[74].

Chemical modification of the isoalloxazine core allows for tailoring of the ground state redox potential of flavins as demonstrated by the group of *Rotello*. Several neutral flavins were synthesized bearing substituents at positions *C*7 and *C*8. While electron withdrawing substituents increase the redox potential compared to the unsubstituted analogue, potentials decrease for electron donating methoxy or dimethylamine substituents.[83] The group of *Cibulka* synthesized CF_3-substituted isoalloxazine and alloxazine derivatives **91** – **93** and estimated their excited state redox potentials (Figure 28A). The electron withdrawing effect of the CF_3 substituent increases the redox potential of both **91** and **92** compared to **RFTA** while it is still lower compared to **93** due to the lack of an additional positive charge. This allows for selective oxidation of electron poor benzylic alcohols to the respective aldehyde without overoxidation to the benzoic acid.[84]

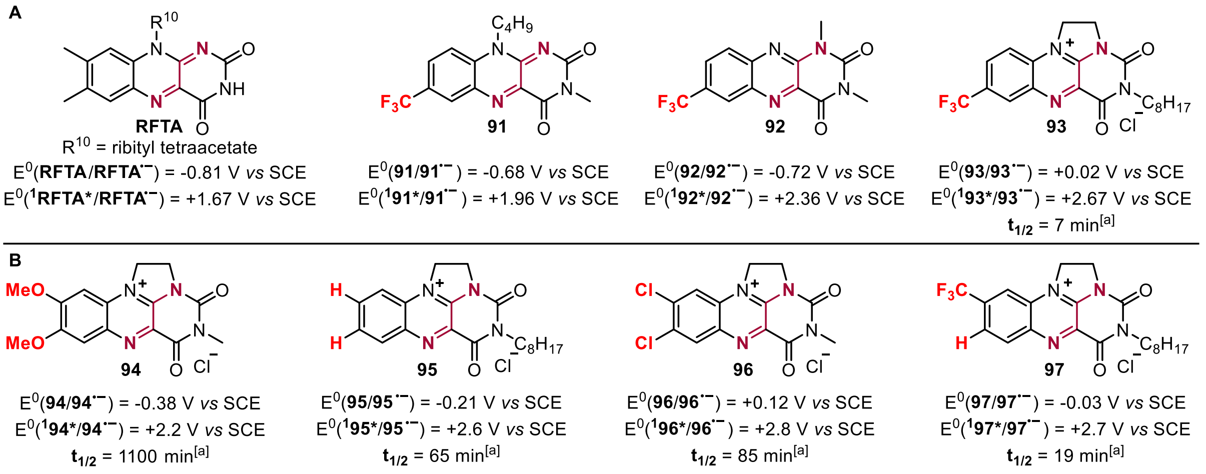
A
R^{10}
RFTA
R^{10} = ribityl tetraacetate
E^0(RFTA/RFTA$^{\bullet-}$) = -0.81 V vs SCE
E^0(^{1}RFTA*/RFTA$^{\bullet-}$) = +1.67 V vs SCE
C_4H_9
F_3C
91
E^0(91/91$^{\bullet-}$) = -0.68 V vs SCE
E^0(^{1}91*/91$^{\bullet-}$) = +1.96 V vs SCE
F_3C
92
E^0(92/92$^{\bullet-}$) = -0.72 V vs SCE
E^0(^{1}92*/92$^{\bullet-}$) = +2.36 V vs SCE
F_3C
C_8H_{17}
93
Cl^-
E^0(93/93$^{\bullet-}$) = +0.02 V vs SCE
E^0(^{1}93*/93$^{\bullet-}$) = +2.67 V vs SCE
$t_{1/2}$ = 7 min[a]
B
MeO
MeO
94
Cl^-
E^0(94/94$^{\bullet-}$) = -0.38 V vs SCE
E^0(^{1}94*/94$^{\bullet-}$) = +2.2 V vs SCE
$t_{1/2}$ = 1100 min[a]
H
H
C_8H_{17}
95
Cl^-
E^0(95/95$^{\bullet-}$) = -0.21 V vs SCE
E^0(^{1}95*/95$^{\bullet-}$) = +2.6 V vs SCE
$t_{1/2}$ = 65 min[a]
Cl
Cl
96
Cl^-
E^0(96/96$^{\bullet-}$) = +0.12 V vs SCE
E^0(^{1}96*/96$^{\bullet-}$) = +2.8 V vs SCE
$t_{1/2}$ = 85 min[a]
F_3C
H
C_8H_{17}
97
Cl^-
E^0(97/97$^{\bullet-}$) = -0.03 V vs SCE
E^0(^{1}97*/97$^{\bullet-}$) = +2.7 V vs SCE
$t_{1/2}$ = 19 min[a]

Figure 28: [a] conditions: 40 equiv. CF_3COD, CD_3CN (25 mM), O_2-atmosphere, T = 40 °C, irradiation; A) Redox potentials of *C*7-CF_3 modified flavins compared to RFTA; B) Redox potentials of selected *N*1,*N*10-ethylene bridged flavinium salts.

A significant increase of redox potentials can be achieved by introducing a positive charge into the flavin scaffold as demonstrated with *N*1,*N*10-ethylene bridged flavinium salts.[44b, 85]

The potential can be modulated further by introducing either electron withdrawing or electron donating substituents at *C*7 and *C*8, some of which are depicted in figure 28B.[85] With this method, singlet excited state redox potentials between −2.2 and −2.8 V *vs* SCE can be achieved as electron donating groups such as methoxy decrease, while electron withdrawing substituents such as CF_3 and Cl increase the potential. However, substitution also influences the photostability of the flavins. Applying the catalysts to the reaction conditions used for the oxidation of unactivated benzylic substrates, electron poor flavinium salts showed considerably lower stability, as seen from their lifetimes, compared to their electron rich analogues, rendering them less suitable for prolonged reaction times while electron rich flavinium salts showed lower catalytic activity in the oxidation of deactivated benzylic substrates in comparison with electron poor flavins.[85]

5. Aim and Motivation

In the previous sections, an overview of the activation of molecular oxygen by flavoenzymes as well as synthetic flavins is given. A special focus was placed on the influence of the enzymatic scaffold on the mechanism as well as the stabilisation of reactive intermediates. Challenges regarding the application of non-enzyme bound riboflavin and its derivatives in chemical synthesis (e.g., low stability of flavin-hydroperoxides and fast elimination of H_2O_2) were outlined. Current solutions involving the use of flavins as mild H_2O_2 sources as well as approaches to stabilise reactive intermediates and tune the flavin's reactivity *via* covalent and non-covalent modifications were presented.

The aim of this work is the design and synthesis of novel, flavin-based catalysts with improved stability and reactivity compared to the parent cofactor (−)-riboflavin, as well as their application in synthetically useful transformations. A non-cationic flavin catalyst is desired due to increased (photo)stability compared to cationic analogues. As target transformations, the biomimetic bromination of oxidation-prone phenolic substrates **98** (Figure 29A) and a sequential dehydrogenation-epoxidation sequence of silyl enol ethers **100** were chosen, both of which rely on the reductive activation of molecular oxygen (Figure 29B).

Bromination of phenolic substrates is traditionally achieved with bromine or electrophilic bromine sources such as NBS, both of which are highly reactive and unselective and often lead to overoxidation. Additionally, the high toxicity of bromine as well as the high reactivity of brominating agents requires additional safety precaution. Therefore, a mild, non-toxic bromination strategy for oxidation prone substrates with a high tolerance for functional groups would be desirable. Desaturation of silyl enol ethers **100** to *α,β*-unsaturated ketones **101** is originally achieved by *Saegusa-Ito* oxidation, which uses stoichiometric amounts of palladium oxidants. Even though improved procedures to circumvent the use of stoichiometric palladium exist, no one-pot strategy to directly transform the silyl enol ethers **100** into synthetically useful *α,β*-epoxyketones **102** has been reported so far. Due to the versatile reactivity of the flavins oxidation states, an oxidative transformation (e.g. *Saegusa-Ito* oxidation of silyl enol ethers) *via* quinoid flavin could be coupled to a reductive process (e.g. activation of O_2) *via* hydroquinoid flavin. This would allow for the direct transformation of silyl enol ethers to *α,β*-epoxyketones in a one-pot fashion.

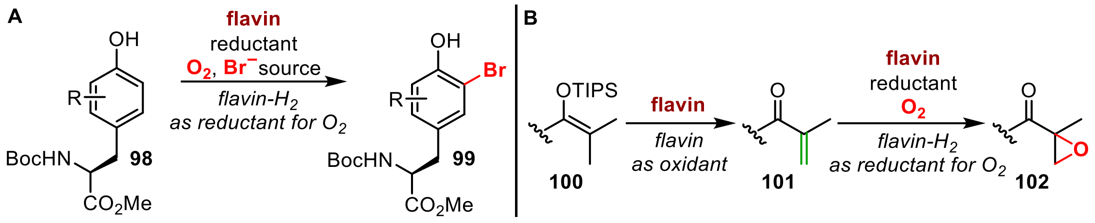

Figure 29: A) Biomimetic, flavin catalysed aerobic bromination; B) Sequential desaturation-epoxidation chosen as proof-of-principle reactions.

To the best of our knowledge, no halogenation strategy mediated by synthetic flavins has been achieved without the use of additional catalysts or mediators. The challenges herein involve:

i) tuning the flavins reactivity and stability by chemical modifications of the isoalloxazine core to ensure sufficient activity but avoid unselective decomposition of both the catalyst and the substrate.

ii) employing a suitable functional group on the flavin, that mimics hydrogen bonding interactions present in the enzymatic scaffold.

iii) identifying a suitable reductant, that is soluble in organic solvents, stable towards reactive intermediates as well as unreactive towards other functional groups present in the catalyst or the substrates.

The sequential desaturation-epoxidation sequence involves two orthogonal flavin activities, namely the oxidation of silyl enol ether substrates to α,β-unsaturated ketones *via* quinoid flavin, followed by the reductive activation of molecular oxygen for subsequent epoxidation to α,β-epoxyketones *via* hydroquinoid flavin. A reliable method for the oxidation has to be identified and at the same time, stability of the tailored flavin has to be ensured to allow for successive reactivity. Additionally, suitable conditions that allow for subsequent epoxidation without substrate decomposition have to be developed. After a reliable protocol for a one-pot desaturation-epoxidation sequence has been established, the substrate scope will be evaluated and furthermore, the applicability of the catalytic system will be demonstrated by realising other sequential transformations.

6. Synthetic C6-Functionalized Aminoflavin Catalysts Enable Aerobic Bromination of Oxidation-Prone Substrates

Title: “Synthetic C6-Functionalized Aminoflavin Catalysts Enable Aerobic Bromination of Oxidation Prone Substrates”

Status: Communication, published online August 13, 2020

Journal: *Angew. Chem. Int. Ed.* **2020**, *59*, 22505−22509.

Publisher: John Wiley and Sons

DOI: 10.1002/anie.202009657; 10.1002/ange.202009657

Authors: Alexandra Walter, Golo Storch

Content: In this publication, the design, synthesis and characterization of novel C_2-symmetric *bis*flavin catalysts containing *C*6-amino modifications on the isoalloxazine core is presented. 2,6-Lutidinium oxalate was identified as a suitable reductant for flavins upon irradiation with blue light. The catalyst’s reactivity towards molecular oxygen was explored in presence of inorganic halide salts and the reductant upon irradiation. Selective conversion of thiourea-containing flavins to *bis*-2-aminobenzothiazol flavins was detected. A reliable protocol for the bromination of phenolic substrates was developed. The high stability of the *bis* 2-aminobenzothiazol flavin under aerobic, catalytic conditions facilitated the selective bromination of eight substrates including tyrosines, flavones and flavanones in yields up to 71%, without the need of additional catalysts or mediators. Unselective substrate decomposition, which was observed with parent RFTA, is suppressed due to the slow release of oxidants by the flavin under catalytic conditions. Additionally, mechanistic experiments with *N*-methylated *bis*flavin analogues revealed catalytic participation of the benzothiazole moiety.

Author Contributions: The flavin catalysts were designed, synthesized and characterized by A. Walter. The catalytic experiments were planned, performed, and analysed by A. Walter. HPLC analysis of the stability of flavin catalysts was performed by A. Walter in cooperation with O. Ackermann. Spectroscopic data was acquired and analysed in cooperation with A. Bauer. The manuscript was written by A. Walter and G. Storch. A. Walter wrote the supplementary information file which contains all experimental data.

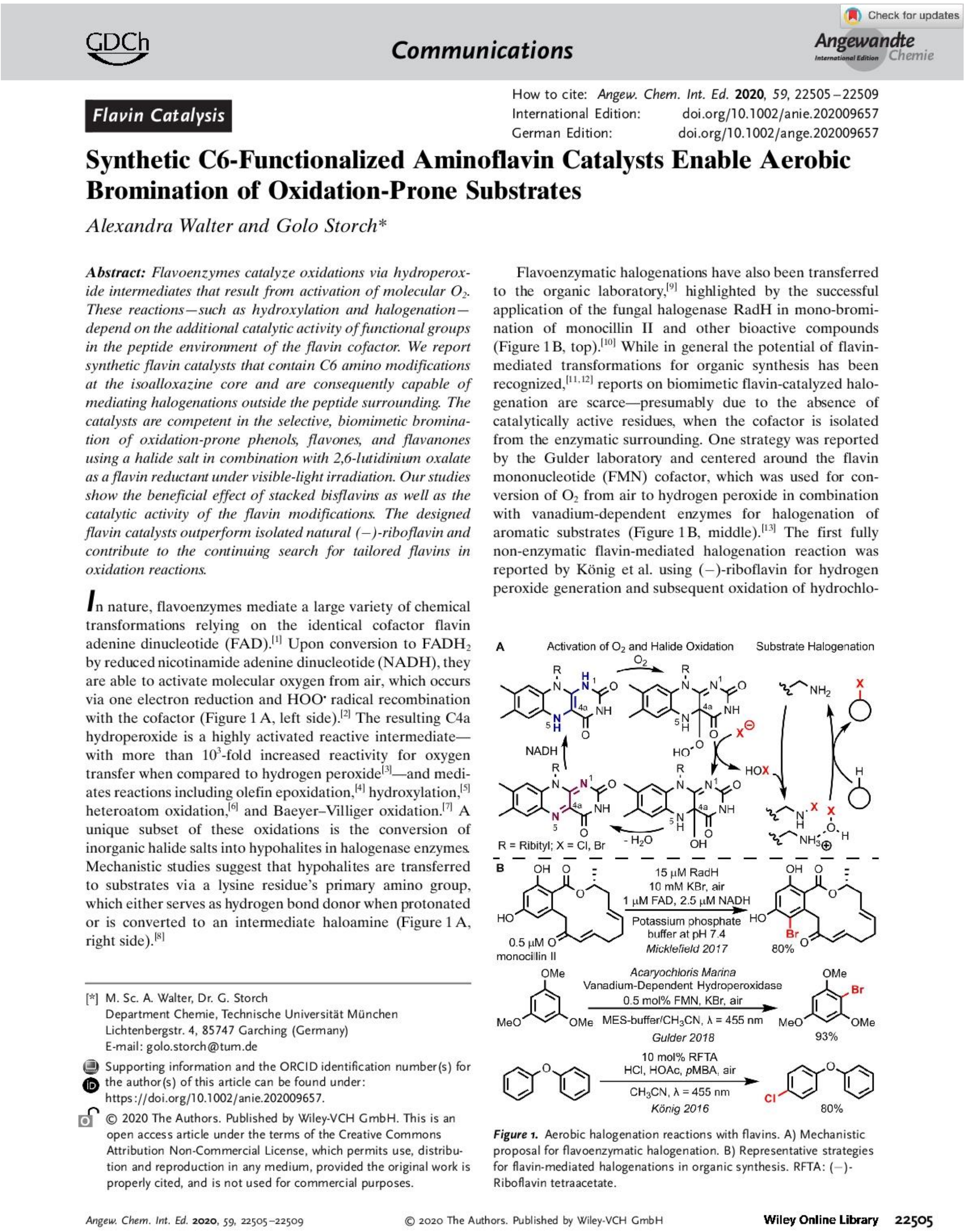

GDCh **Communications** Angewandte Chemie International Edition

Check for updates

Flavin Catalysis

How to cite: *Angew. Chem. Int. Ed.* **2020**, *59*, 22505–22509
International Edition: doi.org/10.1002/anie.202009657
German Edition: doi.org/10.1002/ange.202009657

Synthetic C6-Functionalized Aminoflavin Catalysts Enable Aerobic Bromination of Oxidation-Prone Substrates

*Alexandra Walter and Golo Storch**

Abstract: *Flavoenzymes catalyze oxidations via hydroperoxide intermediates that result from activation of molecular* O_2*. These reactions—such as hydroxylation and halogenation—depend on the additional catalytic activity of functional groups in the peptide environment of the flavin cofactor. We report synthetic flavin catalysts that contain C6 amino modifications at the isoalloxazine core and are consequently capable of mediating halogenations outside the peptide surrounding. The catalysts are competent in the selective, biomimetic bromination of oxidation-prone phenols, flavones, and flavanones using a halide salt in combination with 2,6-lutidinium oxalate as a flavin reductant under visible-light irradiation. Our studies show the beneficial effect of stacked bisflavins as well as the catalytic activity of the flavin modifications. The designed flavin catalysts outperform isolated natural (−)-riboflavin and contribute to the continuing search for tailored flavins in oxidation reactions.*

In nature, flavoenzymes mediate a large variety of chemical transformations relying on the identical cofactor flavin adenine dinucleotide (FAD).[1] Upon conversion to $FADH_2$ by reduced nicotinamide adenine dinucleotide (NADH), they are able to activate molecular oxygen from air, which occurs via one electron reduction and HOO• radical recombination with the cofactor (Figure 1 A, left side).[2] The resulting C4a hydroperoxide is a highly activated reactive intermediate—with more than 10^3-fold increased reactivity for oxygen transfer when compared to hydrogen peroxide[3]—and mediates reactions including olefin epoxidation,[4] hydroxylation,[5] heteroatom oxidation,[6] and Baeyer–Villiger oxidation.[7] A unique subset of these oxidations is the conversion of inorganic halide salts into hypohalites in halogenase enzymes. Mechanistic studies suggest that hypohalites are transferred to substrates via a lysine residue's primary amino group, which either serves as hydrogen bond donor when protonated or is converted to an intermediate haloamine (Figure 1 A, right side).[8]

Flavoenzymatic halogenations have also been transferred to the organic laboratory,[9] highlighted by the successful application of the fungal halogenase RadH in mono-bromination of monocillin II and other bioactive compounds (Figure 1 B, top).[10] While in general the potential of flavin-mediated transformations for organic synthesis has been recognized,[11,12] reports on biomimetic flavin-catalyzed halogenation are scarce—presumably due to the absence of catalytically active residues, when the cofactor is isolated from the enzymatic surrounding. One strategy was reported by the Gulder laboratory and centered around the flavin mononucleotide (FMN) cofactor, which was used for conversion of O_2 from air to hydrogen peroxide in combination with vanadium-dependent enzymes for halogenation of aromatic substrates (Figure 1 B, middle).[13] The first fully non-enzymatic flavin-mediated halogenation reaction was reported by König et al. using (−)-riboflavin for hydrogen peroxide generation and subsequent oxidation of hydrochlo-

Figure 1. Aerobic halogenation reactions with flavins. A) Mechanistic proposal for flavoenzymatic halogenation. B) Representative strategies for flavin-mediated halogenations in organic synthesis. RFTA: (−)-Riboflavin tetraacetate.

---

[*] M. Sc. A. Walter, Dr. G. Storch
Department Chemie, Technische Universität München
Lichtenbergstr. 4, 85747 Garching (Germany)
E-mail: golo.storch@tum.de

Supporting information and the ORCID identification number(s) for the author(s) of this article can be found under: https://doi.org/10.1002/anie.202009657.

© 2020 The Authors. Published by Wiley-VCH GmbH. This is an open access article under the terms of the Creative Commons Attribution Non-Commercial License, which permits use, distribution and reproduction in any medium, provided the original work is properly cited, and is not used for commercial purposes.

15213773, 2020, 50, Downloaded from https://onlinelibrary.wiley.com/doi/10.1002/anie.202009657 by Cochrane Germany, Wiley Online Library on [17/10/2023]. See the Terms and Conditions (https://onlinelibrary.wiley.com/terms-and-conditions) on Wiley Online Library for rules of use; OA articles are governed by the applicable Creative Commons License

ric acid (Figure 1 B, bottom).[14] The authors used *para*-methoxybenzyl alcohol (*p*MBA) as reductant for photo-excited (−)-riboflavin and identified acetic acid as crucial catalytic shuttle for hydrogen peroxide via intermediate peracetic acid formation under the acidic conditions.

We were intrigued by the idea to synthetically modify non-enzymatic flavin catalysts in order to achieve activation of molecular oxygen as well as electrophilic halogenation without the need of additional catalysts or mediators. Moreover, we aimed to facilitate these reactions in organic solvents and also to apply them successfully to oxidation-prone substances containing free phenols, which would significantly increase the synthetic utility of these reactions. Modification of the isoalloxazine core with an amino group seemed promising, since the resulting flavins were anticipated to be less oxidizing,[15] reducing substrate decomposition, while also providing a synthetic handle for installing hydrogen bond donors or nitrogen-based Lewis bases in analogy to the lysine side chain activity. Two synthetic flavin designs were studied (Figure 2 A): First, in flavins based on amine **1**, the C6 position is functionalized in order to position the "side arm" close to the reactive quinoid center. Second, bisflavins **2**, based on *trans*-1,2-diaminocyclohexane,[16] contain two isoalloxazines in a stacked arrangement, thereby locating the C6 functionality proximal to the opposite side's quinoid center as well.

Both synthetic procedures commence with 3-fluoro-2-nitroaniline and consist of a sequence of Cbz protection, S_NAr reaction, nitro group reduction, condensation with alloxan, N3 alkylation, and Cbz deprotection (Figure 2 A). Amines **1** and **2**—bench stable, deep black compounds—were obtained in multigram quantities and N3 dodecylation ensures their solubility in a wide range of organic solvents. The C6 amino groups were converted into urea (**3**) and thiourea (**4**) functionalities, which serve as efficient hydrogen bond donors (Figure 2 B).

With our synthetic route established, we then focused on the reduction of the isoalloxazine core as the first crucial step in aerobic flavin halogenation (see Figure 1 A). A number of suitable reductants is known,[11] including Hantzsch ester, dithionite, zinc, and hydrazine, however, none of the common reductants is (i) soluble in organic solvents, (ii) unreactive towards other functional groups, and additionally (iii) not quenched by oxidizing catalysis intermediates such as hydroperoxides, hypohalous acids, or hydrogen peroxide. Inspired by studies on oxalate oxidase enzymes and the activity of photoexcited (−)-riboflavin in CO_2 release from oxalic acid,[17] we became interested in using the latter as convenient flavin reductant. Oxalic acid itself is insoluble in organic solvent but 2,6-lutidinium oxalate (2:1 mixture, "*LutOx*") indeed acts as a competent reductant for (−)-riboflavin tetraacetate (RFTA) in dichloromethane upon irradiation with blue LED light (Figure 3 A and supporting information).

We then studied the reactivity of thiourea flavin **4** towards hydrogen peroxide—as a mimic for flavin C4a hydroperoxides—in the presence of inorganic halide salt (Figure 3 B).

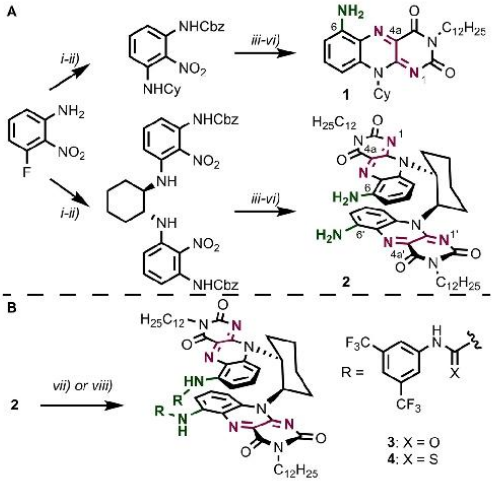

Figure 2. Synthesis of C6 aminoflavin catalysts. A) Route to aminoflavin platform compounds. i) CbzCl, MgO, 71 %. Preparation of **1**: ii) $CyNH_2$, K_2CO_3, 93 %; iii) $SnCl_2$, quant.; iv) alloxan, B_2O_3, 92 %; v) $C_{12}H_{25}I$, K_2CO_3, 65 %; vi) HBr, 77 %. Preparation of **2**: ii) (*R*,*R*)-DACH, K_2CO_3, 78 %; iii) $SnCl_2$, 85 %; iv) alloxan, B_2O_3, 78 %; v) $C_{12}H_{25}I$, K_2CO_3, 94 %; vi) HBr, 86 %. B) Functionalization of **2**: vii) 3,5-bis(trifluoromethyl)phenyl isocyanate, 48 %, viii) 3,5-bis(trifluoromethyl)phenyl isothiocyanate, 65 %. Functionalizations of **1** were performed analogously. DACH: 1,2-diaminocyclohexane.

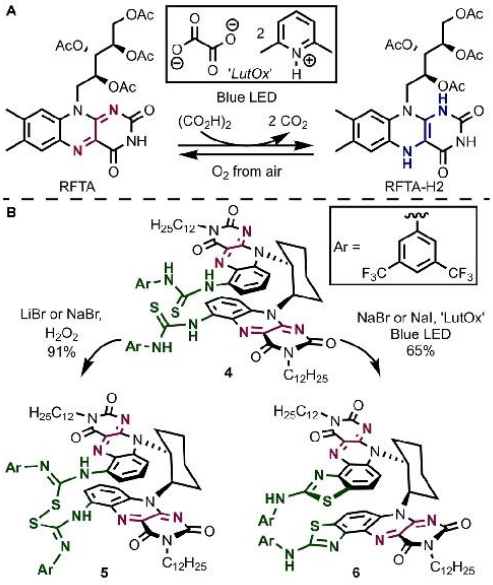

Figure 3. Reversible flavin reduction using 2,6-lutidinium oxalate ("*LutOx*"). A) Reduction of RFTA in dichloromethane. B) Divergent reactivity of thiourea flavin **4** upon exposure to aerobic conditions and halide salt.

© 2020 The Authors. Published by Wiley-VCH GmbH

15213773, 2020, 50, Downloaded from https://onlinelibrary.wiley.com/doi/10.1002/anie.202009657 by Cochrane Germany, Wiley Online Library on [17/10/2023]. See the Terms and Conditions (https://onlinelibrary.wiley.com/terms-and-conditions) on Wiley Online Library for rules of use; OA articles are governed by the applicable Creative Commons License

Within minutes, we observed selective formation (91% isolated yield) of disulfide-type compound **5** by a reaction that proceeds especially well in dilute solution (1.5 mM, see supporting information) and is similar to the dimerization of simple alkyl thioureas.[18] In stark contrast, when irradiated with "*LutOx*" under otherwise similar conditions, clean Jacobsen-Hugershoff-type[19] reaction occurred and *bis*-2-aminobenzothiazole flavin **6** was formed. This divergence is also observed when **4** is treated with excess I_2 under argon, which leads to **5** in the dark while **6** is formed predominantly under blue LED irradiation. We assume that a photoredox mechanism is operative under irradiation and outcompetes sulfur-sulfur bond formation. Consistent with this analysis, the thiourea derived from monoflavin **1** shows 2-aminobenzothiazole (**7**) formation within minutes also when using H_2O_2 and LiBr since no competing intramolecular reaction partner is present.

We then studied, whether benzothiazole flavins **6** and **7** are also reduced by "*LutOx*" via irradiation under inert conditions (Figure 4). They appear as deep red compounds with absorption in the visible range ($\lambda_{max} = 420$ (**6**) and 426 nm (**7**) in CH_2Cl_2) and show fluorescence ($\lambda_{ex} = 410$ nm, see supporting information) at $\lambda_{max} = 593$ (**6**), and 573 nm (**7**). This prompted us to apply blue LED light for excitation and indeed, clean reduction of **7** occurred. When exposed to air, the sample was re-oxidized concomitant to O_2 reduction. This method was also suitable for bisflavin **6** albeit significantly slower when compared to **7**. Urea flavins **3** and **8** (urea derived from **1**) were reduced even more slowly (see supporting information). Decomposition was observed when applying the conditions to disulfide **5**.

Before employing the flavin catalysts in aerobic halogenation reactions with inorganic halide sources, we probed the stability of catalysts **6** and **7** under these conditions. When irradiated ($\lambda_{max} = 457$ nm, LED) under O_2 (Figure 4B, black triangles) in the presence of "*LutOx*" reductant, **7** was observed to be almost fully intact (>90%) after 2 h. However, when inorganic lithium bromide salt was added, rapid decomposition occurred (red triangles). The catalyst lifetime of **6** was much higher (red squares), presumably as a result of the continuous slow generation of Br^+ equivalents. This encouraged us to apply flavin **6** in catalysis.

As a proof-of-principle reaction, we chose the biomimetic halogenation of model tyrosine **9** with molecular O_2 and inorganic bromide salt in dichloromethane as solvent (Figure 5). These conditions were expected to be compatible with the oxidation-prone phenol as well as acid- (*N*-Boc) and base-sensitive (methyl ester) protecting groups. Parent (−)-riboflavin tetraacetate (RFTA) resulted in unselective substrate decomposition, and only 12% bromination products were observed (Entry 1). Shorter reaction times did not result in increased yield. We then moved to C6 amino monoflavins (entries 2–3) and observed that urea catalyst **8** led to less decomposition of **9**, but both reactions did not improve the bromination yield. However, we noted that the experiment with monoflavin **7** had decolored during the course of the reaction, and after applying shorter reaction times, the yield of bromination increased. We aimed for beneficial effects of

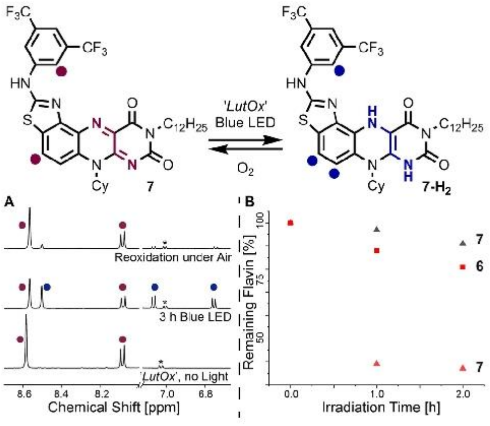

Figure 4. "*LutOx*" reduction of benzothiazole flavin catalysts. A) Under argon, a sample of **7** and "*LutOx*" (5 equiv) in CD_2Cl_2 was irradiated for 3 h with a blue Kessil® LED (43% reduction). The tube was then opened to air. B) Photochemical "*LutOx*" reductions of **6** and **7** under O_2 with (red) and without (black) lithium bromide. Concentrations were monitored by HPLC.

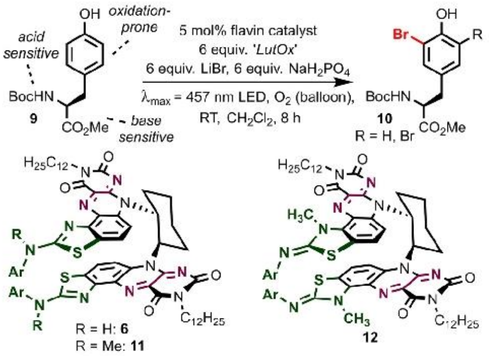

#	Catalyst	Reductant	SM **9** (%)	**10** (R=H, %)	**10** (Σ, %)
1	RFTA	'*LutOx*'	— (—[a], 36[b])	— (—[a], 9[b])	12 (10[a], 9[b])
2	flavin **8**	'*LutOx*'	50	17	17
3	flavin **7**	'*LutOx*'	—	—	10
4	bisflavin **3**	'*LutOx*'	61	11	11
5	bisflavin **5**	'*LutOx*'	82	7	7
6	bisflavin **6**	'*LutOx*'	12	30	58
7	bisflavin **6**	HEH[c]	100	—	—
8	bisflavin **6**	*p*MBA	49	—	7
9	bisflavin **11**	'*LutOx*'	19	26	36
10	bisflavin **12**	'*LutOx*'	—	—	—

Figure 5. Application of C6 aminoflavin catalysts in the aerobic, biomimetic halogenation of model tyrosine **9**. Sodium dihydrogen phosphate was added as a mild proton source. Yields were determined by NMR spectroscopy versus internal standard. [a] Reaction time 4 h. [b] Reaction time 45 min. [c] No irradiation since Hantzsch ester (HEH) reduces **6** in the dark. Ar = 3,5-Bis(trifluoromethyl)phenyl. SM: Starting material.

© 2020 The Authors. Published by Wiley-VCH GmbH

slow and controlled formation of oxidizing species using bisflavins **3**, **5**, and **6** under oxidative halogenation conditions, and indeed decreased decomposition was observed in these cases (entries 4–6). While **3** and **5** did not improve the product yield, benzothiazole **6** resulted in 58% bromination with a good overall mass balance of 70%. Control experiments confirmed that light, flavin catalyst, and reductant are each required (see supporting information, which also contains a solvent screening). The optimal catalyst loading was 5 mol%, which highlights the flavin stability.

Hantzsch ester[20] and *para*-methoxybenzyl alcohol[21]—both competent flavin reductants—did not yield significant quantities of **10** under our conditions (entries 7–8). Interestingly, the *N*-methylated catalyst **11** showed diminished activity, and positional isomer **12** did not even yield **10** in any measurable quantity (entries 9–10). This observation stimulated our interest in probing the catalytic activity of the 2-aminobenzothiazole functionality during halogenation catalysis. Therefore, we studied the activity of flavin **7** in two different routes for bromination of tyrosine derivative **9**, which mimic the early and late stage processes of the full biomimetic halogenation sequence. We first probed for activity when using *tert*-butylhydroperoxide—as flavin C4a hydroperoxide mimic—in combination with lithium bromide under otherwise identical catalytic conditions (see supporting information). Indeed, flavin **7** showed significant catalytic activity. In a second approach, we used *N*-bromosuccinimide as Br^+-source and again found rate enhancement when using flavin **7** as catalyst (see supporting information). Both experiments point towards active catalytic participation of the 2-aminobenzothiazole group in bromination catalysis.

Having observed bromination over unselective substrate decomposition, we expanded our catalysis studies to different kinds of oxidation-prone, phenolic substrates (Figure 6). Other *N*-terminal tyrosine protecting groups such as Cbz (**13**) and Fmoc (**14**) are tolerated, which highlights the compatibility with oxidation-prone benzylic positions. Dipeptides like Boc-Tyr-Val-OMe **15** are suitable substrates as well. Additionally, a variety of flavones, umbelliferon, and flavanones resulted in efficient, regioselective mono-bromination (**16–19**). Throughout all examples, (−)-riboflavin tetraacetate led to decomposition independent of the chosen reaction time (see supporting information).

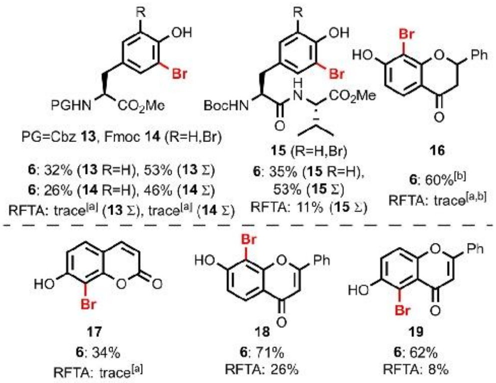

Figure 6. Application of bisflavin **6** in aerobic halogenation of oxidation-prone substrates. Yields were determined by NMR spectroscopy versus internal standard. See Figure 5 for reaction conditions, with 12 equiv "*LutOx*" used for **19** and 15 equiv "*LutOx*" for **16–18**. [a] A yield of ≤5% was observed. [b] Additionally, 29% (with **6**) and 21% (with RFTA) of dibromination observed. PG: Protecting group.

In summary, we report the design and characterization of a series of C6 aminoflavin catalysts and their reactivity under aerobic conditions. We identified 2,6-lutidinium oxalate as organic soluble, inexpensive, and traceless reductant for photoexcited flavins. Applying this reduction strategy, we observed selective transformations of thiourea flavins, resulting in 2-aminobenzothiazole functionalities. Under aerobic conditions, stacked bisflavins were found to be very stable catalysts, which slowly release oxidants upon activation of O_2. Building on these studies, we developed a flavin-mediated halogenation strategy for oxidation-prone substrates including phenolic compounds, flavones, and flavanones. One key advantage when compared to parent (−)-riboflavin is the significantly suppressed substrate decomposition. Mechanistic studies additionally revealed catalytic participation of the 2-aminobenzothiazole modification. The present study is, therefore, anticipated to serve as critical starting point for site-selective flavin catalysis.

Acknowledgements

The Chemical Industry Funds (PhD Fellowship to A.W. and Liebig Fellowship to G.S.) is gratefully acknowledged. Our group is supported by the Technical University of Munich through the Junior Fellow Programme. G.S. is very grateful to Prof. T. Bach for his continuous support. We thank Dr. A. Bauer for assistance with UV/Vis spectroscopy and O. Ackermann for HPLC analyses. Open access funding enabled and organized by Projekt DEAL.

Conflict of interest

The authors declare no conflict of interest.

Keywords: biomimetic halogenation · flavin catalysis · non-covalent interactions · photoredox catalysis · reversible redox interconversion

---

[1] a) T. C. Bruice, *Acc. Chem. Res.* **1980**, *13*, 256–262; b) R. B. Silverman, *Acc. Chem. Res.* **1995**, *28*, 335–342; c) S. O. Mansoorabadi, C. J. Thibodeaux, H.-w. Liu, *J. Org. Chem.* **2007**, *72*, 6329–6342; d) C. T. Walsh, T. A. Wencewicz, *Nat. Prod. Rep.* **2013**, *30*, 175–200.
[2] a) E. Romero, J. R. Gómez Castellanos, G. Gadda, M. W. Fraaije, A. Mattevi, *Chem. Rev.* **2018**, *118*, 1742–1769; b) M. Ismail, L. Schroeder, M. Frese, T. Kottke, F. Hollmann, C. E. Paul, N. Sewald, *ACS Catal.* **2019**, *9*, 1389–1395.
[3] a) C. Kemal, T. C. Bruice, *Proc. Natl. Acad. Sci. USA* **1976**, *73*, 995–999; b) T. C. Bruice, J. B. Noar, S. S. Ball, U. V. Venka-

© 2020 The Authors. Published by Wiley-VCH GmbH

15213773, 2020, 50, Downloaded from https://onlinelibrary.wiley.com/doi/10.1002/anie.202009657 by Cochrane Germany, Wiley Online Library on [17/10/2023]. See the Terms and Conditions (https://onlinelibrary.wiley.com/terms-and-conditions) on Wiley Online Library for rules of use; OA articles are governed by the applicable Creative Commons License

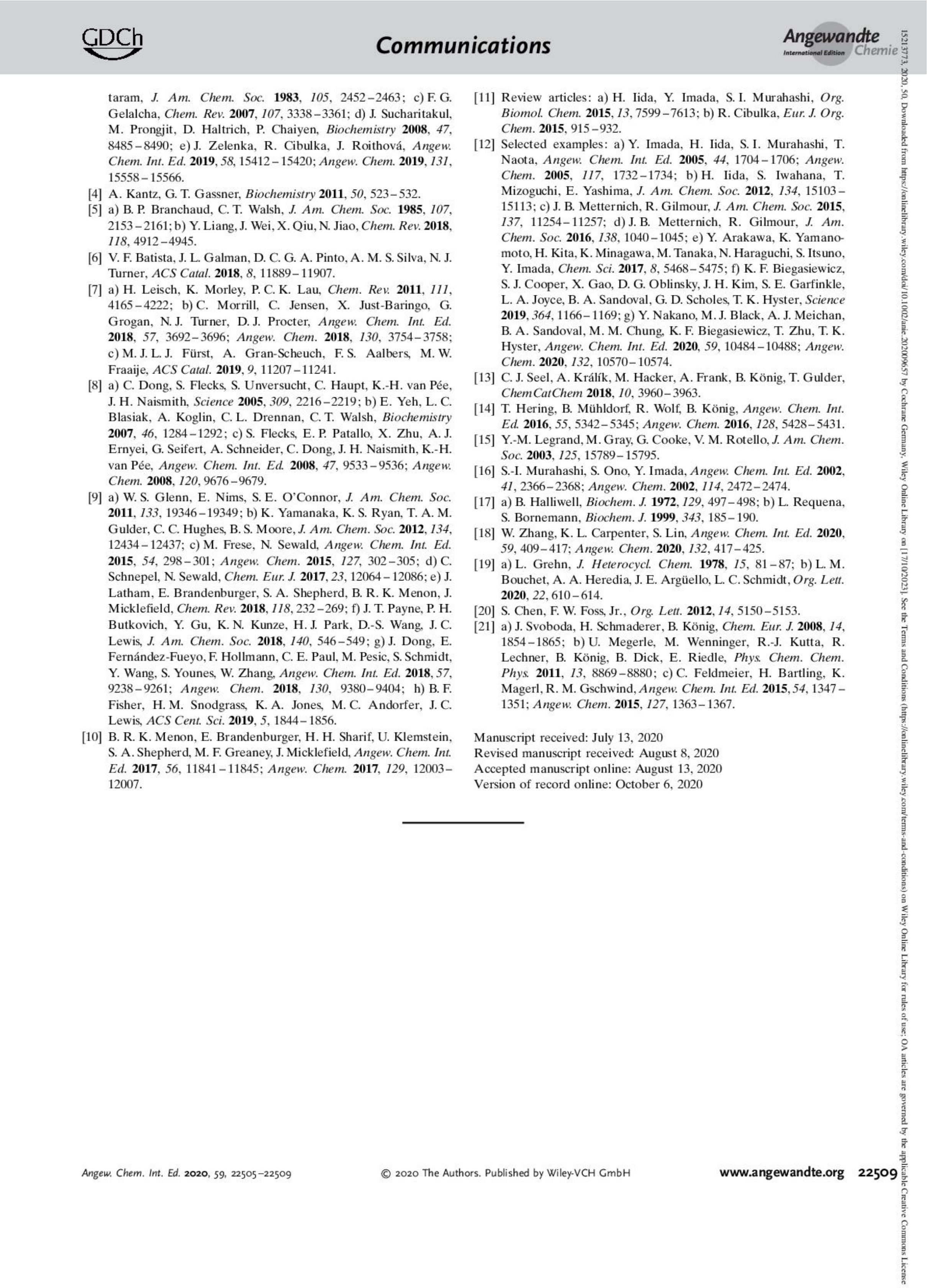

taram, *J. Am. Chem. Soc.* **1983**, *105*, 2452–2463; c) F. G. Gelalcha, *Chem. Rev.* **2007**, *107*, 3338–3361; d) J. Sucharitakul, M. Prongjit, D. Haltrich, P. Chaiyen, *Biochemistry* **2008**, *47*, 8485–8490; e) J. Zelenka, R. Cibulka, J. Roithová, *Angew. Chem. Int. Ed.* **2019**, *58*, 15412–15420; *Angew. Chem.* **2019**, *131*, 15558–15566.

[4] A. Kantz, G. T. Gassner, *Biochemistry* **2011**, *50*, 523–532.

[5] a) B. P. Branchaud, C. T. Walsh, *J. Am. Chem. Soc.* **1985**, *107*, 2153–2161; b) Y. Liang, J. Wei, X. Qiu, N. Jiao, *Chem. Rev.* **2018**, *118*, 4912–4945.

[6] V. F. Batista, J. L. Galman, D. C. G. A. Pinto, A. M. S. Silva, N. J. Turner, *ACS Catal.* **2018**, *8*, 11889–11907.

[7] a) H. Leisch, K. Morley, P. C. K. Lau, *Chem. Rev.* **2011**, *111*, 4165–4222; b) C. Morrill, C. Jensen, X. Just-Baringo, G. Grogan, N. J. Turner, D. J. Procter, *Angew. Chem. Int. Ed.* **2018**, *57*, 3692–3696; *Angew. Chem.* **2018**, *130*, 3754–3758; c) M. J. L. J. Fürst, A. Gran-Scheuch, F. S. Aalbers, M. W. Fraaije, *ACS Catal.* **2019**, *9*, 11207–11241.

[8] a) C. Dong, S. Flecks, S. Unversucht, C. Haupt, K.-H. van Pée, J. H. Naismith, *Science* **2005**, *309*, 2216–2219; b) E. Yeh, L. C. Blasiak, A. Koglin, C. L. Drennan, C. T. Walsh, *Biochemistry* **2007**, *46*, 1284–1292; c) S. Flecks, E. P. Patallo, X. Zhu, A. J. Ernyei, G. Seifert, A. Schneider, C. Dong, J. H. Naismith, K.-H. van Pée, *Angew. Chem. Int. Ed.* **2008**, *47*, 9533–9536; *Angew. Chem.* **2008**, *120*, 9676–9679.

[9] a) W. S. Glenn, E. Nims, S. E. O'Connor, *J. Am. Chem. Soc.* **2011**, *133*, 19346–19349; b) K. Yamanaka, K. S. Ryan, T. A. M. Gulder, C. C. Hughes, B. S. Moore, *J. Am. Chem. Soc.* **2012**, *134*, 12434–12437; c) M. Frese, N. Sewald, *Angew. Chem. Int. Ed.* **2015**, *54*, 298–301; *Angew. Chem.* **2015**, *127*, 302–305; d) C. Schnepel, N. Sewald, *Chem. Eur. J.* **2017**, *23*, 12064–12086; e) J. Latham, E. Brandenburger, S. A. Shepherd, B. R. K. Menon, J. Micklefield, *Chem. Rev.* **2018**, *118*, 232–269; f) J. T. Payne, P. H. Butkovich, Y. Gu, K. N. Kunze, H. J. Park, D.-S. Wang, J. C. Lewis, *J. Am. Chem. Soc.* **2018**, *140*, 546–549; g) J. Dong, E. Fernández-Fueyo, F. Hollmann, C. E. Paul, M. Pesic, S. Schmidt, Y. Wang, S. Younes, W. Zhang, *Angew. Chem. Int. Ed.* **2018**, *57*, 9238–9261; *Angew. Chem.* **2018**, *130*, 9380–9404; h) B. F. Fisher, H. M. Snodgrass, K. A. Jones, M. C. Andorfer, J. C. Lewis, *ACS Cent. Sci.* **2019**, *5*, 1844–1856.

[10] B. R. K. Menon, E. Brandenburger, H. H. Sharif, U. Klemstein, S. A. Shepherd, M. F. Greaney, J. Micklefield, *Angew. Chem. Int. Ed.* **2017**, *56*, 11841–11845; *Angew. Chem.* **2017**, *129*, 12003–12007.

[11] Review articles: a) H. Iida, Y. Imada, S. I. Murahashi, *Org. Biomol. Chem.* **2015**, *13*, 7599–7613; b) R. Cibulka, *Eur. J. Org. Chem.* **2015**, 915–932.

[12] Selected examples: a) Y. Imada, H. Iida, S. I. Murahashi, T. Naota, *Angew. Chem. Int. Ed.* **2005**, *44*, 1704–1706; *Angew. Chem.* **2005**, *117*, 1732–1734; b) H. Iida, S. Iwahana, T. Mizoguchi, E. Yashima, *J. Am. Chem. Soc.* **2012**, *134*, 15103–15113; c) J. B. Metternich, R. Gilmour, *J. Am. Chem. Soc.* **2015**, *137*, 11254–11257; d) J. B. Metternich, R. Gilmour, *J. Am. Chem. Soc.* **2016**, *138*, 1040–1045; e) Y. Arakawa, K. Yamanomoto, H. Kita, K. Minagawa, M. Tanaka, N. Haraguchi, S. Itsuno, Y. Imada, *Chem. Sci.* **2017**, *8*, 5468–5475; f) K. F. Biegasiewicz, S. J. Cooper, X. Gao, D. G. Oblinsky, J. H. Kim, S. E. Garfinkle, L. A. Joyce, B. A. Sandoval, G. D. Scholes, T. K. Hyster, *Science* **2019**, *364*, 1166–1169; g) Y. Nakano, M. J. Black, A. J. Meichan, B. A. Sandoval, M. M. Chung, K. F. Biegasiewicz, T. Zhu, T. K. Hyster, *Angew. Chem. Int. Ed.* **2020**, *59*, 10484–10488; *Angew. Chem.* **2020**, *132*, 10570–10574.

[13] C. J. Seel, A. Králík, M. Hacker, A. Frank, B. König, T. Gulder, *ChemCatChem* **2018**, *10*, 3960–3963.

[14] T. Hering, B. Mühldorf, R. Wolf, B. König, *Angew. Chem. Int. Ed.* **2016**, *55*, 5342–5345; *Angew. Chem.* **2016**, *128*, 5428–5431.

[15] Y.-M. Legrand, M. Gray, G. Cooke, V. M. Rotello, *J. Am. Chem. Soc.* **2003**, *125*, 15789–15795.

[16] S.-I. Murahashi, S. Ono, Y. Imada, *Angew. Chem. Int. Ed.* **2002**, *41*, 2366–2368; *Angew. Chem.* **2002**, *114*, 2472–2474.

[17] a) B. Halliwell, *Biochem. J.* **1972**, *129*, 497–498; b) L. Requena, S. Bornemann, *Biochem. J.* **1999**, *343*, 185–190.

[18] W. Zhang, K. L. Carpenter, S. Lin, *Angew. Chem. Int. Ed.* **2020**, *59*, 409–417; *Angew. Chem.* **2020**, *132*, 417–425.

[19] a) L. Grehn, *J. Heterocycl. Chem.* **1978**, *15*, 81–87; b) L. M. Bouchet, A. A. Heredia, J. E. Argüello, L. C. Schmidt, *Org. Lett.* **2020**, *22*, 610–614.

[20] S. Chen, F. W. Foss, Jr., *Org. Lett.* **2012**, *14*, 5150–5153.

[21] a) J. Svoboda, H. Schmaderer, B. König, *Chem. Eur. J.* **2008**, *14*, 1854–1865; b) U. Megerle, M. Wenninger, R.-J. Kutta, R. Lechner, B. König, B. Dick, E. Riedle, *Phys. Chem. Chem. Phys.* **2011**, *13*, 8869–8880; c) C. Feldmeier, H. Bartling, K. Magerl, R. M. Gschwind, *Angew. Chem. Int. Ed.* **2015**, *54*, 1347–1351; *Angew. Chem.* **2015**, *127*, 1363–1367.

Manuscript received: July 13, 2020
Revised manuscript received: August 8, 2020
Accepted manuscript online: August 13, 2020
Version of record online: October 6, 2020

© 2020 The Authors. Published by Wiley-VCH GmbH

15213773, 2020, 50, Downloaded from https://onlinelibrary.wiley.com/doi/10.1002/anie.202009657 by Cochrane Germany, Wiley Online Library on [17/10/2023]. See the Terms and Conditions (https://onlinelibrary.wiley.com/terms-and-conditions) on Wiley Online Library for rules of use; OA articles are governed by the applicable Creative Commons License

7. Photochemical Desaturation and Epoxidation with Oxygen by Sequential Flavin Catalysis

Title: “Photochemical Desaturation and Epoxidation with Oxygen by Sequential Flavin Catalysis”

Status: Communication, published online October 09, 2023

Journal: *Angew. Chem. Int. Ed.* **2023**, *62*, e202310634.

Publisher: John Wiley and Sons

DOI: 10.1002/anie.202310634; 10.1002/ange.202310634

Authors: Alexandra Walter, Wolfgang Eisenreich, Golo Storch

Content: This publication addresses a sequential desaturation-epoxidation sequence catalysed by a molecular flavin. A photochemical method for a flavin catalysed *Saegusa-Ito* oxidation of silyl enol ethers leading to *α*,*β*-unsaturated ketones was developed and successfully applied to 13 substrates. The flavin catalyst remained stable throughout the reaction and was applied in the subsequent reductive activation of molecular oxygen, leading to the direct conversion of silyl enol ethers to *α*,*β*-epoxyketones (12 examples) in a one-pot fashion. Mechanistic experiments supported the initial formation of an allylic radical *via* single-electron oxidation and deprotonation by the flavin, followed by a second oxidation and desilylation to yield the *α*,*β*-unsaturated ketone. Applicability of the catalytic system was demonstrated by coupling the photocatalytic desaturation to further transformations, namely radical addition, aerobic bromination, and *β*-functionalisation of silyl enol ethers. In an attempt to use O_2 in the photochemical desaturation, selective formation of silyloxy hydroperoxides and *α*-silylperoxy was observed *via* flavin mediates singlet oxygen sensitisation. The reaction was monitored by *in-situ* NMR illumination studies and both reaction products were isolated and characterised.

Author Contributions: All synthetic experiments were planned, performed, and analysed by A. Walter. *In-situ* NMR illumination studies were planned, implemented and analysed by A. Walter and W. Eisenreich. Electrochemical measurements were performed by A. Walter. Spectroscopic data was acquired and analysed by A. Walter in cooperation with J. Großkopf. The manuscript was written by A. Walter, W. Eisenreich and G. Storch. A. Walter wrote the supplementary information, containing all experimental data.

GDCh Communications Angewandte Chemie International Edition
www.angewandte.org

How to cite: *Angew. Chem. Int. Ed.* **2023**, *62*, e202310634
doi.org/10.1002/anie.202310634

Synthetic Methods

Photochemical Desaturation and Epoxidation with Oxygen by Sequential Flavin Catalysis

*Alexandra Walter, Wolfgang Eisenreich, and Golo Storch**

Abstract: Catalytic desaturations are important strategies for the functionalization of organic molecules. In nature, flavoenzymes mediate the formation of α,β-unsaturated carbonyl compounds by concomitant cofactor reduction. Contrary to many laboratory methods for these reactions, such as the *Saegusa-Ito* oxidation, no transition metal reagents or catalysts are required. However, a molecular flavin-mediated variant has not been reported so far. We disclose a photochemical approach for silyl enol ether oxidation, which leads to α,β-unsaturated ketones (13 examples) in very good yields. The flavin catalysts are stable throughout the desaturation reaction, and we successfully applied them in a subsequent aerobic epoxidation by simply changing the reaction conditions. This protocol allowed us to directly convert silyl enol ethers into α,β-epoxyketones in a one-pot fashion (12 examples). Sequential flavin catalysis is not limited to one specific reactivity combination and can, *inter alia*, couple the photochemical oxidation with radical additions. We anticipate that flavin-catalyzed desaturation will be applicable to other substrate classes and that its sequential catalytic activity will enable rapid substrate diversification.

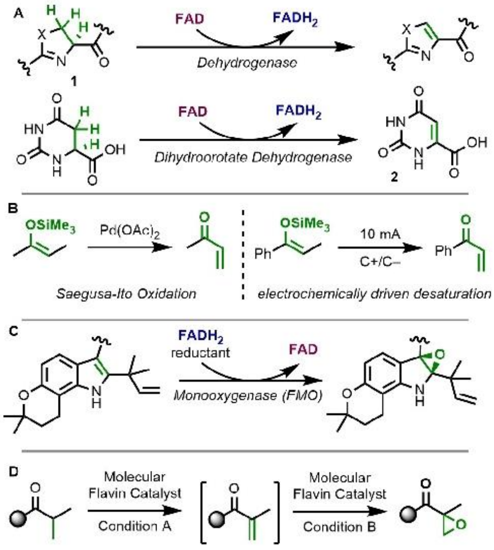

Figure 1. Desaturation and epoxidation catalysis. A) Flavoenzyme desaturation. B) *Saegusa-Ito* reactions in the organic laboratory. C) Flavoenzyme activity in epoxidation with O_2. D) Our strategy for combining both activities in sequential catalysis.

Flavoenzymes mediate a fascinating plethora of transformations.[1] The unique chemical environment around the flavin cofactor controls its oxidation state and substrate accessibility, allowing it to choreograph many different types of reactions.[2] In contrast to the rich enzymatic repertoire, the use of molecular flavin catalysts in organic synthesis is limited.[3] In the present study, we were particularly interested in the ability of molecular flavin catalysts to couple two chemically distinct steps in an iterative one-pot procedure, enabling rapid substrate diversification.[4] Catalytic desaturation[5] and aerobic epoxidation were chosen based on their synthetic utility and reported flavoenzyme activity.

In flavin-dependent desaturase enzymes (Figure 1A), flavin adenine dinucleotide (FAD) accepts a hydride to release the oxidized product concomitant to being reduced to the hydroquinoid state ($FADH_2$). Thiazoline (**1**, X=S) and oxazoline (**1**, X=O) desaturation proceed via this mechanism,[6] which is also operative in *dihydroorotate dehydrogenase*. The latter forms orotidine precursor **2** for uridine biosynthesis.[7] In the organic laboratory, desaturation adjacent to carbonyl positions is typically achieved by silyl enol ether formation and subsequent *Saegusa-Ito* reaction (Figure 1B), which requires stoichiometric amounts of a palladium oxidant.[8] The reaction is very valuable for natural product synthesis and the preparation of active drug molecules.[9] Significant improvements on the original conditions have been reported, including catalytic strategies

---

[*] M.Sc. A. Walter, Prof. Dr. W. Eisenreich, Dr. G. Storch
School of Natural Sciences and Catalysis Research Center (CRC), Technical University of Munich (TUM)
Lichtenbergstr. 4, 85747 Garching (Germany)
E-mail: golo.storch@tum.de

© 2023 The Authors. Angewandte Chemie International Edition published by Wiley-VCH GmbH. This is an open access article under the terms of the Creative Commons Attribution Non-Commercial NoDerivs License, which permits use and distribution in any medium, provided the original work is properly cited, the use is non-commercial and no modifications or adaptations are made.

15213773, 2023, 42, Downloaded from https://onlinelibrary.wiley.com/doi/10.1002/anie.202310634 by Cochrane Germany, Wiley Online Library on [17/10/2023]. See the Terms and Conditions (https://onlinelibrary.wiley.com/terms-and-conditions) on Wiley Online Library for rules of use; OA articles are governed by the applicable Creative Commons License

with a sacrificial oxidant,[10,11] hypervalent iodine reagents,[12] photochemical generation of singlet oxygen,[13] and electrochemical oxidation.[14] However, with the exception of enzyme-mediated examples,[15] flavin-catalyzed desaturations are still lacking as a synthetic method.[16]

In an orthogonal reactivity, flavoenzymes activate molecular O_2 from air for oxygenation reactions (Figure 1C).[17] These reactions require the reduced cofactor ($FADH_2$) and result *inter alia* in the formation of oxiranes.[18] In the organic laboratory, such reactivity typically requires oxidants such as *m*CPBA.[19] It was the aim of this study to enable molecular flavin-catalyzed desaturation and to achieve sequential epoxidation in a one-pot reaction with the same flavin catalyst. This strategy would enable the direct conversion of silyl enol ethers into α,β-epoxyketones.

We initiated our studies with silyl enol ether **3** and probed whether molecular flavins serve as oxidants for desaturation in analogy to the enzymatic transformations. However, no thermal reactivity was observed even under elevated temperatures. This shifted our interest to photochemical conditions,[20] since excited quinoid flavins are strong oxidants with $E_{1/2}(^3\mathbf{4}^*/\mathbf{4}^{\bullet-}) = +1.35$ V vs. SCE and a redox potential of $E_{p/2} = +1.17$ V vs. SCE (CH_3CN) was determined for silyl enol ether **3** (see Supporting Information). We combined flavin **4** with model substrate **3** in a stoichiometric experiment (Figure 2) and irradiated the mixture with blue light in deuterated acetonitrile under an argon atmosphere. This resulted in clean conversion of the quinoid flavin to its reduced counterpart **5**, concomitant to the formation of α,β-unsaturated ketone **6** in 94 % yield (determined versus NMR internal standard; see Supporting Information pages 38–40). When exposed to air, the solution quickly regained the typical flavin color, and oxidation of hydroquinone **5** to quinone **4** was observed. We concluded that photochemical desaturation is indeed feasible with molecular flavins and that all evidence points towards a single-electron oxidation pathway.[21]

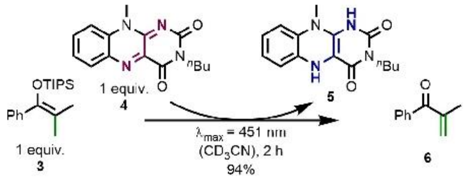

Figure 2. The stoichiometric *Saegusa-Ito* oxidation with a molecular flavin under inert conditions in a J Young NMR tube. Reaction conditions: Flavin **4** (1 equiv.) and silyl enol ether **3** (1 equiv.) were irradiated at $\lambda_{max} = 451$ nm in CD_3CN solution for 2 h. The yield was determined versus NMR internal standard. No silylated reduced flavins were observed, which led to the conclusion that residual water serves as a source of protons (see Supporting Information).

In the next step, we aimed for achieving the *Saegusa-Ito* oxidation in a catalytic fashion (Table 1) with riboflavin tetraacetate (RFTA). We quickly realized that a basic additive (such as Na_2HPO_4) is required to avoid starting material hydrolysis to ketone **7**. The key to success was finding a suitable sacrificial oxidant, which converts hydroquinoid flavin back to the quinoid form. Oxone® only facilitated approximately one turnover, while DDQ and $K_2S_2O_8$ performed better with 34 % and 85 % yield, respectively (Entries 1–3). The oxidation with $K_2S_2O_8$ releases hydrogensulfate,[22] which is quenched by Na_2HPO_4. A stronger base such as Na_3PO_4 was not suitable, presumably as a result of catalyst decomposition (Entry 4).[23] No reactivity was observed in the absence of flavin (Entry 5). We noticed that the reaction solution lost its typical yellow coloration after 2 h of irradiation, indicative of flavin catalyst decomposition. This prompted us to switch to modified flavin **4**, and the reaction times could be extended to 8 h without risk of decoloration. Under these conditions, the unsaturated ketone **6** was formed almost quantitatively (Entry 6). No reactivity was observed without irradiation, and omitting the base additive diminished the yield (Entries 7 and 8).

Table 1: Optimization of the flavin-catalyzed *Saegusa-Ito* oxidation.

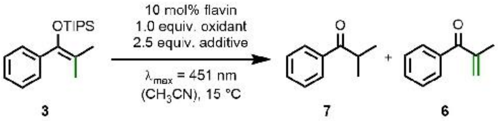

Entry	Flavin	Oxidant	Additive	Time	SM[a]	Yield (6)[a]
#1	RFTA	Oxone®	Na_2HPO_4	2 h	85%	8%
#2	RFTA	DDQ	Na_2HPO_4	2 h	n.d.	34%
#3	RFTA	$K_2S_2O_8$	Na_2HPO_4	2 h	n.d.	85%
#4	RFTA	$K_2S_2O_8$	Na_3PO_4	2 h	69%	n.d.
#5	none	$K_2S_2O_8$	Na_2HPO_4	2 h	>99%	n.d.
#6	4b	$K_2S_2O_8$	Na_2HPO_4	8 h	n.d.	>99%[b]
#7[c]	4b	$K_2S_2O_8$	Na_2HPO_4	8 h	94%	n.d.
#8	4b	$K_2S_2O_8$	none	8 h	n.d.	58%[d]

[a] Determined versus NMR internal standard. [b]: Yield of isolated, volatile product 6: 74%. [c]: No irradiation. [d]: Significant hydrolysis to ketone 7 (approx. 30% yield). SM=Starting material. n.d. = none detected. RFTA=Riboflavin tetraacetate.

© 2023 The Authors. Angewandte Chemie International Edition published by Wiley-VCH GmbH

15213773, 2023, 42, Downloaded from https://onlinelibrary.wiley.com/doi/10.1002/anie.202310634 by Cochrane Germany, Wiley Online Library on [17/10/2023]. See the Terms and Conditions (https://onlinelibrary.wiley.com/terms-and-conditions) on Wiley Online Library for rules of use; OA articles are governed by the applicable Creative Commons License

The scope of the catalytic desaturation was investigated with a series of silyl enol ethers (Figure 3). Our focus was on those substrates leading to aryl isopropenyl ketones, which are traditionally obtained by oxidation of the secondary alcohol or C–C bond formation reactions, while *Saegusa-Ito* protocols are not reported.[24,25] Alkyl-substituted arene substrates (products **8**–**10**) and phenol ethers (products **11**–**13**) led to clean conversion to the corresponding unsaturated ketones. Substrates with electron-deficient arene substituents were found to be less reactive, however, *para*-chloro (**14**) and *para*-fluoro substitution (**15**) worked reasonably well. Biphenyl derivative **16** and methyl ester **17** were equally successful. Our method is not limited to the formation of disubstituted olefins, and cyclohexene product **18** serves as an example of a trisubstituted analog. It is also not necessary to use aryl-substituted silyl enol ethers, which is highlighted by the clean oxidation to unsaturated ketone **19**.

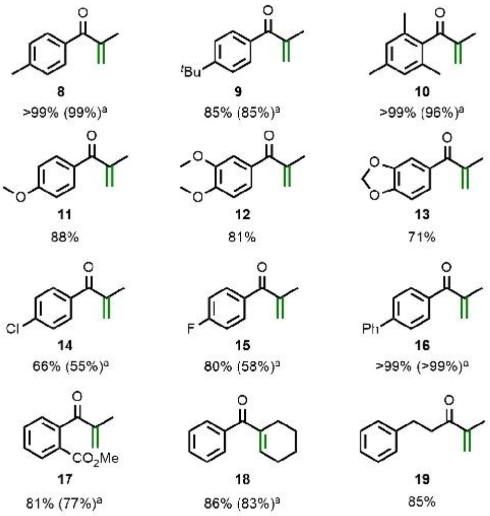

Figure 3. Substrate scope of the catalytic *Saegusa-Ito* reaction. Reaction conditions: See Table 1. Yields are determined versus NMR internal standard. [a] Yields of isolated material.

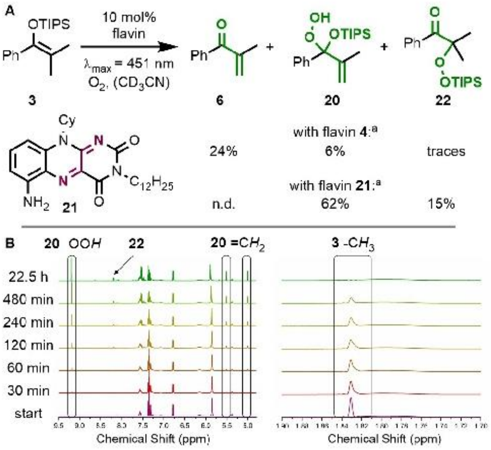

Figure 4. Probing molecular oxygen as a terminal oxidant. A: Products obtained from the reaction of silyl enol ether 3 under an oxygen atmosphere. B: In situ NMR monitoring of the reaction with substrate 3 (1 equiv.) in the presence of aminoflavin 21 (1 equiv.) in CD_3CN. Irradiation was performed with a fiber optics setup and a 5 W LED (λ_{max} = 455 nm; see Supporting Information for details). [a] Yields determined versus NMR internal standard.

We then probed whether molecular oxygen can serve as an oxidant in our catalytic desaturation of silyl enol ether **3**. Interestingly, a catalytic amount of flavin **4** also led to the formation of unsaturated ketone **6** under aerobic conditions, albeit in a poor yield of only 24 %. The reaction proceeded sluggishly, which can be explained by the competing reactivity of silyl enol ethers with singlet oxygen generated by flavin-mediated sensitization.[13,26] In line with this rationale, we identified silyloxy hydroperoxide **20** as a minor byproduct (Figure 4A).[27] This reactive compound could be isolated, which prompted us to investigate its selective formation. We hypothesized that a less oxidizing flavin could be the key here since the excited state redox potential would not be sufficient to oxidize the silyl enol ether, but sensitization of molecular oxygen would still be possible. This succeeded with aminoflavin **21**,[28] which did not show any *Saegusa-Ito* oxidation activity under the standard conditions (see Table 1). However, when irradiated in the absence of an exogenous oxidant under an atmosphere of oxygen, silyloxy hydroperoxide **20** was formed in 62 % yield and could be fully characterized by NMR spectroscopy and HR-ESI-MS (see Supporting Information). This singlet oxygen ene reaction was also monitored by in situ NMR studies via illumination of the sample inside the magnet.[29] This setup allowed us to follow and characterize the conversion to silyloxy hydroperoxide **20** and also to identify aromatic ketone **22** as a third product of this reaction (Figure 4B). The formation of both products can be rationalized based on the competition between a prototropic and a silatropic singlet oxygen ene reaction (Schenck ene reaction[30]).[31]

Encouraged by the stability of flavin catalyst **4** under the photochemical oxidation conditions, we next set out to investigate a sequential reaction that requires the same flavin catalyst to perform a second chemically distinct step in the same reaction vessel. In an orthogonal approach to the singlet oxygen generation under irradiation, reduced flavins are known to react with O_2 via stepwise single-electron transfer leading to flavin hydroperoxides and, ultimately the release of hydrogen peroxide. All unsaturated ketones shown in Figure 3 are potential substrates for epoxidation reactions, which made us wonder whether the addition of a reductant to our reaction vessels after the *Saegusa-Ito* oxidation and exposure to O_2 would trigger the

© 2023 The Authors. Angewandte Chemie International Edition published by Wiley-VCH GmbH

15213773, 2023, 42, Downloaded from https://onlinelibrary.wiley.com/doi/10.1002/anie.202310634 by Cochrane Germany, Wiley Online Library on [17/10/2023]. See the Terms and Conditions (https://onlinelibrary.wiley.com/terms-and-conditions) on Wiley Online Library for rules of use; OA articles are governed by the applicable Creative Commons License

one-pot conversion to epoxyketones. The latter are synthetically interesting reactive electrophiles[32] and also serve as functional groups in proteasome inhibitors.[33] In our one-pot reaction sequences (Table 2), we commenced with silyl enol ether **3** and used the catalytic conditions (c.f., Table 1) that resulted in the nearly quantitative formation of the α,β-unsaturated ketones. Our focus was initially on identifying a suitable reductant for the second reaction step. Zinc is often used as a reductant for flavins,[34] yet its application in our reaction sequence resulted only in trace product formation (Entry 1). A slight improvement was found with Hantzsch ester (HEH) in combination with a carbonate base and methanol as a co-solvent (Entries 2 and 3). Switching to Cs_2CO_3 and adding a small amount of water (0.1 equiv.) improved the yield to 25 %, presumably by increasing the carbonate solubility in the organic solvent mixture (Entry 4). Increasing the reaction temperature to 40 °C led to faster epoxidation and increased levels of product formation (Entries 5 and 6). All yields of epoxyketone **23** refer to the two-step reaction sequence and are based on the silyl enol ether starting material.

These results prompted us to investigate whether analogous sequential reaction conditions can also be applied to the entire set of *Saegusa-Ito* substrates shown in Figure 3. We were pleased to see that all unsaturated ketones were also smoothly converted into the corresponding epoxyketones (Figure 5), with the only exception of ester **17**, which resisted oxygenation. Alkyl-substituted arenes were tolerated best (**24**–**26**), while electron-rich arenes showed slightly lower levels of product formation (**27**–**29**). Halide- and aryl-substitution of the aromatic ketones was well tolerated and led to epoxyketones **30** to **32**. Even the trisubstituted epoxide **33** and aliphatic derivative **34** were obtained, albeit in lower yields. In the latter cases, conversion was observed to be incomplete and much slower.

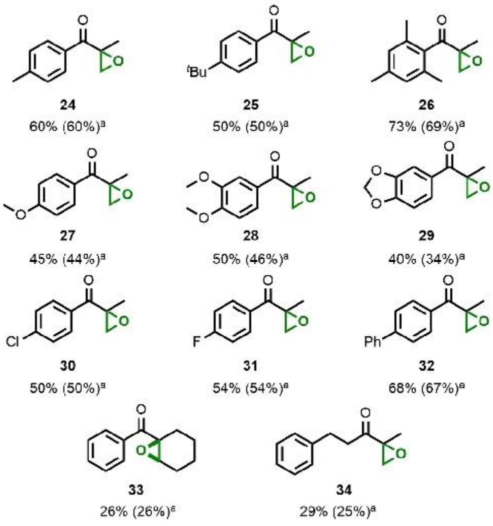

Figure 5. Products of the one-pot desaturation epoxidation sequence. Reaction conditions: See Table 2. Yields were determined versus NMR internal standard [a] Yields of isolated material.

Sequential flavin catalysis is not limited to the combination of desaturation and epoxidation. Subsequent to the *Saegusa-Ito* oxidation step, flavin-catalysis also successfully generates CF_3-radicals from *Langlois* reagent ($NaSO_2CF_3$),[35] which results in addition product **35** in 60 % yield over two steps (Figure 6A). In an orthogonal approach, flavin catalysis leads to C–C bond formation by radical addition to benzylidenemalononitrile (Figure 6B). In analogy to the initial report of this reactivity by *Ooi*,[21a] this requires an allylic radical which is generated by deprotonation of the silyl enol ether radical cation after initial flavin-mediated oxidation of substrate **36**. While dichloromethane performed poorly as a solvent in the *Saegusa-Ito* reaction (see Supporting Information page 42), it was suitable here. The anionic flavin semiquinone radical is proposed to

Table 2: Flavin-mediated one-pot desaturation and epoxidation.

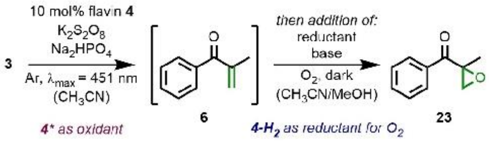

Entry	Reductant	Base	Co-Solvent	Yield[a]
#1	Zinc (5 equiv.)	None	Water (10% v/v)	2%
#2	HEH (4 equiv.)	None	MeOH (25% v/v)	n.d.
#3	HEH (2 equiv.)	K_2CO_3	MeOH (25% v/v)	4%
#4	HEH (2 equiv.)	Cs_2CO_3	MeOH (25% v/v)[b]	25%
#5	HEH (2 equiv.)	Cs_2CO_3	MeOH (25% v/v)[c]	53%
#6	HEH (2 equiv.)	Cs_2CO_3	MeOH (25% v/v)[b,c]	60%[d]

All sequential catalytic reactions were initially irradiated for 8 h (*Saegusa-Ito* oxidation) and then stirred overnight with reductant under an atmosphere of oxygen. [a] Determined versus NMR internal standard. [b] With 0.1 equiv. water. [c] Reaction performed at 40 °C. [d] Yield of isolated material: 46%.

© 2023 The Authors. Angewandte Chemie International Edition published by Wiley-VCH GmbH

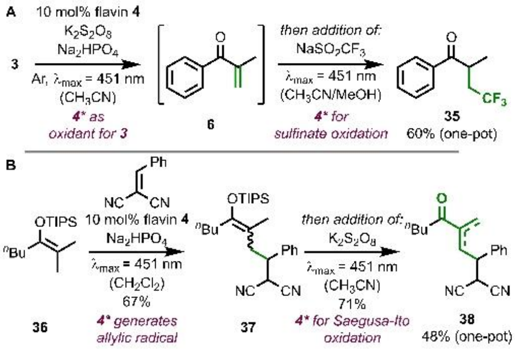

Figure 6. Examples of the application of sequential flavin catalysis: *Saegusa-Ito* oxidation and subsequent radical trifluoromethylation leads to ketone 35 (A). The β-functionalization of silyl enol ether 36 prior to *Saegusa-Ito* oxidation results in elongated, α,β-unsaturated ketone 38 (B). Yields were determined versus NMR internal standard.

deprotonate the substrate intermediate, but adding the additional base Na_2HPO_4 led to further improvement (63 % yield without base; see Supporting Information page 89). The immediate silyl enol ether product **37** can then be subjected to a subsequent flavin-mediated *Saegusa-Ito* oxidation, which leads to α,β-unsaturated ketone **38** (individual steps: 67 % and 71 % yield; one-pot, two-step procedure: 48 % yield). An aerobic halogenation of phenolic substrates with LiBr[28] is also possible after *Saegusa-Ito* oxidation (see Supporting Information pages 85–87).

In summary, we report an unprecedented one-pot strategy for directly converting silyl enol ethers into α,β-epoxyketones which relies on the combination of two orthogonal flavin catalyst activities, namely the photochemical single-electron oxidation and the reductive activation of O_2. While common for flavoenzymes, our two-step reaction sequence with a single molecular flavin catalyst paves the way for similar combination strategies to be used in the organic laboratory. Synthetically valuable sequential reactions are anticipated, for example, by connecting the reductive and oxidative activity of flavins with their function as organocatalysts.

Acknowledgements

The Fonds der Chemischen Industrie (FCI, Ph.D. Fellowship to A.W and Liebig Fellowship to G.S) is gratefully acknowledged. The project was funded by the Deutsche Forschungsgemeinschaft (Emmy Noether Programme, STO 1175/3-1). We thank J. Großkopf for spectroscopic measurements and M. Schick for HPLC separations. Our group is supported by the Technical University of Munich through the Junior Fellow Programme. G.S. is very grateful to Prof. T. Bach for his continuous support. Open Access funding enabled and organized by Projekt DEAL.

Conflict of Interest

The authors declare no conflict of interest.

Data Availability Statement

The data that support the findings of this study are available in the supplementary material of this article.

Keywords: Aerobic Oxidation · Biomimetic Catalysis · Epoxidation · Homogeneous Catalysis · Photochemistry

---

[1] C. T. Walsh, T. A. Wencewicz, *Nat. Prod. Rep.* **2013**, *30*, 175–200.
[2] S. O. Mansoorabadi, C. J. Thibodeaux, H.-W. Liu, *J. Org. Chem.* **2007**, *72*, 6329–6342.
[3] a) R. Cibulka, *Eur. J. Org. Chem.* **2015**, 915–932; b) A. Rehpenn, A. Walter, G. Storch, *Synthesis* **2021**, *53*, 2583–2593.
[4] Examples of multiple activity of flavin catalysts: a) J. B. Metternich, R. Gilmour, *J. Am. Chem. Soc.* **2016**, *138*, 1040–1045; b) T. Morack, J. B. Metternich, R. Gilmour, *Org. Lett.* **2018**, *20*, 1316–1319.
[5] For reviews on general catalytic desaturation, see: a) G. E. Dobereiner, R. H. Crabtree, *Chem. Rev.* **2010**, *110*, 681–703; b) J. Choi, A. H. R. MacArthur, M. Brookhart, A. S. Goldman, *Chem. Rev.* **2011**, *111*, 1761–1779; c) C. Wen, T. Li, Z. Huang, Q.-K. Kang, *Chem. Rec.* **2023**, e202300146, https://doi.org/10.1002/tcr.202300146.
[6] a) R. Sinha Roy, A. M. Gehring, J. C. Milne, P. J. Belshaw, C. T. Walsh, *Nat. Prod. Rep.* **1999**, *16*, 249–263; b) J. O. Melby, X. Li, D. A. Mitchell, *Biochemistry* **2014**, *53*, 413–422.
[7] H. Munier-Lehmann, P.-O. Vidalain, F. Tangy, Y. L. Janin, *J. Med. Chem.* **2013**, *56*, 3148–3167.
[8] Y. Ito, T. Hirao, T. Saegusa, *J. Org. Chem.* **1978**, *43*, 1011–1013.
[9] V. Rodeschini, P. Van de Weghe, E. Salomon, C. Tarnus, J. Eustache, *J. Org. Chem.* **2005**, *70*, 2409–2412.
[10] Examples using palladium catalysts: a) J.-Q. Yu, H.-C. Wu, E. J. Corey, *Org. Lett.* **2005**, *7*, 1415–1417; b) T. Diao, S. S. Stahl, *J. Am. Chem. Soc.* **2011**, *133*, 14566–14569; c) D. Pun, T. Diao, S. S. Stahl, *J. Am. Chem. Soc.* **2013**, *135*, 8213–8221; d) Y. Lu, P. L. Nguyen, N. Lévaray, H. Lebel, *J. Org. Chem.* **2013**, *78*, 776–779; e) Y. Chen, J. P. Romaire, T. R. Newhouse, *J. Am. Chem. Soc.* **2015**, *137*, 5875–5878; f) M. Chen, A. J. Rago, G. Dong, *Angew. Chem. Int. Ed.* **2018**, *57*, 16205–16209.
[11] Examples using copper catalysis: Y. Shang, X. Jie, K. Jonnada, S. N. Zafar, W. Su, *Nat. Commun.* **2017**, *8*, 2273.
[12] K. C. Nicolaou, Y. L. Zhong, P. S. Baran, *J. Am. Chem. Soc.* **2000**, *122*, 7596–7597.
[13] J. Zhang, L. Wang, Q. Liu, Z. Yang, Y. Huang, *Chem. Commun.* **2013**, *49*, 11662–11664.
[14] S. Gnaim, Y. Takahira, H. R. Wilke, Z. Yao, J. Li, D. Delbrayelle, P.-G. Echeverria, J. C. Vantourout, P. S. Baran, *Nat. Chem.* **2021**, *13*, 367–372.
[15] Y. V. S. N. Murthy, Y. Meah, V. Massey, *J. Am. Chem. Soc.* **1999**, *121*, 5344–5345.
[16] For the flavin-mediated reverse (reduction) reaction, see: a) Y. Imada, H. Iida, T. Naota, *J. Am. Chem. Soc.* **2005**, *127*, 14544–14545; b) C. Smit, M. W. Fraaije, A. J. Minnaard, *J. Org. Chem.* **2008**, *73*, 9482–9485.
[17] E. Romero, J. R. Gómez Castellanos, G. Gadda, M. W. Fraaije, A. Mattevi, *Chem. Rev.* **2018**, *118*, 1742–1769.

© 2023 The Authors. Angewandte Chemie International Edition published by Wiley-VCH GmbH

15213773, 2023, 42, Downloaded from https://onlinelibrary.wiley.com/doi/10.1002/anie.202310634 by Cochrane Germany, Wiley Online Library on [17/10/2023]. See the Terms and Conditions (https://onlinelibrary.wiley.com/terms-and-conditions) on Wiley Online Library for rules of use; OA articles are governed by the applicable Creative Commons License

[18] a) A. Minami, M. Shimaya, G. Suzuki, A. Migita, S. S. Shinde, K. Sato, K. Watanabe, T. Tamura, H. Oguri, H. Oikawa, *J. Am. Chem. Soc.* **2012**, *134*, 7246–7249; b) S. Li, J. M. Finefield, J. D. Sunderhaus, T. J. McAfoos, R. M. Williams, D. H. Sherman, *J. Am. Chem. Soc.* **2012**, *134*, 788–791.

[19] a) P. S. Baran, E. J. Corey, *J. Am. Chem. Soc.* **2002**, *124*, 7904–7905; b) Z. Bian, C. C. Marvin, M. Pettersson, S. F. Martin, *J. Am. Chem. Soc.* **2014**, *136*, 14184–14192.

[20] Examples: a) S. Bloom, C. Liu, D. K. Kölmel, J. X. Qiao, Y. Zhang, M. A. Poss, W. R. Ewing, D. W. C. MacMillan, *Nat. Chem.* **2018**, *10*, 205–210; b) J. Zelenka, R. Cibulka, J. Roithová, *Angew. Chem. Int. Ed.* **2019**, *58*, 15412–15420; c) M. Chilamari, J. R. Immel, S. Bloom, *ACS Catal.* **2020**, *10*, 12727–12737; d) O. J. Knowles, L. O. Johannissen, G. E. M. Crisenza, S. Hay, D. Leys, D. J. Procter, *Angew. Chem. Int. Ed.* **2022**, *61*, e202212158.

[21] Photochemical reactions via single-electron oxidation of silyl enol ethers: a) K. Ohmatsu, T. Nakashima, M. Sato, T. Ooi, *Nat. Commun.* **2019**, *10*, 2706; b) F. Schäfers, L. Quach, J. L. Schwarz, M. Saladrigas, C. G. Daniliuc, F. Glorius, *ACS Catal.* **2020**, *10*, 11841–11847; c) T. Nakashima, H. Fujimori, K. Ohmatsu, T. Ooi, *Chem. Eur. J.* **2021**, *27*, 9253–9256.

[22] L. M. Bouchet, A. A. Heredia, J. E. Argüello, L. C. Schmidt, *Org. Lett.* **2020**, *22*, 610–614.

[23] a) T. Harayama, Y. Tezuka, T. Taga, F. Yoneda, *J. Chem. Soc. Perkin Trans. 1* **1987**, 75–83; b) S. B. Smith, T. C. Bruice, *J. Am. Chem. Soc.* **1975**, *97*, 2875–2881.

[24] Examples by C–C bond formation: a) H. Ebel, K. Zeitler, W. Steglich, *Synthesis* **2003**, *1*, 0101–0106; b) D.-Y. Zhu, W.-D. Li, C. Yang, J. Chen, J.-B. Xia, *Org. Lett.* **2018**, *20*, 3282–3285.

[25] Examples by alcohol oxidation: a) G. Liang, Y. Xu, I. B. Seiple, D. Trauner, *J. Am. Chem. Soc.* **2006**, *128*, 11022–11023; b) G. Sudhakar, K. Satish, *Chem. Eur. J.* **2015**, *21*, 6475–6480.

[26] a) C. W. Jefford, C. G. Rimbault, *Tetrahedron Lett.* **1977**, *18*, 2375–2378; b) E. Friedrich, W. Lutz, *Chem. Ber.* **1980**, *113*, 1245–1263.

[27] I. Saito, R. Nagata, K. Yuba, T. Matsuura, *Tetrahedron Lett.* **1983**, *24*, 1737–1740.

[28] A. Walter, G. Storch, *Angew. Chem. Int. Ed.* **2020**, *59*, 22505–22509.

[29] W. Eisenreich, M. Joshi, B. Illarionov, G. Richter, W. Römisch-Margl, F. Müller, A. Bacher, M. Fischer, *FEBS J.* **2007**, *274*, 5876–5890.

[30] P. Bayer, R. Pérez-Ruiz, A. Jacobi von Wangelin, *ChemPhotoChem* **2018**, *2*, 559–570.

[31] a) G. M. Rubottom, M. I. Lopez Nieves, *Tetrahedron Lett.* **1972**, *13*, 2423–2425; b) W. Adam, A. Alzerreca, J.-C. Liu, F. Yany, *J. Am. Chem. Soc.* **1977**, *99*, 5768–5773.

[32] Examples: a) F. Nowrouzi, J. Janetzko, R. A. Batey, *Org. Lett.* **2010**, *12*, 5490–5493; b) A. Kondoh, N. Tasato, T. Aoki, M. Terada, *Org. Lett.* **2020**, *22*, 5170–5175.

[33] a) D. Bhattarai, M. J. Lee, A. Baek, I. J. Yeo, Z. Miller, Y. M. Baek, S. Lee, D.-E. Kim, J. T. Hong, K. B. Kim, *J. Med. Chem.* **2020**, *63*, 3763–3783; b) M. J. Lee, D. Bhattarai, H. Jang, A. Baek, I. J. Yeo, S. Lee, Z. Miller, S. Lee, J. T. Hong, D.-E. Kim, W. Lee, K. B. Kim, *J. Med. Chem.* **2021**, *64*, 10934–10950.

[34] Y. Arakawa, K. Yamanomoto, H. Kita, K. Minagawa, M. Tanaka, N. Haraguchi, S. Itsuno, Y. Imada, *Chem. Sci.* **2017**, *8*, 5468–5475.

[35] L. Zhu, L.-S. Wang, B. Li, B. Fu, C.-P. Zhang, W. Li, *Chem. Commun.* **2016**, *52*, 6371–6374.

Manuscript received: July 25, 2023
Accepted manuscript online: August 28, 2023
Version of record online: September 12, 2023

15213773, 2023, 42, Downloaded from https://onlinelibrary.wiley.com/doi/10.1002/anie.202310634 by Cochrane Germany, Wiley Online Library on [17/10/2023]. See the Terms and Conditions (https://onlinelibrary.wiley.com/terms-and-conditions) on Wiley Online Library for rules of use; OA articles are governed by the applicable Creative Commons License

© 2023 The Authors. Angewandte Chemie International Edition published by Wiley-VCH GmbH

8. Summary

For the biomimetic bromination, a reliable synthetic route for C_2-symmetric *bis*flavin **104** was developed which required six steps starting from commercially available 3-fluoro-2-nitroaniline **103** (Figure 30). The amino group in the *C*6-position served as synthetic handle for the introduction of biomimetic halogen bond donors such as thiourea. *Bis*flavin **105** as well as *mono*flavin **106** were synthesized, to demonstrate the advantages of the stacked *bis*flavin arrangement. Additionally, oxalic acid in combination with two equivalents of lutidine was identified as a suitable reductant for flavins. This novel reductant "*LutOx*" is readily available, inexpensive, and is oxidized to inert CO_2.[86]

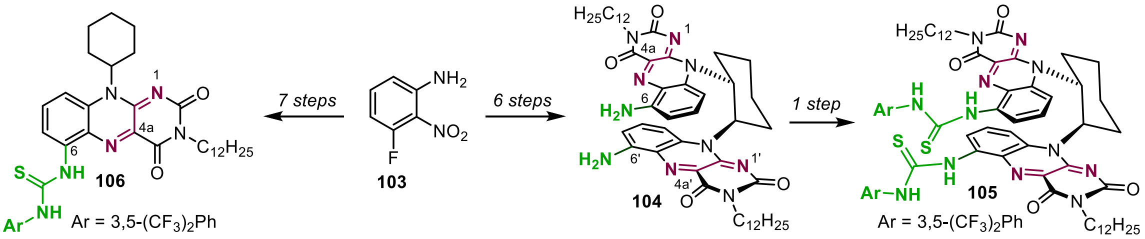

Figure 30: Synthesis of thiourea-containing *bis*flavin **105** and *mono*flavin **106** starting from 3-fluoro-2-nitroaniline **103**.

The stability of *bis*flavin **105** under catalytic conditions was tested by irradiation in presence of "*LutOx*" as reductant and a halide source under O_2, where a clean *Jacobsen-Hungershoff*-type reaction to the respective *bis*-2-aminobenzothiazole **107** was observed (Figure 31). In contrast, when the stability of **105** towards H_2O_2 in presence of a halide salt in the dark was tested, clean and almost quantitative formation of disulfide **108** occurred. These findings can be explained by a photoredox mechanism taking place upon irradiation, which kinetically outcompetes the sulfur-sulfur bond formation. This hypothesis is supported by the finding that *mono*flavin **106** forms the respective 2-aminobenzothiazole **109** in the dark in presence of H_2O_2 and an inorganic halide salt, due to the lack of a second competing intramolecular reaction partner.[86]

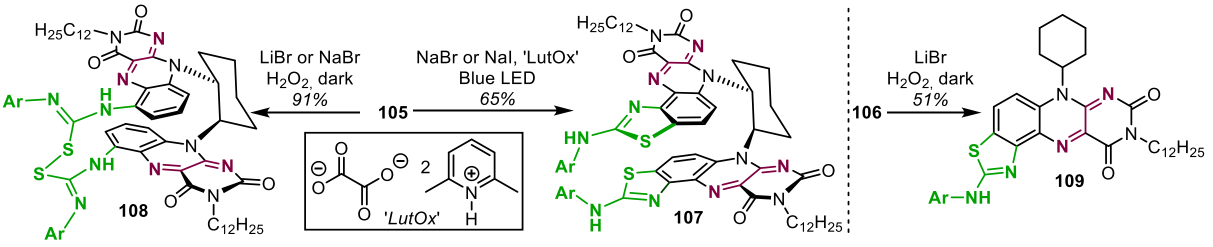

Figure 31: Formation of 2-aminobenzothiazole flavins **107** and **109** as well as disulfide **108** from the respective thiourea containing flavins **105** and **106**.

Analysis of both 2-aminobenzothiazole flavins **107** and **109** in presence of "*LutOx*" revealed clean reduction to the hydroquinoid flavin upon irradiation. To test the stability, both flavins were irradiated in presence of "*LutOx*" and LiBr under aerobic conditions. After 2 h of irradiation, over 80% of *bis*flavin **107** remained intact while only 37% of *mono*flavin **109** remained, presumably due to the slower generation of Br^+ equivalents by **107**. A protocol for the biomimetic halogenation was developed with Boc-Tyr-OMe **98** as a proof-of-principle substrate, as it contains both acid- and base- sensitive protecting groups. *Mono*- and *bis*-brominated tyrosine **99** was obtained in 58% total yield (Figure 32). This method was successfully applied to eight phenolic substrates including tyrosines, flavones, a dipeptide, a flavanone, and a coumarin.[86]

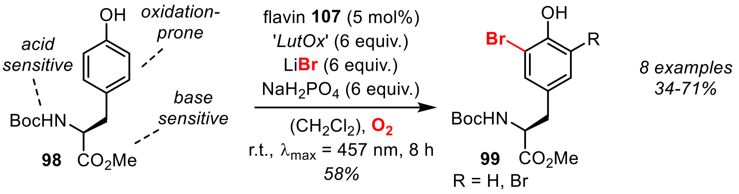

Figure 32: Conditions for the biomimetic bromination of Boc-Tyr-OMe using *bis*-2-aminobenzothiazole flavin **22**.

The advantages of *bis*flavin **107** were highlighted by comparing the results with **RFTA** and *mono*flavin **109**, where high levels of decomposition of both catalyst and substrate and low yields were observed. Additionally, mechanistic studies using methylated derivatives of 2-aminobenzothiazole catalysts **107** and **109** indicated catalytic participation of the 2-aminobenzothiazole moiety.[86]

In a second project, the multifunctionality of *bis*flavin **107** and flavin **110** was demonstrated in sequential transformations by combining two orthogonal steps, namely the photooxidation of silyl enol ethers followed by the reductive activation of molecular oxygen for sequential epoxidation and bromination. Flavin **110** was used in the sequential dehydrogenation-epoxidation sequence of silyl enol ethers **100**, where the same flavin catalyst is used in two orthogonal reactivities, a photocatalytic *Saegusa-Ito*-oxidation step followed by the reductive activation of O_2.[87] Since no thermal reactivity could be observed, the excited state redox potential of flavin **110** ($E^0(^3\mathbf{110}^*/\mathbf{110}^{\bullet-})$ = +1.35 V *vs* SCE) as well as the ground state redox potential of **100a** ($E_{p/2}$ = +1.17 V *vs* SCE) were determined and revealed that photochemical oxidation of **100a** by **110** was indeed feasible (Figure 33A). A reliable protocol for the photocatalytic oxidative dehydrogenation of **100** to *α,β*-unsaturated ketones **101** under inert atmosphere using **110** as well as an oxidant for catalyst regeneration was developed

(Figure 33B). Alkyl-isopropyl as well as various aryl-isopropyl ketones bearing electron-donating and electron-withdrawing substituents as well as an aryl-cyclohexyl derivative were successfully converted using this method. **RFTA** also led to a certain degree of product formation, but decomposed during the reaction, rendering it unsuitable for sequential transformations. Catalyst **110** on the other hand remained stable, presumably due to the lack of the sensitive ribityl backbone.[87]

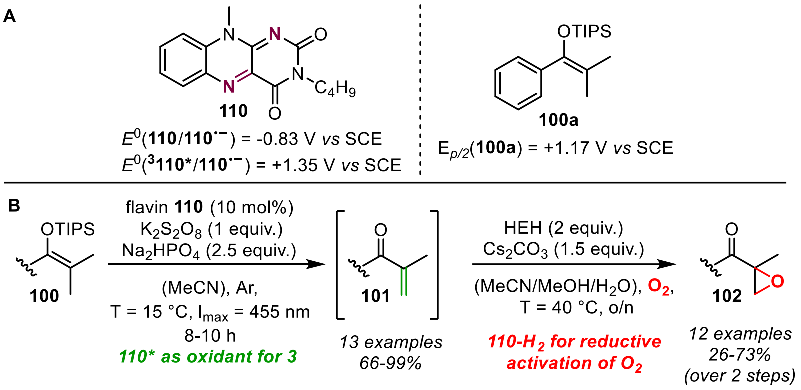
A
110
E^0(110/110$^{\bullet-}$) = -0.83 V vs SCE
E^0(^{3}110*/110$^{\bullet-}$) = +1.35 V vs SCE
OTIPS
100a
$E_{p/2}$(100a) = +1.17 V vs SCE
B
OTIPS
100
flavin 110 (10 mol%)
$K_2S_2O_8$ (1 equiv.)
Na_2HPO_4 (2.5 equiv.)
(MeCN), Ar,
T = 15 °C, I_{max} = 455 nm
8-10 h
110* as oxidant for 3
101
13 examples
66-99%
HEH (2 equiv.)
Cs_2CO_3 (1.5 equiv.)
(MeCN/MeOH/H_2O), O_2,
T = 40 °C, o/n
110-H_2 for reductive activation of O_2
102
12 examples
26-73%
(over 2 steps)

Figure 33: A) (Excited state) redox potentials determined for **110** and 100**a**; B) Procedure for the one-pot *Saegusa-Ito* oxidation-epoxidation sequence catalysed by **110**.

Following these observations, reaction conditions for a one-pot procedure, yielding *α*,*β*-epoxyketones **102** were identified. By exchanging the argon atmosphere for O_2 and adding *Hantzsch* ester (HEH) as sacrificial reductant after the first oxidation step, 12 silyl enol ethers **100** were successfully converted into *α*,*β*-epoxyketones **102**. Electron rich arenes showed slightly lower product formation while alkyl-substituted arenes gave the best results and aliphatic as well as trisubstituted epoxides were obtained in lower yields.[87]

In an attempt to replace $K_2S_2O_8$ as stoichiometric oxidant with molecular O_2, formation of silyloxy hydroperoxide **111** as byproduct (Figure 34A, right) *via* a singlet oxygen pathway was observed. Replacing flavin **110** with aminoflavin **113** (Figure 34A, left), which exhibited no activity in the *Saegusa-Ito* oxidation but efficiently mediated $^1O_2$ sensitization, allowed for selective formation of **111** *via* prototropic ene reaction. α-Silylperoxy ketone **112** (Figure 24A, right) was identified as minor product, presumably formed *via* a competing silatropic ene reaction. The formation of both products was monitored by *in-situ* NMR studies where **100a** was illuminated in deuterated MeCN in presence of **113** (Figure 34B). Both **111** and **112** were successfully isolated by column chromatography and characterized using NMR-spectroscopy and HR-ESI-MS.[87]

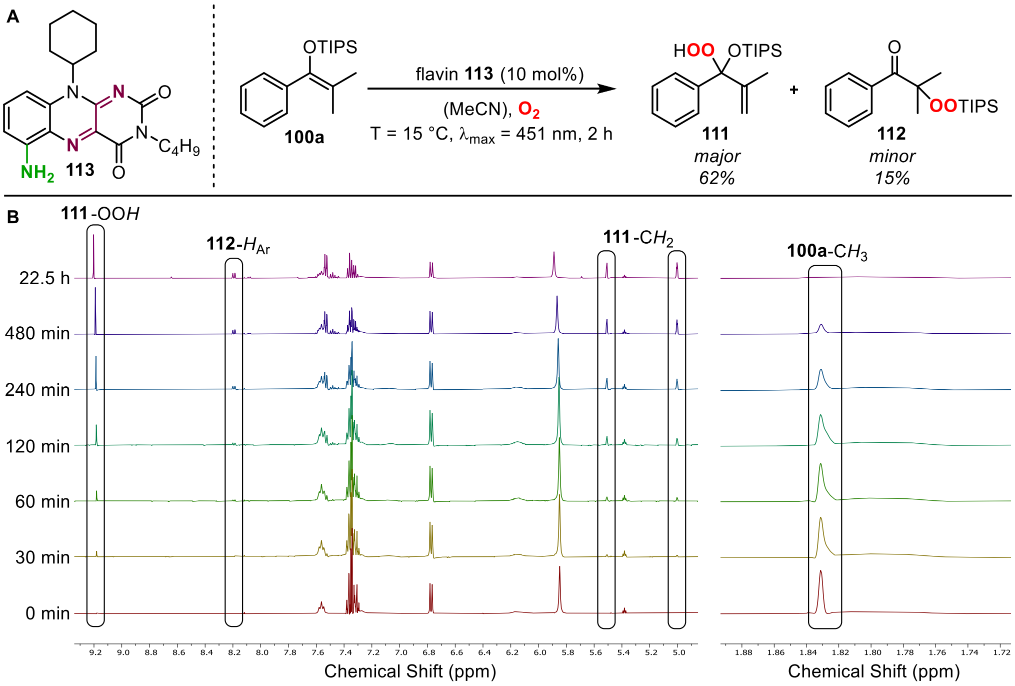
A
NH2 113
OTIPS
100a
flavin 113 (10 mol%)
(MeCN), O2
T = 15 °C, λmax = 451 nm, 2 h
HOO OTIPS
111
major
62%
+
OOTIPS
112
minor
15%
B
111-OOH
112-HAr
111-CH2
100a-CH3
22.5 h
480 min
240 min
120 min
60 min
30 min
0 min
Chemical Shift (ppm)
Chemical Shift (ppm)

Figure 34: A) Chemical structure of *C*6-aminoflavin **113** (left) and transformation of **100a** to **111** and **112** by **113** *via* $^1O_2$ sensitization; B) Monitoring of the reaction by *in-situ* NMR illumination studies.

To highlight the applicability of our catalytic system other sequential transformations were investigated. A one-pot procedure involving *Saegusa-Ito* oxidation of **100a** and sequential addition of a CF$_3$-radical to the *Michael* system resulted in the formation of ketone **114** (Figure 35A). In the second reaction step, **110** mediates the formation of CF$_3$-radicals from *Langlois* reagent (NaSO$_2$CF$_3$) by oxidation. Additionally, *C*$_2$-symmetric *bis*flavin **107** was successfully applied in a *Saegusa-Ito* oxidation-bromination sequence of silyl enol ether **115**, which features a phenol moiety (Figure 35B). Oxidation to the respective *α,β*-unsaturated ketone **116** by flavin **107** was successful, which highlights the flavins versatile reactivity. Since flavin **107** remained stable over the course of the reaction and *α,β*-unsaturated ketone **116** contains the required structural motive for the biomimetic bromination mentioned above, we developed a one-pot procedure for the transformation of silyl enol ether **115** to the respective brominated phenol **117**. By switching to the reaction conditions after the first oxidation step to the ones presented for the aerobic bromination of phenols, the brominated product **117** was obtained in a total yield of 40%.[87]

The mechanism of the oxidation is anticipated to involve a single-electron oxidation of **100** by flavin **110**, followed by deprotonation by anionic, semiquinoid flavin, which results in a neutral allylic radical. This radical species was successfully trapped by benzylidenemalononitrile, yielding *β*-functionalised silyl enol ether **119** from silyl enol ether

118 (Figure 35C). Using CH_2Cl_2 instead of MeCN suppressed the competing *Saegusa-Ito* oxidation of **118** and the addition of Na_2HPO_4 improved the yield slightly from 63% to 67%, presumably by facilitating deprotonation of the radical cation. Successive *Saegusa-Ito* oxidation of **119** was feasible as well by simply exchanging the solvent for MeCN and adding $K_2S_2O_8$ as sacrificial oxidant. With this method, functionalised *α*,*β*-unsaturated ketones **120** are accessible *via* a redox neutral *β*-functionalisation coupled with an photocatalytic *Saegusa-Ito* oxidation.[87]

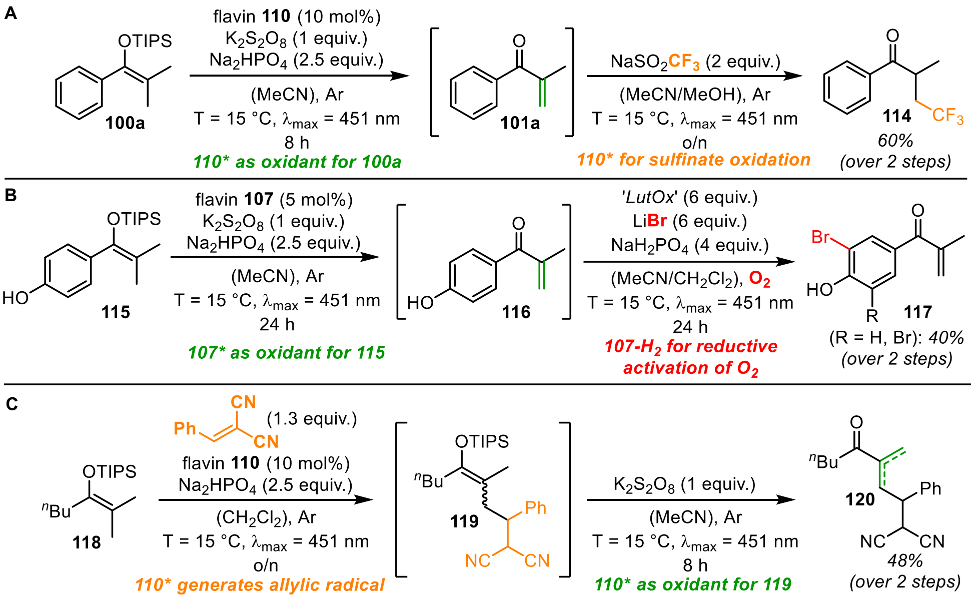
A
OTIPS
100a
flavin 110 (10 mol%)
K2S2O8 (1 equiv.)
Na2HPO4 (2.5 equiv.)
(MeCN), Ar
T = 15 °C, λmax = 451 nm
8 h
110* as oxidant for 100a
101a
NaSO2CF3 (2 equiv.)
(MeCN/MeOH), Ar
T = 15 °C, λmax = 451 nm
o/n
110* for sulfinate oxidation
114
CF3
60%
(over 2 steps)
B
OTIPS
HO
115
flavin 107 (5 mol%)
K2S2O8 (1 equiv.)
Na2HPO4 (2.5 equiv.)
(MeCN), Ar
T = 15 °C, λmax = 451 nm
24 h
107* as oxidant for 115
HO
116
'LutOx' (6 equiv.)
LiBr (6 equiv.)
NaH2PO4 (4 equiv.)
(MeCN/CH2Cl2), O2
T = 15 °C, λmax = 451 nm
24 h
107-H2 for reductive activation of O2
Br
HO
R
117
(R = H, Br): 40%
(over 2 steps)
C
OTIPS
nBu
118
Ph
CN
CN
(1.3 equiv.)
flavin 110 (10 mol%)
Na2HPO4 (2.5 equiv.)
(CH2Cl2), Ar
T = 15 °C, λmax = 451 nm
o/n
110* generates allylic radical
OTIPS
nBu
119
Ph
NC
CN
K2S2O8 (1 equiv.)
(MeCN), Ar
T = 15 °C, λmax = 451 nm
8 h
110* as oxidant for 119
nBu
120
Ph
NC
CN
48%
(over 2 steps)

Figure 35: A) *Saegusa-Ito* oxidation-trifluoromethylation sequence mediated by **110**; B) *Saegusa-Ito* oxidation-bromination sequence mediated by **107**; C) Sequential *β*-silyl enol ether modification and *Saegusa-Ito* oxidation of silyl enol ether **118**.

In conclusion, two flavin catalysts **107** and **110** with improved reactivity and stability compared to **RFTA** were established. *Bis*flavin **107** was successfully applied in a biomimetic bromination of oxidation prone phenolic substrates, where the 2-aminobenzothiazole moiety was found to be advantageous for catalytic activity. Additionally, a one-pot *Saegusa-Ito* oxidation-bromination sequence using a phenolic silyl enol ether transformation was realised. Flavin **110** was successfully applied in different sequential transformations including *Saegusa-Ito* oxidation-epoxidation, *Saegusa-Ito* oxidation-trifluoromethylation as well as a *β*-functionalisation-*Saegusa-Ito* oxidation sequence. Mechanistic experiments supported the initial formation of a neutral allylic radical *via* single-electron oxidation and deprotonation by **110**.

9. Licenses

Both publications “Synthetic C6-Functionalized Aminoflavin Catalysts Enable Aerobic Bromination of Oxidation Prone Substrates” and “Photochemical Desaturation and Epoxidation with Oxygen by Sequential Flavin Catalysis” are “open access” publications. Therefore, no licenses are needed and the publications as well as the respective supplementary information can be accessed free of charge *via* the following links:

Synthetic C6-Functionalized Aminoflavin Catalysts Enable Aerobic Bromination of Oxidation Prone Substrates

https://onlinelibrary.wiley.com/doi/full/10.1002/anie.202009657

Photochemical Desaturation and Epoxidation with Oxygen by Sequential Flavin Catalysis

https://onlinelibrary.wiley.com/doi/10.1002/anie.202310634

10.List of Abbreviations

acac	acetylacetone
Ar	aryl
Bu	butyl
BVMO	*Baeyer-Villiger monooxygenase*
BzlNAH	*N*-Benzyl-1,4-dihydronicotinamide
CKX	*cytokinin dehydrogenase*
DCE	1,2-dichloroethane
DCM	dichloromethane
DMB	5,6-dimethylbenzimidazole
DNA	deoxyribonucleic acid
EDTA	ethylenediaminetetraacetic acid
Equiv.	equivalent
Et	ethyl
EtOAc	ethyl acetate
EtOH	ethanol
FAD	flavin adenine dinucleotide
FMN	flavin adenine mononucleotide
HEH	*Hantzsch* ester
HPAH	*para-hydroxyphenylacetate 3-hydroxylase*
LutOx	lutidinium oxalate
*m*CPBA	*meta*-chloroperoxybenzoic acid
Me	methyl
MeCN	acetonitrile
MES	2-(*N*-Morpholino)ethanesulfonic acid
MeOH	methanol
MS	molecular sieves
NBS	*N*-Bromosuccinimide
NAD(P)H	nicotinamide adenine dinucleotide (phosphate)

P2O	*oxidase*
PCET	proton coupled electron transfer
Ph	phenyl
*p*MBA	*para*-methoxybenzyl alcohol
PrnA	*halogenase*
RebH	*halogenase*
RFTA	riboflavin tetraacetate
RFTB	riboflavin tetrabutyrate
RutA	*monooxygenase*
r.t.	room temperature
T	temperature
t	time
TEMPO	(2,2,6,6-tetramethylpiperidin-1-yl)oxyl
THF	tetrahydrofurane
TIPS	triisopropylsilyl
SCE	saturated calomel electrode
SET	single-electron transfer
VHPO	*vanadium-dependent haloperoxidase*
λ	wavelength

11.References

[1] C. J. T. S. O. Mansoorabadi, H.-W. Liu, *J. Org. Chem.* **2007**, *72*, 6329-6342.

[2] A. W. Blyth, *J. Chem. Soc., Trans.* **1879**, *35*, 530-539.

[3] R. Kuhn, P. György, T. Wagner-Jauregg, *Ber. Dtsch. Chem. Ges. (A and B Series)* **1933**, *66*, 576-580.

[4] K. G. Stern, *Nature* **1933**, *132*, 784-785.

[5] T. Pavlovska, R. Cibulka, in *Flavin-Based Catalysis*, **2021**, pp. 1-27.

[6] P. Karrer, K. Schöpp, F. Benz, *Helv. Chim. Acta* **1935**, *18*, 426-429.

[7] R. Kuhn, F. Weygand, *Ber. Dtsch. Chem. Ges. (A and B Series)* **2006**, *67*, 2084-2085.

[8] R. Kuhn, H. Rudy, F. Weygand, *Ber. Dtsch. Chem. Ges. (A and B Series)* **2006**, *69*, 1543-1547.

[9] W. C. O. Warburg, *Biochem. Ztschr.* **1938**, *298*, 150-168.

[10] G. W. K. S. M. H. Christie, A. R. Todd, *J. Chem. Soc.* **1954**, 46-52.

[11] a) A. M. Edwards, I. Ahmad, F. H. M. Vaid, M. V. Encinas, C. Previtali, N. A. Garcia, S. N. Criado, W. A. Massad, R. P. Goodrich, R. A. Edrich, L. L. Goodrich, C. A. Scott, K. J. Manica, D. J. Hlavinka, N. A. Hovenga, E. T. Hansen, D. Gampp, S. D. Keil, D. I. Gilmour, J. Li, C. B. Martin, M. S. Platz, F. Quina, C. W. M. Kay, A. Bacher, M. Fischer, G. Richter, E. Schleicher, S. Weber, W. R. Briggs, A. Losi, A. Murakami, M. Iseki, S. Matsunaga, M. Watanabe, J. T. M. Kennis, M. T. A. Alexandre, E. S. Photobiology, in *Flavins Photochemistry and Photobiology, Vol. 6* (Eds.: E. Silva, A. M. Edwards, D.-P. Hader, G. Jori), The Royal Society of Chemistry, **2006**, p. 0; b) P. Macheroux, B. Kappes, S. E. Ealick, *FEBS J.* **2011**, *278*, 2625-2634.

[12] E. Romero, J. R. Gomez Castellanos, G. Gadda, M. W. Fraaije, A. Mattevi, *Chem. Rev.* **2018**, *118*, 1742-1769.

[13] P. F. Heelis, *Chem. Soc. Rev.* **1982**, *11*, 15-39.

[14] C. T. Walsh, T. A. Wencewicz, *Nat. Prod. Rep.* **2013**, *30*, 175-200.

[15] F. Xu, *Ind. Biotechnol.* **2005**, *1*, 38-50.

[16] V. Massey, *J. Biol. Chem.* **1994**, *269*, 22459-22462.

[17] V. Massey, *Biochem. Soc. Trans.* **2000**, *28*, 283-296.

[18] A. W. Galston, *Proc. Natl. Acad. Sci. USA* **1949**, *35*, 10-17.

[19] R. Cibulka, M. W. Fraaije, in *Flavin-Based Catalysis*, **2021**, pp. 97-124.

[20] A. M. M. W. Fraaje, *Trends Biochem. Sci.* **2000**, *25*, 126-132.

[21] a) W. S. M. M. Mewies, N. S. Scrutton, *Protein Sci.* **2009**, *7*, 7-20; b) J. Drenth, M. W. Fraaije, in *Flavin-Based Catalysis*, **2021**, pp. 29-65.

[22] M. E. Taga, N. A. Larsen, A. R. Howard-Jones, C. T. Walsh, G. C. Walker, *Nature* **2007**, *446*, 449-453.

[23] C. Dong, S. Flecks, S. Unversucht, C. Haupt, K.-H. van Pée, J. H. Naismith, *Science* **2005**, *309*, 2216-2219.

[24] M. Bučko, P. Gemeiner, A. Schenkmayerová, T. Krajčovič, F. Rudroff, M. D. Mihovilovič, *Appl. Microbiol. Biotechnol.* **2016**, *100*, 6585-6599.

[25] K. Thotsaporn, P. Chenprakhon, J. Sucharitakul, A. Mattevi, P. Chaiyen, *J. Biol. Chem.* **2011**, *286*, 28170-28180.

[26] A. Matthews, R. Saleem-Batcha, J. N. Sanders, F. Stull, K. N. Houk, R. Teufel, *Nat. Chem. Biol.* **2020**, *16*, 556-563.

[27] M. Toplak, R. Teufel, *Biochemistry* **2022**, *61*, 47-56.

[28] S. Keller, T. Wage, K. Hohaus, M. Holzer, E. Eichhorn, K. H. van Pee, *Angew. Chem. Int. Ed.* **2000**, *39*, 2300-2302.

[29] K.-H. van Pée, E. P. Patallo, *Appl. Microbiol. Biotechnol.* **2006**, *70*, 631-641.

[30] a) S. Flecks, E. P. Patallo, X. Zhu, A. J. Ernyei, G. Seifert, A. Schneider, C. Dong, J. H. Naismith, K. H. van Pee, *Angew. Chem. Int. Ed.* **2008**, *47*, 9533-9536; b) E. Yeh, L. C. Blasiak, A. Koglin, C. L. Drennan, C. T. Walsh, *Biochemistry* **2007**, *46*, 1284-1292.

[31] J. Sucharitakul, M. Prongjit, D. Haltrich, P. Chaiyen, *Biochemistry* **2008**, *47*, 8485-8490.

[32] T. Wongnate, P. Surawatanawong, S. Visitsatthawong, J. Sucharitakul, N. S. Scrutton, P. Chaiyen, *J. Am. Chem. Soc.* **2014**, *136*, 241-253.

[33] J. Sucharitakul, M. Prongjit, D. Haltrich, P. Chaiyen, *Biochemistry* **2008**, *47*, 8485-8490.

[34] J. Frebortova, M. W. Fraaije, P. Galuszka, M. Sebela, P. Pec, J. Hrbac, O. Novak, K. D. Bilyeu, J. T. English, I. Frebort, *Biochem. J.* **2004**, *380*, 121-130.

[35] a) H. Fu, T. Qiao, J. M. Carceller, S. N. MacMillan, T. K. Hyster, *J. Am. Chem. Soc.* **2023**, *145*, 787-793; b) X. Huang, B. Wang, Y. Wang, G. Jiang, J. Feng, H. Zhao, *Nature* **2020**, *584*, 69-74; c) B. A. Sandoval, P. D. Clayman, D. G. Oblinsky, S. Oh, Y. Nakano, M. Bird, G. D. Scholes, T. K. Hyster, *J. Am. Chem. Soc.* **2021**, *143*, 1735-1739.

[36] M. A. Sheraz, S. H. Kazi, S. Ahmed, Z. Anwar, I. Ahmad, *Beilstein J. Org. Chem.* **2014**, *10*, 1999-2012.

[37] G. Merenyi, J. Lind, *J. Am. Chem. Soc.* **1991**, *113*, 3146-3153.

[38] K. Tamao, T. Hayashi, Y. Ito, *J. Chem. Soc., Chem. Commun.* **1988**, 795-797.

[39] M. M. Mader, P.-O. Norrby, *J. Am. Chem. Soc.* **2001**, *123*, 1970-1976.

[40] Y. Imada, H. Iida, T. Kitagawa, T. Naota, *Chem. Eur. J.* **2011**, *17*, 5908-5920.

[41] T. Hering, B. Mühldorf, R. Wolf, B. König, *Angew. Chem. Int. Ed.* **2016**, *55*, 5342-5345.

[42] C. J. Seel, A. Králík, M. Hacker, A. Frank, B. König, T. Gulder, *ChemCatChem* **2018**, *10*, 3960-3963.

[43] Y. Shiogai, M. Oka, H. Iida, *Org. Biomol. Chem.* **2023**, *21*, 2081-2085.

[44] a) R. Lechner, S. Kummel, B. Konig, *Photochem. Photobiol. Sci.* **2010**, *9*, 1367-1377; b) J. Zelenka, E. Svobodova, J. Tarabek, I. Hoskovcova, V. Boguschova, S. Bailly, M. Sikorski, J. Roithova, R. Cibulka, *Org. Lett.* **2019**, *21*, 114-119; c) B. Mühldorf, R. Wolf, *Angew. Chem. Int. Ed.* **2016**, *55*, 427-430.

[45] A. Hassan Tolba, M. Krupička, J. Chudoba, R. Cibulka, *Org. Lett.* **2021**, *23*, 6825-6830.

[46] A. Takeda, H. Okai, K. Watabe, H. Iida, *J. Org. Chem.* **2022**, *87*, 10372-10376.

[47] C. Suadee, S. Nijvipakul, J. Svasti, B. Entsch, D. P. Ballou, P. Chaiyen, *J. Biochem.* **2007**, *142*, 539-552.

[48] a) R. Cibulka, *Eur. J. Org. Chem.* **2015**, *2015*, 915-932; b) C. Kemal, T. W. Chan, R. C. Bruice, *J. Am. Chem. Soc.* **1977**, *99*, 7272-7286.

[49] A. Rehpenn, A. Walter, G. Storch, *Synthesis* **2021**, *53*, 2583-2593.

[50] C. Kemal, T. C. Bruice, *Proc. Natl. Acad. Sci. USA* **1976**, *73*, 995-999.

[51] S. Murahashi, T. Oda, Y. Masui, *J. Am. Chem. Soc.* **1989**, *111*, 5002-5003.

[52] Y. Imada, H. Iida, S. Ono, S.-I. Murahashi, *J. Am. Chem. Soc.* **2003**, *125*, 2868-2869.

[53] Y. Imada, H. Iida, S. Ono, Y. Masui, S.-I. Murahashi *Chem. Asian. J.* **2006**, *1*, 136-147.

[54] Y. Imada, T. Kitagawa, H.-K. Wang, N. Komiya, T. Naota, *Tetrahedron Lett.* **2013**, *54*, 621-624.

[55] S. Murahashi, D. Zhang, H. Iida, T. Miyawaki, M. Uenaka, K. Murano, K. Meguro, *Chem. Commun.* **2014**, *50*, 10295-10298.

[56] Y. Imada, H. Iida, T. Naota, *J. Am. Chem. Soc.* **2005**, *127*, 14544-14545.

[57] Y. Imada, H. Iida, S. Murahashi, T. Naota, *Angew. Chem. Int. Ed.* **2005**, *44*, 1704-1706.

[58] H. Iida, R. Demizu, R. Ohkado, *J. Org. Chem.* **2018**, *83*, 12291-12296.

[59] M. März, M. Babor, R. Cibulka, *Eur. J. Org. Chem.* **2019**, *2019*, 3264-3268.

[60] H. Kotoucova, I. Strnadova, M. Kovandova, J. Chudoba, H. Dvorakova, R. Cibulka, *Org. Biomol. Chem.* **2014**, *12*, 2137-2142.

[61] S. Chen, F. W. Foss, Jr., *Org. Lett.* **2012**, *14*, 5150-5153.

[62] a) R. Ohkado, T. Ishikawa, H. Iida, *Green Chem.* **2018**, *20*, 984-988; b) H. Okai, K. Tanimoto, R. Ohkado, H. Iida, *Org. Lett.* **2020**, *22*, 8002-8006; c) A. Takeda, M. Oka, H. Iida, *J. Org. Chem.* **2023**, *88*, 7551-7556; d) K. Tanimoto, H. Okai, M. Oka, R. Ohkado, H. Iida, *Org. Lett.* **2021**, *23*, 2084-2088.

[63] T. Mizushima, M. Oka, Y. Imada, H. Iida, *Adv. Synth. Catal.* **2022**, *364*, 2443-2448.

[64] A. T. Murray, P. Matton, N. W. G. Fairhurst, M. P. John, D. R. Carbery, *Org. Lett.* **2012**, *14*, 3656-3659.

[65] T. Ishikawa, M. Kimura, T. Kumoi, H. Iida, *ACS Catal.* **2017**, *7*, 4986-4989.

[66] Y. Arakawa, K. Yamanomoto, H. Kita, K. Minagawa, M. Tanaka, N. Haraguchi, S. Itsuno, Y. Imada, *Chem. Sci.* **2017**, *8*, 5468-5475.

[67] Y. Chevalier, Y. Lock Toy Ki, D. le Nouen, J.-P. Mahy, J.-P. Goddard, F. Avenier, *Angew. Chem. Int. Ed.* **2018**, *57*, 16412-16415.

[68] S. D. M. Islam, A. Penzkofer, P. Hegemann, *Chem. Phys.* **2003**, *291*, 97-114.

[69] M. Insińska-Rak, E. Sikorska, J. L. Bourdelande, I. V. Khmelinskii, W. Prukała, K. Dobek, J. Karolczak, I. F. Machado, L. F. V. Ferreira, E. Dulewicz, A. Komasa, D. R. Worrall, M. Kubicki, M. Sikorski, *J. Photochem. Photobiol. A* **2007**, *186*, 14-23.

[70] *Chemical Photocatalysis*, De Gruyter, Berlin, Boston, **2013**.

[71] a) J. Dad'ová, E. Svobodová, M. Sikorski, B. König, R. Cibulka, *ChemCatChem* **2012**, *4*, 620-623; b) T. Neveselý, E. Svobodová, J. Chudoba, M. Sikorski, R. Cibulka, *Adv. Synth. Catal.* **2016**, *358*, 1654-1663.

[72] M. Bregnhøj, M. Westberg, F. Jensen, P. R. Ogilby, *Phys. Chem. Chem. Phys.* **2016**, *18*, 22946-22961.

[73] C. Dang, L. Zhu, H. Guo, H. Xia, J. Zhao, B. Dick, *ACS Sustainable Chem. Eng.* **2018**, *6*, 15254-15263.

[74] D. Shen, F. Zhong, L. Li, H. Zhang, T. Ren, C. Sun, B. Wang, M. Guo, M. Chao, S. Fukuzumi, *Org. Chem. Front.* **2023**, *10*, 2653-2662.

[75] A. Wolnicka-Glubisz, A. Pawlak, M. Insinska-Rak, A. Zadlo, *J. Photochem. Photobiol. B* **2020**, *205*, 111820.

[76] J. B. Metternich, R. Gilmour, *J. Am. Chem. Soc.* **2016**, *138*, 1040-1045.

[77] L. M. Bouchet, A. A. Heredia, J. E. Argüello, L. C. Schmidt, *Org. Lett.* **2020**, *22*, 610-614.

[78] M. März, M. Kohout, T. Neveselý, J. Chudoba, D. Prukała, S. Niziński, M. Sikorski, G. Burdziński, R. Cibulka, *Org. Biomol. Chem.* **2018**, *16*, 6809-6817.

[79] N. P. Ramirez, B. Konig, J. C. Gonzalez-Gomez, *Org. Lett.* **2019**, *21*, 1368-1373.

[80] S. Bloom, C. Liu, D. K. Kolmel, J. X. Qiao, Y. Zhang, M. A. Poss, W. R. Ewing, D. W. C. MacMillan, *Nat. Chem.* **2018**, *10*, 205-211.

[81] S. A. Baker Dockrey, A. R. H. Narayan, *Org. Lett.* **2020**, *22*, 3712-3716.

[82] B. Muhldorf, R. Wolf, *Chem. Commun.* **2015**, *51*, 8425-8428.

[83] Y.-M. Legrand, M. Gray, G. Cooke, V. M. Rotello, *J. Am. Chem. Soc.* **2003**, *125*, 15789-15795.

[84] A. H. Tolba, F. Vávra, J. Chudoba, R. Cibulka, *Eur. J. Org. Chem.* **2020**, *2020*, 1579-1585.

[85] A. Pokluda, Z. Anwar, V. Boguschová, I. Anusiewicz, P. Skurski, M. Sikorski, R. Cibulka, *Adv. Synth. Catal.* **2021**, *363*, 4371-4379.

[86] A. Walter, G. Storch, *Angew. Chem. Int. Ed.* **2020**, *59*, 22505-22509.

[87] A. Walter, W. Eisenreich, G. Storch, *Angew. Chem. Int. Ed.* **2023**, *62*, e202310634.